UNIVERSITÀ DEGLI STUDI DI PADOVA

Facoltà di Scienze MM.FF.NN.
Dipartimento di Biologia

Scuola di Dottorato di Ricerca in Biochimica e Biotecnologie
Indirizzo in Biotecnologie
Ciclo XXI

INTERACTIONS BETWEEN FATZ AND MYOTILIN FAMILIES AND ENIGMA FAMILY PROTEINS AT THE SARCOMERIC Z-DISC

Direttore della Scuola
Ch.mo Prof. Giuseppe Zanotti

Supervisore
Ch.mo Prof. Giorgio Valle

Dottorando
Chiara Gardin

A.A. 2008/2009

TABLE OF CONTENTS

SUMMARY

The Z-disc of striated muscle cells is a highly specialized three-dimensional structure which delineates the boundary of the individual sarcomeres. It accomplishes a unique role by anchoring actin filaments and acts as a molecular trigger for contraction. Beyond a well-defined structural role, in recent years it is emerging the hypothesis that Z-disc may be directly involved in the perception and transmission of muscular stress signals. To achieve these complex functions, many Z-disc proteins are involved in multiple protein interactions. The importance of these interactions is indicated by the fact that mutations in several Z-disc proteins can result in muscular dystrophies and/or cardiomyopathies in human and mice. Functional studies on the Z-disc interactome and its regulation will greatly improve the understanding of the biology of the Z-disc and its muscular disorders.

The main goal of my project was to understand the complex network of protein-protein interactions occurring at the Z-disc of skeletal and cardiac muscle. In particular, my work focused on two groups of Z-disc proteins: the FATZ and myotilin protein families on one hand, and some proteins belonging to the enigma family on the other hand. This work led to the identification of a specific interaction between the PDZ domain of enigma family members and the C-terminal five amino acids of the FATZ and myotilin families.

The work of this thesis was part of a wider project involving the groups of Dr. G. Faulkner at ICGEB, Trieste, and Prof. O. Carpen at University of Turku, Finland. Together with our collaborators we noted that the C-terminal five amino acids of FATZ-1 (ETEEL), FATZ-2 (ESEDL), FATZ-3 (ESEEL), myotilin (ESEEL), palladin (ESEDL) and myopalladin (ESDEL) are highly similar. Searches in protein sequence databases revealed that this E-[S/T]-[D/E]-[D/E]-L motif is restricted in Vertebrates to the FATZ and myotilin families of proteins, and it is evolutionary conserved from zebrafish to humans, indicating its importance for their biological function. The ELM program (a source for predicting functional sites in eukaryotic proteins) predicted that the terminal four amino acids of the FATZ and myotilin families constitute a binding motif for class III PDZ domain proteins (X-[D/E]-X-[V/I/L]). The first object of my work was to determine if the proteins with this new type of class III PDZ binding motif at their C-terminal could effectively bind PDZ domains. We knew from the literature that ZASP binds to all the three members of the FATZ family and from preliminary

observations of our Finnish collaborators that myotilin interacts with ZASP. In addition to ZASP, other two members of the enigma family of PDZ proteins, ALP and CLP-36, were included in this study. Both the full-length and the truncated (lacking the last five amino acids) version of the FATZ and myotilin families were produced as native proteins and tested for PDZ binding using the AlphaScreen (Amplified Luminescence Proximity Homogeneous Assay) technique. Biotinylated phosphorylated and non-phosphorylated peptides corresponding to the C-terminal five amino acids of the FATZ and myotilin families were also used in AlphaScreen interaction experiments, as well as a control peptide having E instead of L as its last amino acid (ESEEE). The results presented in this thesis show that the final five amino acids of the FATZ and myotilin families of proteins are responsible for the binding to the PDZ domains of ZASP, ALP and CLP-36, and that the nature of the last amino acid of the motif is crucial for the interaction. We also show that phosphorylation of the ligand sequence (on the serine or threonine residue) modulates the ability of the peptides to bind to the PDZ domains of the enigma family. α-actinin-2 was included in this study as its C-terminus (GESDL) is classified as a class I PDZ binding motif (X-[S/T]-X-[V/I/L]) and it had bind shown to bind to the PDZ domains of ZASP and ALP. AlphaScreen experiments confirm the binding of both the full-length and the C-terminal phosphorylated and non-phosphorylated peptides of α-actinin-2 to the PDZ domains of ZASP and ALP, and they also reveal an interaction with the PDZ domain of CLP-36.

These interactions were verified using another *in vitro* binding technique, the TranSignal PDZ Domain Array. Based on the results of the PDZ arrays, RIL, another member of the enigma family, is capable of binding the E-[S/T]-[D/E]-[D/E]-L motif. Therefore, these final five amino acids can be considered a novel type of class III PDZ binding motif specific for the PDZ domains of enigma proteins.

To better quantify the strength of the noted interactions, SPR (Surface Plasmon Resonance) experiments were performed in the laboratory of Dr. A. Baines at University of Kent, UK. The affinities of the interactions between the PDZ domain of ZASP and some of the phosphorylated and non-phosphorylated peptides of the FATZ and myotilin families result to be in the nM range. The SPR results also demonstrate a new interaction between the PDZ domain of ZASP and ANKRD2. This protein is a member of the MARP family and it is thought to be involved in muscle stress response pathways. ANKRD2 localizes both in the sarcomeric I-band and the nucleus, and it is able to bind to several transcription factors, including YB-1, PML and p53. This interaction strengthens the

hypothesis that, besides having a structural function, Z-disc could also have a role in cell signalling.

It is worth noting that many Z-disc proteins can interact with the same partners therefore it would be helpful to define the level and pattern of expression of the individual proteins in different muscle tissues to understand which interactions actually occur. Therefore, another aim of my work was to measure the abundance of mRNAs of some Z-disc proteins using the Real-Time PCR technique. Four different muscles from adult mice were considered: tibialis (a fast-twitch skeletal muscle), soleus (a slow-twitch skeletal muscle), gastrocnemius (a skeletal muscle with mixed fibers) and heart (cardiac muscle). The different distribution of the FATZ proteins, myotilin and the alternatively spliced variants of ZASP suggests that, at least in mouse, the interactions between these proteins could be compartmentalized in distinct fiber types.

RIASSUNTO

Il disco-Z del muscolo striato è una struttura molecolare altamente specializzata a livello della quale si instaurano numerose interazioni proteina-proteina. Il disco-Z delinea il confine dei singoli sarcomeri, fornendo un punto di ancoraggio per i filamenti sottili di actina; il loro scorrimento sui filamenti spessi di miosina produce la forza meccanica responsabile della contrazione. Al di là di un evidente significato strutturale, negli ultimi anni sta diventando sempre più consistente l'ipotesi di un coinvolgimento del disco-Z anche nella percezione e nella trasmissione di segnali. L'importanza delle interazioni tra le proteine del disco-Z è indicata dal fatto che mutazioni in molte di queste proteine possono risultare in distrofie muscolari e/o cardiomiopatie sia in uomo sia in topo. Una più ampia conoscenza delle interazioni che si articolano a livello del disco-Z e, in generale, degli eventi che le regolano, aiuterebbe a chiarire la biologia del disco-Z e l'insorgenza di eventuali patologie associate. Il mio progetto di Dottorato è stato incentrato su due gruppi di proteine sarcomeriche e sulle loro interazioni: le proteine delle famiglie FATZ e miotilina da un lato, e alcune proteine appartenenti alla famiglia enigma dall'altro. Questo lavoro ha portato all'identificazione di una specifica interazione tra i domini PDZ delle proteine della famiglia enigma e gli ultimi cinque residui aminoacidici presenti nelle proteine delle famiglie FATZ e miotilina.

Il lavoro di questa tesi si inserisce in un progetto più ampio che coinvolge i gruppi coordinati dalla Dr.ssa G. Faulkner dell'ICGEB, Trieste, e il Prof. O. Carpen dell'Università di Turku, Finlandia. Grazie alla loro collaborazione, è stato possibile notare che i cinque residui C-terminali delle proteine FATZ-1 (ETEEL), FATZ-2 (ESEDL), FATZ-3 (ESEEL), miotilina (ESEEL), palladina (ESEDL) e miopalladina (ESDEL) sono molto simili. Una ricerca effettuata in *database* di sequenze proteiche ha rivelato che questo motivo, E-[S/T]-[D/E]-[D/E]-L, è quasi esclusivamente ristretto nei Vertebrati alle proteine delle famiglie FATZ e miotilina; inoltre, esso sembra essere conservato da *zebrafish* ad uomo, suggerendo la sua importanza per le proteine che lo contengono. Il programma ELM (che predice siti funzionali in proteine eucariotiche) ha predetto che gli ultimi quattro amino acidi delle proteine FATZ, miotilina, palladina e miopalladina costituiscono un motivo di legame per le proteine con domini PDZ di classe III (X-[D/E]-X-[V/I/L]). Il mio primo obiettivo è stato quello di verificare se le proteine caratterizzate da questo nuovo motivo C-terminale

potessero effettivamente legare domini PDZ. E' noto dalla letteratura che i tre componenti della famiglia FATZ legano ZASP. Sappiamo inoltre, da osservazioni preliminari dei nostri collaboratori finlandesi, che miotilina interagisce con ZASP. Oltre a ZASP, altri due membri della famiglia enigma, ALP e CLP-36, sono stati inclusi nello studio. Le proteine della famiglia FATZ e miotilina sono state prodotte sia in versione *full-length* sia priva degli ultimi cinque amino acidi per essere utilizzate in saggi di interazione AlphaScreen (*Amplified Luminescence Proximity Homogeneous Assay*). Peptidi biotinilati, fosforilati e non, corrispondenti ai cinque amino acidi finali delle FATZ, miotilina, palladina e miopalladina sono stati inoltre impiegati nei saggi AlphaScreen, così come un peptide di controllo avente in ultima posizione un acido glutammico (E) invece che una leucina (L). I risultati riportati in questa tesi dimostrano che gli ultimi cinque amino acidi delle proteine delle famiglie FATZ e miotilina sono responsabili del legame ai domini PDZ di ZASP, ALP e CLP-36, e che la natura dell'ultimo residuo aminoacidico è cruciale per questa interazione. Inoltre, la fosforilazione del residuo di serina o treonina del ligando C-terminale può influenzare il legame dei peptidi nei confronti dei domini PDZ della famiglia enigma. La proteina α-actinina-2 è stata introdotta nello studio, poiché la sua sequenza C-terminale (GESDL) è classificata come motivo di legame per i domini PDZ di classe I (X-[S/T]-X-[V/I/L]). Gli esperimenti AlphaScreen hanno confermato l'interazione di α-actinina-2 (sia della forma *full-length* sia dei peptidi C-terminali, fosforilati e non) con i PDZ di ZASP e ALP, e hanno fatto emergere una nuova interazione con il PDZ di CLP-36.

Molte di queste interazioni sono state verificate con un altro metodo di interazione proteina-proteina *in vitro*, il *TranSignal PDZ Domain Array*. Sulla base dei risultati di PDZ *array* è stato possibile identificare un altro membro della famiglia di proteine enigma, RIL, in grado di legare il motivo E-[S/T]-[D/E]-[D/E]-L. Possiamo considerare questi cinque amino acidi C-terminali come un nuovo motivo di legame per le proteine con domini PDZ di classe III, specifico per i domini PDZ delle proteine enigma.

Per poter meglio quantificare la forza delle interazioni studiate, alcuni esperimenti di SPR (*Surface Plasmon Resonance*) sono stati eseguiti nel laboratorio del Dr. A. Baines all'Università di Kent, UK. Le affinità delle interazioni tra il dominio PDZ di ZASP e alcuni dei peptidi fosforilati e non-fosforilati delle famiglie di proteine FATZ e miotilina risultano essere nell'ordine del nM. Gli esperimenti di SPR hanno portato anche all'identificazione di un'interazione tra il PDZ di ZASP e ANKRD2. Si pensa che questa proteina, membro della famiglia MARP, sia coinvolta nelle vie di risposta a stress muscolari. ANKRD2 può trovarsi sia nella

banda-I del sarcomero sia nel nucleo ed è in grado di legare diversi fattori di trascrizione, come YB-1, PML e p53. La scoperta di questa interazione rafforza l'ipotesi che il disco-Z, oltre ad un ruolo strutturale, potrebbe essere coinvolto in vie di segnalazione.

Dal momento che a livello del disco-Z molte proteine hanno più di un *partner* proteico, sarebbe utile cercare di definire il livello e il profilo di espressione delle singole proteine in tessuti muscolari con diverse caratteristiche. Un altro obiettivo del mio lavoro è stato, quindi, quello di valutare l'abbondanza degli mRNA di alcune delle proteine del disco-Z da me studiate con la *Real-Time PCR*. Allo scopo sono stati presi in considerazione quattro tessuti muscolari di topo adulto: il tibiale (un muscolo scheletrico a contrazione rapida), il soleo (un muscolo scheletrico a contrazione lenta), il gastrocnemio (un muscolo scheletrico con fibre miste) e il muscolo cardiaco. La differente distribuzione delle FATZ, miotilina e ZASP (con le sue varianti di *splicing*) suggerisce che, almeno in topo, le interazioni tra queste proteine potrebbero essere compartimentalizzate in distinte fibre muscolari.

LIST OF ORIGINAL ARTICLES

The knowledge and experimental data produced during my PhD fellowship led to the publication of the following articles:

von Nandelstadh P, Ismail M, Gardin C, Suila H, Zara I, Belgrano A, Valle G, Carpen O, Faulkner G (2009). A class III PDZ binding motif in myotilin and FATZ families binds Enigma family proteins - a common link for Z-disc myopathies. *Mol Cell Biol*. 29(3):822-834.

Feltrin E, Campanaro S, Diehl AD, Ehler E, Faulkner G, Fordham J, Gardin C, Harris M, Hill D, Knoell R, Laveder P, Mittempergher L, Nori A, Reggiani C, Sorrentino V, Volpe P, Zara I, Valle G, and Deegan J (2009). Muscle Research and Gene Ontology: New standards for improved data integration. *BMC Medical Genomics*. 2(6). [Epub ahead of print].

ABBREVIATIONS

SI prefixes

n	nano- (10^{-9})
μ	micro- (10^{-6})
m	milli- (10^{-3})
k	kilo- (10^{3})

SI units

g	gram
L	litre
min	minute
mol	mole
s	second
°C	degrees Celsius
Å	angstrom

Other units / abbreviations

aa	amino acid
A-band	anisotropic in polarized light
ABD	actin-binding domain
ALP	actinin-associated LIM protein
AlphaScreen	amplified luminescent proximity homogeneous assay
ANF	atrial natriuretic factor
ANKRD2	ankyrin repeat domain 2 protein
AR LGMD	autosomal recessive limb-girdle muscular dystrophy
ATP	adenine triphosphate
bp	base pair
C2C12	mouse myoblast cell line
CARP	cardiac ankyrin repeat protein
CBB	coomassie brilliant blue
cDNA	complementary DNA
CH	calponin homology
CLP	C-terminal LIM domain protein with a molecular weight of 36 kDa
CRIBI	*Centro di Ricerca Interdipartimentale per le Biotecnologie Innovative*

Ct	threshold cycle
Da	dalton
DARP	diabetes-related ankyrin repeat protein
DCM	dilated cardiomyopathy
DEPC	diethylpyrocarbonate
Dlg	discs large protein
DNA	deoxyribonucleic acid
DTT	dithiothreitol
ECL	enhanced chemiluminescence
EDC	1-ethyl-3-(3-dimethylaminopropyl) carbodiimide
EDTA	ethylene-diamine tetraacetic acid
ELM	eukaryotic linear motif
ENH	enigma homology protein
EST	expressed sequence tag
FATZ	γ-filamin, α-actinin, and telethonin binding protein of the Z-disc
FL	full length
GABA	gamma amino-butyric acid
GAPDH	glyceraldehyde 3-phosphate dehydrogenase
GLGF	glycine-leucine-glycine-phenylalanine motif
GST	glutathione-S-transferase
HCM	hypertrophic cardiomyopathy
hCLIM1	human 36-kDa carboxyl terminal LIM domain
HEPES	N-2-Hydroxyethylpiperazine-N'-2-ethanesulfonic acid
HIS	histidine
HPLC	high performance liquid chromatography
HRP	horseradish peroxidase
I-band	isotropic in polarized light
ICGEB	International Centre for Genetic Engineering and Biotechnology
Ig	immunoglobulin
IPTG	isopropyl-β-D-thiogalactoside
K_A	equilibrium association constant or affinity constant
K_a	association rate constant or on-rate constant (K_{on})
K_D	equilibrium dissociation constant
K_d	dissociation rate constant or off-rate constant (K_{off})
LB	Luria Bertani broth
LGMD	limb girdle muscular dystrophy
LIM domain	acronym derived from the first three described LIM-domain containing proteins: Lin-11, Isl-1 and Mec-3

Ln	natural logarithm
Log	common logarithm
M	molar
MARP	muscle ankyrin repeat protein
M-band	mittel, meaning middle in German
MFM	myofibrillar myopathy
MLP	muscle LIM protein
mRNA	messenger RNA
NFAT	nuclear factor of activated T-cells
NHS	n-hydroxysuccinimide
Ni-NTA	nickel-nitrilotriacetic acid
NMR	nuclear magnetic resonance
OD_{600}	optical density at 600 nm
O/N	overnight
PAGE	polyacrylamide gel electrophoresis
PBS	phosphate buffered saline
PCR	polymerase chain reaction
PDLIM	PDZ and LIM domain protein
PDZ domain	acronym derived from the first three described PDZ-domain containing proteins: PSD-95, Dlg and ZO-1
PEST	protein-destabilizing motif
pI	isoelectric point
PKC	protein kinase C
PSD-95	postsynaptic density 95 kDa
PVDF	polyvinyldifluoride
R_{eq}	response at equilibrium
RIL	reversion-induced protein
RNA	ribonucleic acid
RP	reverse phase
rpm	revolutions per minute
RT	room temperature
RU	response or resonance units
SDS	sodium dodecyl-sulphate
SH_3	Src homology domain
siRNA	small interfering RNA
SLRs	spectrin-like repeats
SMART	simple modular architecture research tool
SPR	surface plasmon resonance

TEMED	N,N,N/,N/-tetramethylethylenediamine
Tris	2-amino-2-(hydroxymethyl)propane-1-3-diol
Tween-20	polyoxyethylene (20) sorbitan monolaurate
UV	ultraviolet light
v/v	volume per volume
w/v	weight per volume
ZASP	Z-band alternatively spliced PDZ-motif protein
Z-disc	zwischen, meaning between in German
ZO-1	zonula occludens 1 protein

I INTRODUCTION

I-1 The muscle: structure and function

Muscle is the contractile tissue of the body, responsible for both locomotion of the organism itself and movement of internal organs. There are three types of muscle which all have the ability to contract: skeletal, cardiac, and smooth muscle.
Skeletal muscle is a voluntary striated muscle. It is anchored by tendons to bone and is used to affect skeletal movement such as locomotion and in maintaining posture. An average adult male has 40–50% (as percentage of body mass) of skeletal muscle and an average adult female is made up of 30–40%. An individual skeletal muscle consists of hundreds of muscle cells called muscle fibers or myofibers that are cylindrical and multinucleated. The nuclei are located in the periphery of the cell, just under the plasma membrane. Myofibers are bundled together and wrapped in a connective tissue sheath called the epimysium (Figure 1). Portions of the epimysium project inward to divide the muscle into compartments. Each compartment contains a bundle of muscle fibers, forming a fascicle, which is surrounded by a layer of connective tissue called the perimysium. Within the fascicle, each individual myofiber is surrounded by connective tissue called the endomysium. Each muscle fiber contains many myofibrils. Myofibrils are made up of sarcomeres, the basic contractile unit of muscle that is composed of thick and thin filaments. Thick filaments are mainly composed of myosin whereas thin filaments are composed of actin filaments associated with tropomyosin and troponin. In addition to myofibrils, there are also other specialized structures in skeletal muscle cells. Other cytoskeletal filament systems (described below) connect myofibrils to the sarcolemma (plasma membrane) and its invaginations (T-tubules) as well as to the sarcoplasmic reticulum (endoplastic reticulum) (Burkitt HG et al., 1993).

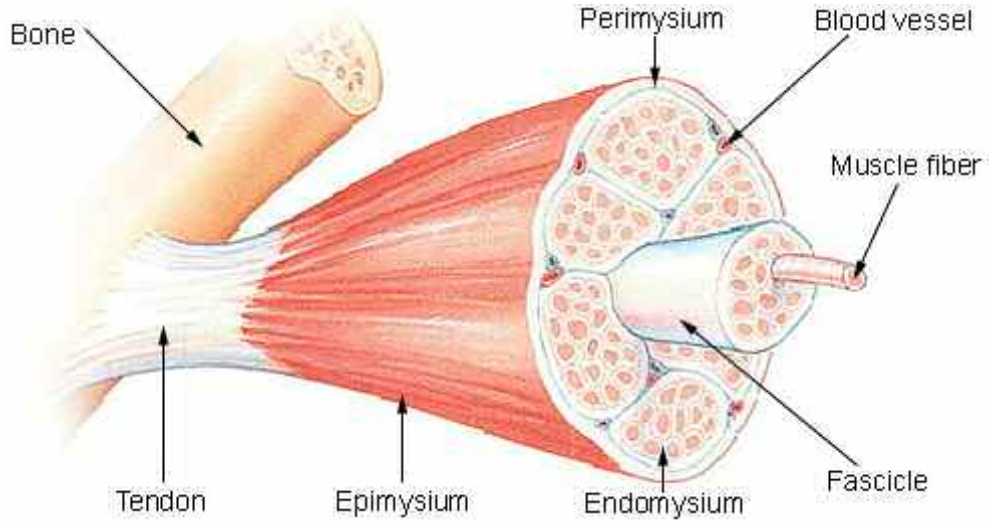

Figure 1. Representation of a muscle showing the relationship between muscle fibers and the connective tissues of the tendon, epimysium, perimysium and endomysium (http://training.seer.cancer.gov/module_anatomy/images/illu_muscle_structure).

Different fiber types can be distinguished in each skeletal muscle; the myosin heavy chain (MHC) isoform composition is commonly adopted as the criteria for fiber classification (Bottinelli R, and Reggiani C, 2000). The fiber type composition, varying from muscle to muscle, is the basis of the well-known structural and functional muscular diversity. The fibers can change their characteristics in response to a large variety of stimuli leading to muscular plasticity (Berchtold MW et al., 2000). Type I, slow-twitch or slow-oxidative fibers contain large amounts of myoglobin, many mitochondria and many blood capillaries. Type I fibers are red, split ATP at a slow rate, have a slow contraction velocity, are very resistant to fatigue and have a high capacity to generate ATP by oxidative metabolic processes. Such fibers are found in large numbers in the postural muscles of the neck. Type II fibers can be distinguished in IIA and IIX in humans; in rodents also fibers IIB exist (Spangenburg EE, and Booth FW, 2003). Type IIA, fast-twitch or fast oxidative fibers contain very large amounts of myoglobin, a lot of mitochondria and blood capillaries. These fibers are red, have a very high capacity for generating ATP by oxidative metabolic processes, split ATP at a very rapid rate, have a fast contraction velocity and are resistant to fatigue. Such fibers are infrequently found in humans. Type IIX and IIB, fast-twitch or fast-glycolytic fibers contain a low content of myoglobin, relatively few mitochondria, relatively few blood capillaries and large amounts of glycogen. These fibers are white, generate ATP by anaerobic metabolic processes, split ATP at a fast rate and have a fast contraction velocity. Such fibers are found in large numbers in the muscles of the arms.

Cardiac muscle is an involuntary striated muscle. It is quite similar in structure to skeletal muscle, and is found only in the heart. Cardiac muscle cells called

myocytes are not fused together to form continuous multinucleated myofibers. Instead, the adjacent myocites are connected to each other by intercalated discs, which have three main junctional complexes (Clark KA et al., 2002). The gap junctions enable the chemical connection between adjacent cardiomyocyte, whereas adherens-junctions and desmosomes connect the filamentous systems, such as actin, to the membrane.

In skeletal and cardiac muscle the sarcomeres of adjacent myofibrils are aligned, and this generates the striated appearance of these tissues in microscopic preparations.

Smooth muscle is an involuntary non-striated muscle. It is found within the walls of organs and structures such as the esophagus, stomach, intestines, bronchi, uterus, urethra, bladder, and blood vessels. The cytoskeleton of smooth muscle is not organized into myofibrils, although some similarities exist (Small JV, and Gimona M, 1998). Dense bodies, also called Z-bodies, are located in the cytosol (and contain α-actinin), whereas dense bands/dense plaques are electron-dense areas close to the cell membrane (that contain vinculin and talin). Both dense bodies and dense bands act as anchoring sites for the actin filaments of opposite polarities, and dense bodies together with the thin and thick filaments form the contractile unit of the smooth muscle (Bond M, and Somlyo AV, 1982).

I-2 Muscle contraction

Although the three types of muscle have significant differences all of them use the movement of actin against myosin to generate contraction.

Skeletal muscle contraction is under somatic nervous system control. In skeletal muscle, motor neurons branch within a muscle to form motor units, which supply a group of muscle fibers. Acetylcholine is released from the nerve terminal at the neuromuscular junction, where the neuronal end is attached to the muscle membrane. The binding of acetylcholine to its receptors on the sarcolemma causes the receptor channels to open, which enables Na^{2+} influx leading to the depolarization of sarcolemma (Lodish H et al., 1995). This depolarization extends to the myofibrils via the T-tubule system, which leads to Ca^{2+} release from the sarcoplasmic reticulum. The cytosolic Ca^{2+} concentration is increased about 100-fold. Ca^{2+} binds to troponin C on the troponin-tropomyosin complex located on thin filaments. In relaxed muscle, tropomyosin blocks the myosin binding site on actin. Ca^{2+} binding to troponin C causes a shift in the tropomyosin position and exposes the myosin binding site. Actin filament binding, in turn, activates the

myosin power cycle. The myosin head domain mediates the connection to the actin filaments and the power stroke, where the energy of ATP hydrolysis is converted to mechanical work. This results in a sliding movement of actin and myosin filaments at the sarcomeric level and in a muscle contraction at the organ level (Berchtold MW et al., 2000).

In contrast to skeletal muscle, cardiac muscle has an intrinsic ability to contract without stimulation from the central nervous system. However, the intrinsic contraction rate is regulated by the autonomous nervous system and hormones. The stimulation of cardiac contraction is mediated by modified cardiac cells known as pacemakers that initiate action potentials. In cardiac muscle the cells are not fused; however, intercalated discs permit spreading of the depolarization from one cell to another (Burkitt HG et al., 1993). The normal heartbeat begins with an action potential in the pacemaker cells located in the sinoatrial node that spreads rapidly through the electrically coupled cells of the atria. After a slight delay, the action potential stimulates the depolarization of the atrioventricular node and the impulses are transmitted to the ventricles via the bundle of His and Purkinje fibers. The contractile machinery and the sliding mechanism of thin and thick filaments are similar to that of skeletal muscle.

Smooth muscle contraction is under the control of the autonomous nervous system and hormones (Somlyo AP, and Somlyo AV, 1994). The Ca^{2+} flux from the sarcoplasmic reticulum is also the first initiator after a nerve signal in smooth muscle. The interaction of sliding actin and myosin filaments is similar in smooth muscle compared to cardiac and skeletal muscles, but there are differences in the proteins involved in contraction. Instead of a troponin-tropomyosin system, the contraction is regulated by a calmodulin-myosin light chain kinase/phosphatase system (Stephens NL, 2001). Ca^{2+} binds to calmodulin, which activates the myosin light chain kinase. The calcium-calmodulin-myosin light chain kinase complex phosphorylates serine-19 on the myosin regulatory light chain. This allows myosin ATPase activation by the thin filament leading to the contraction. Herrera and coworkers (Herrera AM et al., 2005) suggest that in contrast to striated muscle, the contraction machinery of smooth muscle is flexible. The changes in the number of contractile units and the changes in thick filament length account for the length changes of smooth muscle cells.

I-3 The sarcomere

All muscles use actin and myosin for contraction, but only in skeletal and cardiac muscle these proteins are organized into sarcomeres, which are the fundamental contractile unit of striated muscle. The mammalian sarcomere is approximately 2 μm in length, and can shorten to about 70% of its original length during contraction (Au Y, 2004). The individual units of the sarcomere include four major filamentous systems: the thin, thick, titin, and nebulin filaments. The striation appearance of the muscle fibers results from an alternating pattern of dark and light bands when they are viewed under a polarized light microscope. Figure 2 shows the sarcomere depicting its organization in bands and lines. The **A-band** (Anisotropic in polarized light, dark) resides in the centre of the sarcomere and it is composed mainly of thick filaments. The length of the A-band is equal to the length of a typical thick filament (about 1.5 μm). The A-band, which also includes portions of thin filaments, contains the following three subdivisions: the M-line, the H-zone, and the zone of overlap. The **M-line** (Mittel, meaning middle in German) is composed by proteins that connect the central portion of each thick filament to its neighbors. These dark-staining proteins help stabilize the position of the thick filaments. The **H-zone** (Heller, meaning bright in German) is a lighter region on either side of the M-line without any actin-myosin overlap. The H-zone contains thick filaments but no thin filaments. The **zone of overlap** is the region where thick and thin filaments interdigitate. Electron microscopy images of the A-band showed that each thin filament is surrounded by three thick filaments, and each thick filament is surrounded by six thin filaments; myosin heads extend to interact with actin forming cross-bridges. The region containing only thin filaments is termed **I-band** (Isotropic in polarized light, light) and it extends from the A-band of one sarcomere to the A-band of the next sarcomere. The **Z-disc** (Zwischen, meaning between in German) marks the boundary between adjacent sarcomeres. From the Z-discs at either end of the sarcomere, thin filaments extend toward the M-line and into the zone of overlap. The actin filaments are polar structures, and Z-disc proteins serve to provide a mechanical link between actin arrays of opposite polarity from adjacent sarcomeres (Huxley HE, 2008).

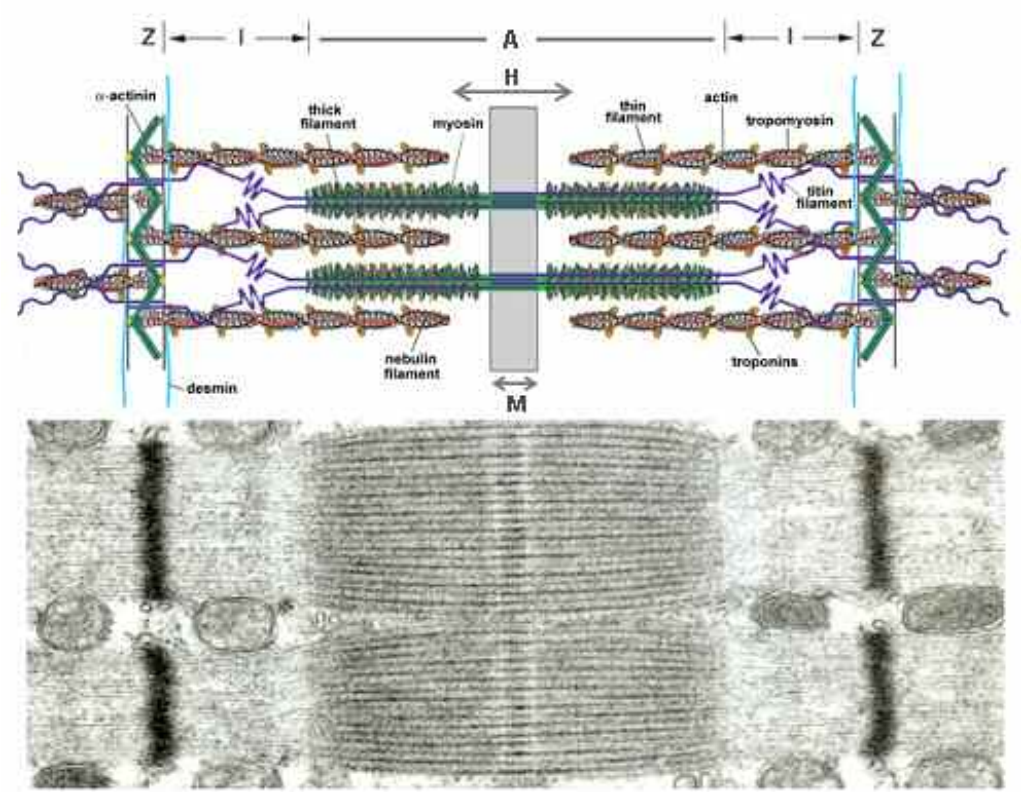

Figure 2. Simplified model of two muscle sarcomeres in parallel (top), and electronmiscroscopic photograph of the ultrastructural organization of sarcomeres in parallel (bottom) (Ottenheijm CA et al., 2008).

I-3.1 The actin cytoskeleton: actin and myosin

Actin is one of the most abundant and highly conserved proteins. Actin proteins mediate contractile function in muscle cells and determine the morphology and motility in non-muscle cells. In mammals, there are at least six different actin isoforms, each encoded by a separate gene (Yao X et al., 1995). The expression of each isoactin gene is regulated in a developmental and tissue-specific manner. Two main types of actin are distinguished on the basis of both protein sequence and tissue-specific expression: the muscle actins with four isoforms, two in striated muscles (α-skeletal and α-cardiac) and two in smooth muscles (α-vascular and γ-visceral), and the non-muscle or cytoplasmic actins present in every cell, with two isoforms, the β- and γ- isoforms. The identity of the actin isoforms at the protein sequence level is 93-99.5%, being higher between muscle actins than between cytoplasmic isoforms (Mounier N, and Sparrow JC, 1997). Globular actin monomers (G-actin) polymerize to form actin filaments (F-actin), which have the appearance of two twisted α-helices. Actin filaments are polarized, with a fast-growing barbed-end or plus (+) end and a slow-growing pointed-end or minus (-) end. In sarcomeres, the fast-growing barbed-ends of actin polymers

point toward the Z-discs. CapZ binds to these plus ends, inhibiting polymerization, whereas tropomodulin caps the minus end, preventing dissociation of actin monomers. Capping at both ends cause the actin filaments to be very stable (Lodish H et al., 1995). In muscle, actin filaments associate with the proteins tropomyosin and troponin, which are important in the regulation of muscle contraction.

Myosins form the second filamentous system of myofibrils. There are 15 classes in the myosin superfamily. As a general feature, myosins can bind actin and act as motor proteins. Filament forming muscle and non-muscle myosins constitute class II. Members of this class are hexameric enzymes composed of two myosin heavy chains (MHC), two essential myosin light chains (MLC), and two regulatory MLC (Reggiani C et al., 2000). There are a number of isoforms of both myosin heavy and light chains, which can combine with each other to produce various isomyosins. The expression of isomyosins is regulated to fulfill the different contraction requirements depending on muscle type. Head and tail regions constitute the myosin molecule. The head region contains the N-terminal parts of the heavy chains and the regulatory and essential light chains. The head region is the motor domain binding to actin, hydrolyzing ATP and generating movement. The myosin tail region contains a coiled-coil forming region, which enables the dimerization of two myosin heavy chains in a bipolar order. In striated muscle, these hexameres are bundled together by parallel interactions along the filaments to form thick myosin filaments (Sellers JR, 2000). The tails of bipolar myosins are anchored at the M-line, where myosin filaments are crosslinked by M-bridges. Myomesin and M-protein are potential candidates for crosslinking thick filaments at the M-line. In particular, myomesin can form anti-parallel dimers and it is thought that these dimers crosslink the contractile filaments in the M-band similar to α-actinin in the Z-disc (Lange S et al., 2005).

I-3.2 The giant proteins: titin and nebulin

In addition to thin and thick filaments, vertebrate striated muscle contains a third and a fourth filament system formed by the giant proteins titin and nebulin (Frank D et al., 2006).

Titin, also called connectin, is one of the largest proteins known in humans having a molecular weight of about 3700 kDa (Miller MK et al., 2004). Titin is a multifunctional protein spanning from the Z-disc to the M-line. The N-terminal ends overlap in the Z-disc, whereas the C-terminal ends overlap at the M-line; thus, two titin molecules create a continuous filament system through the entire

sarcomere. Titin can be separated into different regions based on the sarcomeric location and function: the Z-disc titin, the I-band titin, the A-band titin, and the M-line titin (Gregorio CC et al., 1999). The Z-disc titin contains several Ig-like repeats (Z1 and Z2) followed by a series of alternatively spliced z-repeats (zr1-zr7), which have been implicated in the regulation of the Z-disc thickness (Gautel M et al., 1996). The I-band region functions as a molecular spring, which is responsible for the elasticity of muscle (Granzier HL, and Labeit S, 2004). The A-band region may act as a template in thick filament assembly, whereas the M-line region contains a kinase domain, which links titin to signalling cascades. Based on its assembly properties, multiple protein interactions and modular structure, titin is believed to regulate the assembly of actin and myosin filaments, to maintain sarcomeric organization, as well as to function as a sarcomeric stretch sensor (Miller MK et al., 2004).

Nebulin is another sarcomeric giant protein (600-900 kDa). Alternatively splicing accounts for its size variation (Labeit S, and Kolmerer B, 1995). Nebulin is an inextensible protein anchored at the Z-disc by its C-terminal region and spans the length of the thin filament ending at the edge of the H-zone. As the size of nebulin correlates with the length of thin filaments, it has been suggested that nebulin may act as a ruler regulating the number of actin monomers that polymerize into each filament during the formation of mature muscle fibers (Kruger M et al., 1991). Nebulin may also regulate contraction by preventing actin-myosin interaction. It was thought that nebulin was not expressed in heart. Instead, a smaller nebulin-like protein called nebulette (107 kDa), that is highly homologous to the C-terminal of nebulin, has been found in cardiac muscle (Millevoi S et al., 1998). Although a mechanism of thin filament length regulation may also exist in cardiac muscle, nebulette could only participate in length regulation at the barbed-end because, in contrast to nebulin, nebulette is too short to span up to the pointed-end of the thin filament. Nevertheless, the C-terminal homology between nebulin and nebulette is thought to be necessary to conserve their binding to the Z-disc (Moncman CL, and Wang K, 1995).

I-4 The Z-disc

The Z-disc is an identifying feature of striated muscle that delineates the border of the individual sarcomeric unit. It crosslinks thin filaments of adjacent sarcomeres, thereby transmitting force generated by the acto-myosin interaction during muscular contraction. Z-discs of adjacent myofibrils are aligned, providing a

means to coordinate contractions between individual myofibrils to a focal point where the Z-disc is linked to the muscle membrane (Clark KA et al., 2002). Furthermore, the Z-disc occupies a unique position at the interface of the sarcomere, the cytoskeleton, the sarcoplasmic reticulum, and sarcolemma (Pyle WG, and Solaro RJ, 2004), suggesting that it has additional functions in the transmission and sensing of external and internal signals (Frey N, and Olson EN, 2002).

The Z-discs are composed of a large number of proteins and other molecules. The formation of mature Z-discs requires the addition and organization of Z-disc proteins to form a stable unit that can support contractile forces of the muscle. During myofibrillogenesis, Z-discs assemble by the lateral fusion of the Z-bodies of premyofibrils and nascent myofibrils (McKenna NM et al., 1986). In the transition from Z-bodies to Z-discs, the number of proteins in the Z-band increases, and this may lead to increased organization and stability needed for contraction (Sanger JW, and Sanger JM, 2001). The earliest Z-bodies in premyofibrils contain actin, α-actinin, filamin and nebulin (Moncman CL, and Wang K, 1995). Z-disc proteins that also interact with the sarcolemma, such as talin and vinculin become localized after the Z-bodies of nascent myofibrils have fused laterally to form Z-discs of the mature myofibrils (Sanger JW et al., 2000). Between the earliest Z-body stage and the mature Z-disc stage, titin becomes localized in Z-bodies. At this time muscle-specific myosin II filaments begin to align along the forming myofibrils in a process thought to be guided by titin (Wang K, and Wright J, 1988).

The Z-disc in every vertebrate striated muscle has a precisely defined width that is presumably related to the mechanical properties of the muscle. Z-discs width ranges from approximatively 30-50 nm in fast skeletal muscle fibers to 100-140 nm in cardiac muscle and slow skeletal muscle fibers (Luther PK et al., 2002). In longitudinal electron micrograph sections of Z-discs, a characteristic zig-zag pattern is observed. Narrow Z-discs in fast muscles show one or two zig-zag layers, while slow muscle Z-discs show three or four zig-zag layers. Each zig-zag layer corresponds to overlapping sets of Z-links. An important component of these Z-links is α-actinin, which crosslinks the actin filaments. The Z-discs width thus reflects the number of crosslinks mediated by α-actinin, which in turn depend on the interaction with the titin z-repeats (Young P et al., 1998).

I-5 Z-disc proteins

The Z-disc of striated muscle cells is a highly complex and specialized three-dimensional structure, consisting of dozens of different proteins assembled into a multiprotein complex. Although α-actinin has been viewed as the major Z-disc protein in all striated muscles, it accounts for less than 20% of the total protein content of Z-discs (Pyle WG, and Solaro RJ, 2004). In recent years, an increasing number of Z-disc proteins have been identified but the precise interactions, and mechanisms of assembly are still poorly understood. It is important to remark that most Z-disc proteins have two or more binding partners, which makes the Z-disc a very complex network of protein interactions (Figure 3).

The special role of Z-disc and of Z-disc protein interactions is indicated by the fact that mutations in several proteins that are either Z-disc components or bind to Z-disc proteins have been associated to the development of dilated cardiomyopathy and/or muscular dystrophy.

In the following, I will give you a general overview on some Z-disc proteins, focusing in particular on their molecular interaction partners and on the pathologies eventually associated to them. Most of Z-disc proteins have a structural role, since they are involved in the assembly of the Z-disc structure or in the maintenance of its integrity during muscle contraction. Nevertheless, some of them serve as docking sites for transcription factors, Ca^{2+} signalling proteins, and for kinases and phosphatases that affect function and gene expression. For this reason, the Z-disc has been compared to a way station for proteins that regulate transcription and move between the Z-disc and the nucleus (Pyle WG, and Solaro RJ, 2004). The idea that the Z-disc may be a coordinator of intracellular signalling is supported by the evidence that some muscle disorders seem to be associated with an altered recruitment of molecules participating in intracellular signalling more than with the alteration of each sarcomeric interaction (Arimura T et al., 2004).

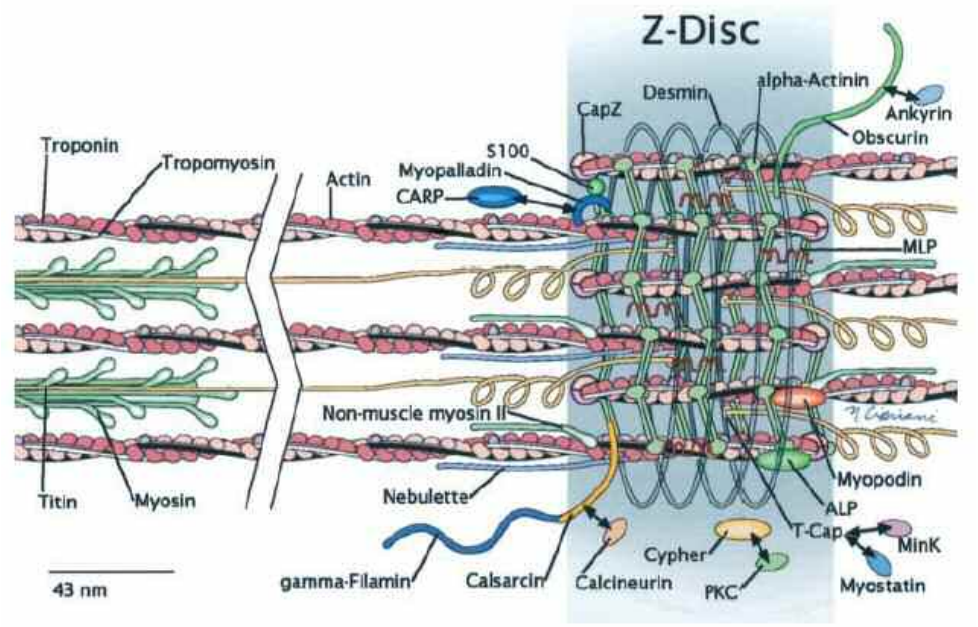

Figure 3. Cartoon of the network of proteins making up the Z-disc (Pyle WG, and Solaro RJ, 2004).

I-5.1 α-actinins

α-actinin is a member of a highly conserved family of actin binding proteins that also includes spectrins, dystrophin and utrophin. α-actinin is a functional anti-parallel dimer, with a polypeptide chain mass of 94-103 kDa. α-actinin is composed of a N-terminal actin-binding domain (ABD), connected via a flexible neck region to four spectrin-like repeats (SLRs) forming the central rod that is followed by a C-terminal calmodulin (CaM)-like domain. The ABD is composed of two calponin homology (CH) domains, CH1 and CH2. The CH1 is responsible for the binding to actin, whereas the CH2 increases the binding affinity (Gimona M et al., 2002). The SLRs are the most variable parts of the α-actinin molecule that mediate α-actinin dimerization and are also important interaction sites for multiple structural and signalling proteins (Djinovic-Carugo K et al., 2002). The C-terminal CaM-like domain consists of two pairs of EF-hands and displays functional divergence among α-actinin isoforms. In humans, there are four α-actinin genes encoding proteins with about 80% sequence identity (Beggs AH et al., 1992). α-actinin isoforms can be generally divided into two classes based on the differences in the C-terminal domain. Non-muscle cytoskeletal isoforms (α-actinin-1 and 4) contain two functional EF-hand motifs, which bind Ca^{2+} and thereby regulate the actin-binding activity. Muscle sarcomeric isoforms (α-actinin-2 and 3) contain non-functional EF-hand motifs, do not bind Ca^{2+} at physiological concentrations, and thereby bind to actin filaments in a Ca^{2+}-

insensitive manner (Tang J et al., 2001). Non-muscle α-actinin-1 and 4 are located in focal contacts, stress fibers, and cortical networks. In particular, α-actinin-1 is concentrated at the ends of stress fibers in focal contacts and adherens junctions, whereas α-actinin-4 localizes on stress fibers and can also translocate to the nucleus (Honda K et al., 1998). The isoform expressed in smooth muscle dense plaques and dense bodies is a product of alternative splicing of the α-actinin-1 gene (Waites GT et al., 1992). α-actinin-2 and 3 are restricted to striated muscle, where they are enriched especially at the Z-discs, but can also be found in the sarcolemma. α-actinin-2 is expressed in all skeletal muscle fibers, whereas expression of α-actinin-3 is limited to a subset of type II (fast) fibers. Furthermore, α-actinin-3 is absent in cardiac muscle and it is not found in approximatively 16% of the world population, suggesting that α-actinin isoforms can compensate for the loss of another family member (North KN et al., 1999).

In the past decade, several new Z-disc components have been discovered and many of them directly bind α-actinin. At the Z-disc, α-actinin-2 crosslinks only anti-parallel actin filaments, which come to the Z-disc from opposing sarcomeres. α-actinin-2 has two interactions sites with the titin Z-disc portion: the C-terminal domain interacts with z-repeats whereas the rod region binds to a different area of titin (Young P et al., 1998). Furthermore, titin interaction with the α-actinin-2 EF-region is controlled by phosphatydlinositol 4, 5 bisphosphate (PIP2), which binds to the CH2 domain of α-actinin-2 (Young P, and Gautel M, 2000). The binding of PIP2 may release the α-actinin-2 EF-region from an autoinhibitory state, enabling titin binding. α-actinin-2 also interacts with nebulin (Nave R et al., 1990). In addition to the filamentous and giant muscle proteins, α-actinin-2 interacts with a consistent number of smaller Z-disc components. α-actinin-2 binds to muscle LIM protein (MLP), which has a central role in the Z-disc stretch sensor machinery (Louis HA et al., 1997). Other two groups of α-actinin-2 interaction partners are the three members of the myotilin/palladin/myopalladin family (Otey CA et al., 2005), and the members of the filamin, actinin and telethonin-binding proteins of the Z-disc (FATZ family) (Faulkner G et al., 2000). Given its diverse protein-protein interactions, it appears obvious that α-actinin plays a key role in mediating and integrating molecular interconnections at the Z-disc. The multifunctionality of α-actinin is even more evident considering its interactions with costameric proteins such as β1-integrin, vinculin and dystrophin. These costameric connections show that α-actinin is also involved in connecting the contractile machinery to the sarcolemma. Furthermore, α-actinin interacts with several kinases, suggesting that the role of α-actinin in muscle ranges from a structural

crosslinker at the Z-disc to a docking site for various signalling cascades (Klaavuniemi T, 2006).
Thus, it is not surprising that mutations in the α-actinin genes can lead to human diseases. In particular, a mutation that resides close to the N-terminus disrupts the binding with MLP and it has been associated with dilated cardiomyopathy (DCM) (Mohapatra B et al., 2003). Furthermore, it has also been found that overexpression of a C-terminal deletion of α-actinin is linked to hypertrophied Z-discs (Schultheiss T et al., 1992).

I-5.2 MLP

Muscle LIM protein (MLP) is a member of cysteine-rich protein (CRP)-family, a group of evolutionarily conserved cytoskeletal proteins expressed in a variety of muscle tissues (Louis HA et al., 1997). MLP localizes at the periphery of the Z-disc (Arber S et al., 1997), and at the intercalated disc (Ehler E et al., 2001). The protein comprises two LIM domains, the first of which directly binds to α-actinin (Harper BD et al., 2000). It has been proposed that MLP may be a nuclear regulator of myogenic differentiation by enhancing the DNA-binding ability of MyoD (Kong Y et al., 1997), and it is also implicated in the communication with the nucleus especially in response to hypertrophic signals (Ecarnot-Laubriet A et al., 2000). However, several cytoplasmatic binding partners have been identified beyond α-actinin, including telethonin/T-Cap.
Mice that harbor a deficiency in the MLP protein develop DCM and a point mutation in the human gene has also been associated with this disease. This single nucleotide mutation results in a severe charge change within the N-terminal telethonin interacting domain of MLP, thus disrupting the binding between the two proteins and causing a miss-localization of telethonin and Z-disc disruption. It has been suggested that the complex between MLP and telethonin, which is a docking protein of titin, is part of the cardiac stretch sensing machinery (Knoll R et al., 2002). MLP also interacts with the calcineurin protein and it is essential for its anchorage to the Z-disc, thus providing a molecular basis for the link between MLP and the calcineurin–NFAT pathway (Heineke J et al., 2005).

I-5.3 Telethonin

Telethonin is a small sarcomeric protein with a molecular weight of 19 kDa identified as one of the most abundant transcripts expressed in striated muscle (Valle G et al., 1997). The protein is also known as T-Cap (Gregorio CC et al.,

1998). It colocalizes with actin in the Z-disc and it can also bind to FATZ (Faulkner G et al., 2000) and the N-terminal Z1-Z2 domains of titin. This interaction is critical for sarcomeric structure since overexpression of either telethonin or the Z1–Z2 region of titin in cardiac myocytes disrupts Z-disc structure and sarcomere organization. This observation suggests that telethonin plays a key role in positioning and anchoring the N-terminal of titin at the Z-disc (Gregorio CC et al., 1998). Moreover, telethonin may be phosphorylated by the titin kinase region activated by calcium/calmodulin binding during myocyte differentiation. The titin kinase domain is located at the edge of the M-band, whereas telethonin is in the Z-disc. For this reason, it has been proposed that during myofibrillogenesis the cytoskeleton undergoes reorganization and the titin C-terminal could be transiently in close proximity to telethonin thus allowing phosphorylation (Mayans O et al., 1998).

Telethonin was the first sarcomeric protein associated with an autosomal recessive Limb-Girdle Muscular Dystrophy (AR LGMD) (Moreira ES et al., 2000). LGMDs are a genetically heterogeneous group of disorders that affect mainly the proximal musculature. Two different mutations in the telethonin gene were identified, giving rise to premature stop codons and resulting in truncated telethonin. Interestingly, the C-terminal truncation eliminates the domain of telethonin that is phosphorylated by titin kinase. Mutations in telethonin have also been found in patients with hypertrophic cardiomyopathy (HCM) and DCM (Hayashi T et al., 2004). In particular, mutations causing the HCM phenotype are associated with a stronger interaction with titin, MLP and FATZ-2. It has been hypothesized that stronger binding could increase passive tension and thereby increase calcium sensitivity of muscle contraction (Cazorla O et al., 2001), a phenomenon observed in other HCM-causing sarcomeric protein mutations before. On the contrary, in a DCM-associated mutation, these interactions were impaired.

Telethonin also binds to ANKRD2 (Kojic S et al., 2004), a protein upregulated in skeletal muscle hypertrophy and a member of the MARP family. The members of this family interact with the I-band region of titin forming a complex with myopalladin and calpain protease p94 (Miller MK et al., 2003). It has been proposed that MARPs are able to sense muscle stress/stretch, and in response to this trigger transmit signals to the nucleus that result in the regulation of gene expression (Kojic S et al., 2004).

In cardiac muscle telethonin can bind to minK, the β-subunit of a component of the delayed rectifier potassium current I_{Ks} channel. It has been proposed that telethonin may act as link between myofibrillar components of the sarcomere with

the β-subunit of the I_{Ks} channel found in the T-tubular membrane, thus suggesting the possibility of a stretch-dependent regulation of potassium flux in cardiac muscle (Furukawa T et al., 2001).

I-5.4 Filamins

Filamins belong to a family of dimeric proteins that crosslink actin filaments. There are three isoforms: α-, β- and γ-filamins. All of these isoforms have a N-terminal actin-binding domain followed by 24 Ig-like repeats and a C-terminal domain necessary for the dimerization. γ-filamin is the striated muscle-specific isoform and a unique insertion in its twentieth Ig repeat has been shown to be responsible for targeting the protein to Z-disc of striated muscle (van der Ven PF et al., 2000). Several binding partners of γ-filamin have been identified, including γ- and δ -sarcoglycan (Thompson TG et al., 2000), myotilin (van der Ven PF et al., 2000), the FATZ family of proteins (Faulkner G et al., 2000; Takada F et al., 2001), and the β1-integrin subunit (Loo DT et al., 1998). It has been shown that the binding to sarcoglycans is affected by calpain 3, a muscle-specific calcium-dependent protease, which is able to cleave the C-terminal region of γ-filamin (Guyon JR et al., 2003). Based on these protein interactions, it was suggested that γ-filamin may be a link between the sarcolemma and the sarcomeric cytoskeleton. Moreover, several γ-filamin binding partners are mutated or implicated in different forms of LGMD, indicating that they act together to stabilize the muscle cytoskeleton (Nigro V et al., 1996). Recently, it has been shown that a mutation in the dimerization domain of γ-filamin can cause myofibrillar myopathy (MFM) (Vorgerd M et al., 2005).

I-5.5 The myotilin, palladin and myopalladin family

Myotilin, palladin and myopalladin form a novel subfamily of Ig-like domain-containing cytoskeletal proteins that seem to be important for the regulation and assembly of actin-based arrays in different muscle and non-muscle cells in all classes of vertebrates (Otey CA et al., 2005).

I-5.5.1 Myotilin

Myotilin was the first member of this family to be identified. The protein, with a molecular weight of 57 kDa, has been named myotilin (myofibrillar protein with titin-like Ig domains) as it has similarities with the Ig domains of titin. Structurally, the protein consists in a N-terminal region rich in serine residues, a 23 aa hydrophobic region, and a C-terminal region with two Ig-like domains highly homologous to the Ig domains of palladin, myopalladin, and Z-disc Ig domains 7 and 8 of titin (Salmikangas P et al., 1999). The myotilin gene locates in chromosome 5q31 inside a region, which contains the LGMD1A disease gene (Bartoloni L et al., 1998). Subsequent analysis demonstrated that mutations in myotilin were associated with LGMD1A (Hauser MA et al., 2000) and also a subgroup of MFM (Selcen D, and Engel AG, 2004). Muscle diseases caused by mutations in the myotilin gene are now referred to as myotilinopathies (Olivé M et al., 2005), and the main morphological features consist of myofibrillar lesions, particularly Z-disc abnormalities. These changes include Z-disc streaming and accumulation of fibrillar material originating from the thin filaments. All known myotilinopathies are caused by missense mutations in the N-terminus of myotilin, and several of the mutated residues are putative phosphorylation sites (Moza M et al., 2007). Myotilin expression pattern both in human and mouse is strictly controlled, with highest expression in skeletal muscle, moderate expression in heart and peripheral nerves, and little or no expression in other tissues. Myotilin binds to F-actin and efficiently crosslinks actin filaments into tightly packed bundles; furthermore, myotilin stabilizes the assembled actin bundles, probably by decreasing the rate of actin monomers depolymerization from filament ends. It is thought that the capacity to crosslink actin filaments relies on the ability of myotilin to form dimers via its two Ig-like domains. Myotilin expression starts late during myofibrillogenesis, when preassembled myofibrils begin to align. This view is supported by experiments in which premature myotilin expression in differentiating myoblasts prevents normal sarcomere assembly, as typical alignment of contractile proteins is not observed upon differentiation (Salmikangas P et al., 2003). All these findings suggest that myotilin might have an important role in the assembly and maintenance of Z-disc integrity (von Nandelstadh P et al., 2005). Others binding partners have been described for myotilin, and all of them are Z-disc components. Myotilin binds via its first 214 residues to the spectrin repeats 3-4 of α-actinin, whereas the myotilin C-terminal region containing the Ig-like domains binds to the Ig-like domains 19-21 of γ-filamin (van der Ven PF et al., 2000). Not only γ-filamin, but also α-filamin, β-

filamin and β_{var-1} filamin variant are able to bind to myotilin (Gontier Y et al., 2005). Myotilin has also been shown to bind to the FATZ family members FATZ-1 and FATZ-2 (Gontier Y et al., 2005); in particular, the entire molecule of myotilin seems to contribute to the interaction with FATZ-1, as both N- or C-terminal truncations abrogate binding. The association with FATZ proteins links myotilin to the calcineurin signalling pathway, while an interaction with the ubiquitin ligases MURF-1 (muscle specific ring-finger protein 1) and MURF-2 could involve myotilin in the titin-based signalling events (Witt SH et al., 2005).

I-5.5.2 Palladin

Palladin was simultaneously discovered by two different groups: the murine palladin was discovered by Parast MM and colleagues (Parast MM, and Otey CA, 2000), whereas the human ortholog was identified by Mykkänen OM and colleagues (Mykkänen OM et al., 2001). The protein was named palladin in honor of the Renaissance architect Palladio, to reflect the association of the protein with architectural elements of the cell (Parast MM, and Otey CA, 2000). Palladin is the most widely expressed member of the family, being present in a variety of tissues. In muscles, palladin is highly expressed in smooth and poorly in skeletal, whereas in non-muscle tissues a higher expression of palladin is found in prostate, testis, ovary, small intestine and colon (Mykkänen OM et al., 2001). Palladin expression is greatly reduced in a number of adult tissues including heart, skeletal muscle, liver and kidney. One explanation could be that palladin is involved in establishing the cytoskeletal organization of cells during differentiation, and then replaced by other proteins in fully differentiated cells (Parast MM, and Otey CA, 2000). Both mouse and human palladin may be expressed as several isoforms, possibly dependent on the cell type. The most abundant form in both species, which is also the most widely expressed, is the 90-92 kDa isoform. The 140 kDa isoform is less abundant and is predominantly found in embryonic mice, while in adult mice it is mostly detected in smooth muscles (Mykkänen OM et al., 2001). A 200 kDa isoform was first found in the developing heart, and subsequently in embrionic and neonatal bone as well (Otey CA et al., 2005).

Palladin (the most common isoform) contains three Ig domains: the most N-terminal one has the highest homology to the N-terminal Ig domains of titin, whereas palladin's middle and C-terminal Ig domains are most homologous to myotilin Ig domains and titin C-terminal Ig domains (Parast MM, and Otey CA, 2000). Palladin and myotilin share high homology in their N-terminal regions and in the C-terminal Ig-domains but, unlike myotilin, palladin contains a poly-proline

region in the N-terminal half of the molecule. Proline-rich sequences have been shown to play an important role in the reorganization of the actin cytoskeleton. The structural difference with the other two family members may be related to the fact that the organization of actin in the sarcomere is strictly regulated, whereas in cells that express palladin, dynamic modulation of actin filaments by polymerization/depolymerization is a continuous process (Mykkänen OM et al., 2001). Palladin colocalizes with α-actinin in focal adhesions, cell-cell junctions, and stress fiber striations. A short sequence of palladin upstream of the first Ig domain was found to bind to the C-terminal EF-hands 3–4 of α-actinin (Rönty M et al., 2004). The palladin-α-actinin interaction could serve to target palladin to sites of actin remodelling, since α-actinin seems to function as an actin-bundling protein and also as a scaffold to recruit complexes of signalling molecules to the cytoskeleton (Otey CA et al., 2005). Moreover, palladin C-terminal Ig domains are responsible for the interaction with ezrin, a member of the ezrin-radixin-moesin (ERM) protein family of membrane-cytoskeleton linker proteins (Mykkänen OM et al., 2001). Instead, the poly-proline stretch in the N-terminal region of palladin is responsible for the binding to members of the vasodilator-stimulated phosphoproteins (VASPs) (Boukhelifa M et al., 2004). It could be possible that the ezrin-palladin complex recruit VASPs as part of a mechanism that regulates actin polymerization at precise regions within the stress fibers. Recently, a mutation in the human palladin gene was implicated in a penetrant form of inherited pancreatic cancer (Pogue-Geile KL et al., 2006). It has been suggested that the mutated palladin may cause cytoskeletal changes in the pancreatic cancer cells, responsible for strong invasive and migratory abilities of these cancers.

I-5.5.3 Myopalladin

Myopalladin is a 145 kDa protein originally identified in a yeast two-hybrid assay when searching for potential Z-disc binding partners of nebulin and nebulette (Bang ML et al., 2001). A proline-rich stretch near the center of myopalladin is sufficient for the binding to the Src homology (SH_3) C-terminal domains of nebuline/nebulette. The protein, which structurally contains two N-terminal and three C-terminal Ig-domains, was termed myopalladin based on its homology to palladin (Parast MM, and Otey CA, 2000). Like myotilin, also myopalladin expression is strictly limited to skeletal and cardiac muscle, where it localizes to the Z-disc and to narrow portions of the I-band on either side of the Z-disc. A common feature among the three family members is the ability to bind α-actinin.

However, myopalladin binding to α-actinin requires all three C-terminal Ig domains, whereas myotilin and palladin both bind to the α-actinin via homologous sequences upstream of their Ig domains (Otey CA et al., 2005). It has been suggested that the interaction of myopalladin with α-actinin and nebuline/nebulette could serve for the integrity of the sarcomere since overexpression of the N-terminal region of myopalladin leads to Z-disc disruption and sarcomere disassembly (Bang ML et al., 2001). An interesting feature of myopalladin is its ability to bind to members of the MARP family. In particular, it has been shown an interaction with cardiac ankyrin repeat protein (CARP) by means of the N-terminal region of myopalladin (Bang ML et al., 2001). CARP is involved in the regulation of muscle gene expression during both heart development and in response to various cellular stresses. The interaction between myopalladin and CARP could therefore provide a link from the Z-disc to transcriptional regulation of cardiac genes. Recently, mutations in the myopalladin gene have been associated with idiopathic DCM (Duboscq-Bidot L et al., 2008).

I-5.6 The FATZ family

FATZ is an acronym for γ-filamin-, α-actinin-, and telethonin-binding protein of the Z-disc (Faulkner G et al., 2000), indicating its repertoire of binding partners. FATZ was originally identified as part of systematic sequencing project for human skeletal muscle ESTs at *Centro di Ricerca Interdipartimentale per le Biotecnologie Innovative* (CRIBI) of Padova (Lanfranchi G et al., 1996). Two other laboratories independently identified FATZ by yeast two-hybrid assay: one discovered calsarcin as a calcineurin-binding protein (Frey N et al., 2000), the other identified myozenin as a α-actinin- and γ-filamin-binding Z-disc protein (Takada F et al., 2001). The protein can be divided into three domains: the N- and C- terminal regions are α-helical domains separated by a glycine-rich central domain (Faulkner G et al., 2000; Takada F et al., 2001). These domains led to the identification of two other family members that also display a high degree of sequence similarity within these defined regions (Frey N et al., 2000; Frey N, and Olson EN, 2002), suggesting a conservation of functional properties and protein-binding domains. The FATZ proteins represent a family of sarcomeric proteins localized in the striated muscle Z-disc, comprising the three members FATZ-1, FATZ-2 and FATZ-3. The colocalization and direct interaction with several key Z-disc proteins such as α-actinin, telethonin and γ-filamin suggests that FATZs serve as a crosslinker for these proteins, probably contributing to the formation

and maintenance of the Z-disc. Furthermore, the binding with the phosphatase calcineurin, an important transducer of calcium-dependent signals in a variety of cell types, links FATZs to cell signalling (Frey N, and Olson EN, 2002).

I-5.6.1 FATZ-1 (calsarcin-2, myozenin-1)

The FATZ-1 human gene has been mapped to chromosome 10q22.1 (Faulkner G et al., 2000); it contains six exons that encode for a 32 kDa protein. The identity of human and mouse FATZ-1 is 89.5% at the nucleotide level and 90% at the amino acid level. The proteins share the same pattern of distribution, being higher in skeletal muscle tissues and lower in heart, testis and prostate. In skeletal muscle, FATZ-1 is predominantly expressed in fast-twitch fibers. Furthermore, FATZ-1 can be detected both in human and mouse undifferentiated muscle cells but its expression increases with time of differentiation (Faulkner G et al., 2000). Secondary-structure predictions suggest the presence of two α-helical domains consisting of amino acids residues 1-72 and 187-244, and indicated as CD1 and CD2 respectively. The flexible central part of the protein is less conserved; it is particularly rich in glycine and it has been named glycine-rich domain (GRD). The protein then ends with a C-terminal tail of approximatively 55 aa (Faulkner G et al., 2000; Takada F et al., 2001). As mentioned above (par. I-5.6), FATZ-1 binds to several sarcomeric proteins and some of these binding sites have been mapped. FATZ-1 interacts with both α-actinin and γ-filamin by means of its C-terminal domain. The FATZ-1 binding site on α-actinin-2 resides in the region that spans the SLRs 3 and 4, whereas sequences in repeat 23 near the C-terminal region of γ-filamin are essential for FATZ-1 binding to that protein. Interestingly, γ-filamin repeat 24 contains sequences responsible for the dimerization as well as the central repeats of α-actinin are the site of dimerization for this protein. Thus, it has been hypothesized that FATZ-1 could modulate both γ-filamin and α-actinin dimerization, probably regulating the spacing between monomers and hence the spacing of thin filaments (Takada F et al., 2001). Nevertheless, α-actinin and γ-filamin binding to FATZ-1 appeared to be competitive, because both proteins interact with the C-terminal region of FATZ-1. This observation suggested that FATZ-1 could be multifunctional, having similar roles in binding either α-actinin or γ-filamin, but not simultaneously. FATZ-1 is able to bind not only to γ-filamin, but also to the C-terminal region of α-filamin, β-filamin and $\beta_{var\text{-}1}$ filamin variant (Gontier Y et al., 2005). The interaction between FATZ-1 and telethonin (Faulkner G et al., 2000) also occurs but the precise binding site has not been mapped on both proteins. In addition, FATZ-1 revealed interactions with Z-band

alternatively spliced PDZ-motif (ZASP) protein (Frey N, and Olson EN, 2002) and myotilin (Gontier Y et al., 2005); the CD2 domain of FATZ-1 is sufficient for its binding to myotilin, whereas the entire molecule of myotilin appears to contribute to the interaction with FATZ-1. Immunofluorescence experiments demonstrated that in double-transfected chinese hamster ovary (CHO) cells, in which FATZ-1 and myotilin were coexpressed, the two proteins colocalize and the periodical distribution pattern of FATZ-1 is lost. This indicates that myotilin can have a direct or indirect effect in reorganizing the subcellular distribution of FATZ-1 (Gontier Y et al., 2005). Interestingly, FATZ-1 has been shown to interact with the phosphatase calcineurin at the Z-disc (Frey N et al., 2000). It is thought that FATZ-1 may serve to localize calcineurin in proximity of an intracellular calcium pool where it can interact with specific upstream activators or downstream substrates.

Recently, two synonymous single nucleotide substitutions have been found in the FATZ-1 gene of DCM patients (Arola AM et al., 2007). The potential role of these mutations is still unclear but it seems that they do not play a significant role in the genetic etiology of idiopathic DCM. Nevertheless, since FATZ-1 is part of an intricate network of interactions with several Z-disc proteins, its secondary role in the pathogenesis of DCM can not be excluded.

I-5.6.2 FATZ-2 (calsarcin-1, myozenin-2)

The FATZ-2 human gene has been mapped to chromosome 4q26-q27, and it encodes for a protein of 30 kDa. Sequence comparison revealed 88% identity between the mouse and the human proteins (Frey N et al., 2000). FATZ-2 is expressed in all striated muscle tissues throughout development, and becomes restricted to cardiac muscle and slow-twitch skeletal muscle fibers in adult. FATZ-2 is able to bind to α-actinin-2 and α-actinin-3 as well as to calcineurin. Coimmunoprecipitation experiments demonstrated that calcineurin could only be precipitated by α-actinin in the presence of FATZ-2, indicating a trimeric complex. The C-terminal region (aa 217-240) of FATZ-2 is responsible for calcineurin binding, whereas residues 153-200 appear to be necessary for the interaction with α-actinin SLRs 2 and 3 (Frey N et al., 2000). Like FATZ-1, FATZ-2 is localized to the Z-disc and has the ability to bind several other Z-disc proteins, including γ-filamin, telethonin, myotilin and ZASP, suggesting overlapping functional properties for the two proteins (Gontier Y et al., 2005). FATZ-2 is not required for pre- or post-natal development, since mice lacking FATZ-2 did not show any abnormalities and had a normal life-span. FATZ-1 and

FATZ-3 expression was not upregulated in the heart of FATZ-2-null mice, therefore they do not compensate for the lack of FATZ-2 (Frey N et al., 2004). However, in these mice the expression of calcineurin was notably increased, supporting the idea that FATZ-2 negatively modulates calcineurin activity. The upregulation of calcineurin induces a fetal gene program, which typically is associated with cardiac hypertrophy. Despite the lack of hypertrophy in the heart of FATZ-2-null mice, there was a marked induction of the hypertrophic program genes, the atrial natriuetic factor (ANF) and the brain natriuretic peptide (BNP), suggesting that they are regulated by calcineurin (Frey N et al., 2004). Also the fiber type composition was evaluated in mice lacking FATZ-2, since it is known that calcineurin has a role in directing the slow fiber phenotype (Berchtold MW et al., 2000). Indeed, the number of slow fibers was increased in soleus (a slow) muscle of these mice, and the slow fibers size was significantly decreased. This possibly reflects a mechanism of maintaining overall muscle size, because calcineurin it is not involved in the control of skeletal muscle fiber size (Naya FJ et al., 2000). To define the functions of FATZ-2 *in vivo*, transgenic mice expressing a constitutively active form of calcineurin were crossed with FATZ-2-null mice. The hearts of these mice showed a high level of cardiac hypertrophy with an almost four-fold increase in cardiac mass compared to normal mice. In addition, calcineurin transgenic mice lacking FATZ-2 had a reduced lifespan with death by the age of 20-28 days. Furthermore, FATZ-2 deficient mice were sensitized to pathological biomechanical stress, again resulting in exaggerated hypertrophy (Frey N et al., 2004). In conclusion, it has been proposed that FATZ-2 shows an important role in modulating calcineurin-dependent signalling as well as in the transduction of biomechanical stress (Frank D et al., 2006).

Recently, two mutations in the FATZ-2 gene have been identified in patients with HCM (Osio A et al., 2007). The authors speculate that FATZ-2 mutations cause HCM by activating the calcineurin pathway. Nevertheless, these mutations are not localized within the known binding sites for calcineurin or α-actinin; therefore, it has been hypothesized that structural changes in the FATZ-2 protein could affect the interactions. However, alternative possibilities have been proposed, including FATZ-2 interactions with proteins other than calcineurin to cause HCM. Very recently, more than 400 patients with familial HCM were screened; however, a disease-associated mutation in FATZ-2 gene was not identified. Thus, combining these results with previous reports, it can be concluded that FATZ-2 mutations are rare causes of familial HCM (Posch MG et al., 2008).

I-5.6.3 FATZ-3 (calsarcin-3, myozenin-3)

The FATZ-3 human gene has been mapped to chromosome 5q31, it contains seven exons that encode for a 27 kDa protein. Sequence comparison revealed 75% identity between human and mouse FATZ-3 at the amino acid level. Alignment of human FATZ-3 with FATZ-1 and FATZ-2 displays the highest homology to the N- and C-termini of the other two family members, whereas the central portion is less conserved (Frey N, and Olson EN, 2002). FATZ-3 is exclusively expressed in skeletal muscle, being enriched in fast-twitch fibers; no expression is detected in the adult heart. Similarly to FATZ-1 and FATZ-2, FATZ-3 is able to mediate protein-protein interactions with α-actinin-2, γ-filamin, telethonin and calcineurin. The N-terminal portion of FATZ-3, comprising aa 50-110, allows binding to γ-filamin, telethonin and calcineurin. In the case of α-actinin, two independent domains of FATZ-3 are sufficient to bind that protein: aa 186-207 are necessary for the C-terminal interaction, whereas aa 50-67 at N-termini also mediate association with α-actinin. In addition, FATZ-3 has been shown to bind to ZASP like FATZ-1 and FATZ-2. These interactions occurred with both the short ZASP isoforms (having only the N-terminal PDZ domain) and the long ones (with the C-terminal LIM domains), suggesting that the binding involves the N-terminal region of ZASP (Frey N, and Olson EN, 2002). Given the overlap of several protein interaction domains in FATZ-3, it could be possible that some of these interactions are mutually exclusive rather than simultaneous.
A form of myopathy, the vocal cord and pharyngeal weakness with autosomal dominant distal myopathy (VCPDM), has been mapped to chromosome 5q31, where the human FATZ-3 gene is predicted to be located (Feit H et al., 1998).

I-5.7 The enigma family

The enigma family is a newly emerging group of cytoskeletal PDZ and LIM domain (PDLIM) proteins. Indeed, they are characterized by a N-terminal PDZ domain (acronym derived from the first three described PDZ-domain containing proteins: PSD-95, Dlg and ZO-1), and one or three C-terminal LIM domains (acronym derived from the first three described LIM-domain containing proteins: Lin-11, Isl-1 and Mec-3). To date, the family contains seven members, grouped in two subclasses depending on the number of LIM domains. The enigma subfamily defines the class with three LIM domains, and it is formed by enigma (Wu RY, and Gill GN, 1994), enigma homology protein (ENH) (Kuroda S et al., 1996) and ZASP/cypher/oracle (Faulkner G et al., 1999; Zhou Q et al., 1999; Passier R et al.,

2000). The ALP subfamily contains proteins with a single LIM domain, and consists of actinin-associated LIM protein (ALP) (Xia H et al., 1997), C-terminal LIM domain protein with a molecular weight of 36 kDa (CLP-36) (Wang H et al, 1995), reversion-induced LIM protein (RIL) (Kiess M et al., 1995) and mystique (Torrado M et al., 2004).

Of the seven PDZ-LIM family members, ALP, ZASP and CLP-36 contain a conserved region, named ZASP-like motif (ZM), in the internal region between the PDZ and LIM domain (Schultz J et al., 1998). The motif is composed of 26-27 residues. Neither the structural or functional characteristics of the internal region are known. On the contrary, the PDZ and LIM domains are conserved folds found in numerous other proteins mediating various functions. It has been suggested that PDZ-LIM proteins act as adapters recruiting signalling molecules to the actin cytoskeleton. This is based on the ability of some of them to associate with cytoskeletal structures via the PDZ domain, and also on the binding capacity of several PDZ-LIM proteins with kinases by means of the LIM domains (Vallenius T et al., 2004). The sequence identity within the family in the conserved domains is high, being higher within subfamilies. For instance, the human PDZ domains of ALP and CLP-36 have a 62% identity, whereas the PDZ domain identity between human ALP and ZASP PDZ is 54%. The identity in the LIM domains is also high, being 66% between ALP and CLP-36 (Klaavuniemi T, 2006). In contrast, the identity in the internal region decreases to 30%.

I-5.7.1 The enigma subfamily: enigma

Enigma is also known as LIM mineralization protein (LIM-1) (Liu Y et al., 2002), and PDZ and LIM domain 7 (PDLIM7). Enigma is expressed in brain and skeletal muscle, where it localizes mostly at the Z-disc, and also at the boundary between the I-band and Z-disc (Guy PM et al., 1999). In cultured cells, enigma is detected in the cytoplasm and membrane ruffles rich in actin filaments (Barrès R et al., 2005). The three enigma LIM domains were found to interact with protein kinase C (PKC) α, βI and ζ (Kuroda S et al., 1996). PKC are a group of serine/threonine kinase, which has been shown to play a critical role in the development of cardiac hypertrophy and ischemic preconditioning both *in vitro* and *in vivo* (Dempsey EC et al., 2000). In addition, it has been shown that enigma interacts with several receptors. The LIM domains 2 and 3 of the protein recognize the insulin receptor, the tyrosine kinases Ret, and also Ret oncoproteins carrying mutations associated with multiple endocrine neoplasia (MEN) cancer syndromes (Wu R et al., 1996; Borrello MG et al., 2002). These findings suggest that enigma may function as a

link between the Z-disc and signal transduction. Enigma was observed to associate via its PDZ domain to the actin filaments in non-muscle cells (Durick K et al., 1998), whereas in skeletal muscle this association occurs through binding of enigma PDZ domain to the C-terminal region of skeletal β-tropomyosin (Guy PM et al., 1999). It is possible that this PDZ domain interaction may anchor enigma to the boundary of the Z-disc and I-band, where skeletal β-tropomyosin is distributed, thus recruiting kinases to the cytoskeleton via enigma LIM domains. Another explanation is that enigma-skeletal β-tropomyosin interaction may have a role in the the cytoskeleton assembly in muscle. In particular, tropomyosin isoforms bind the actin filaments and are assembled into dimers as result of an interaction between the N- and C-termini. Codistribution of enigma and skeletal β-tropomyosin along the margin of the Z-disc and I-band indicates that enigma binds to skeletal β-tropomyosin at the barbed-end of actin filaments, thus preventing β-tropomyosin actin binding and dimerization at the Z-disc (Guy PM et al., 1999).

I-5.7.2 The enigma subfamily: ENH

ENH, also known as PDLIM5, was originally identified in a yeast two-hybrid assay of rat brain cDNAs using PKC βI as bait (Kuroda S et al., 1996). The name enigma homology protein (ENH) comes from the similarity to enigma, since approximately 37% of the amino acids residues are identical between the two proteins. The PDZ domains of enigma and ENH have 69% identity, whereas their three LIM domains are 51, 59, and 70% identical (Guy PM et al., 1999). ENH could be a scaffold protein involved in recruiting PKC to its substrates; in the brain tissue, a specific interaction between ENH and both PKC ε and N-type Ca^{2+} channels has been described, leading to the formation of a macromolecular complex (Maeno-Hikichi Y et al., 2003). ENH has been found to be expressed also in skeletal and cardiac muscle, where it interacts via its PDZ domain with actin and α-actinin, thus localizing at the Z-disc (Nakagawa N et al., 2000). Two additional isoforms have been described, called ENH2 and ENH3, which lack the three LIM domains. Another ENH isoform, ENH4, was discovered later (Niederländer N et al., 2004). Unlike ENH1, and as ENH2 and ENH3, this new isoform is a PDZ only protein. The distribution pattern of the different isoforms is specific: ENH1 is expressed in cardiac muscle, ENH2 and ENH4 in skeletal muscle, whereas ENH3 both in skeletal and cardiac muscle (Niederländer N et al., 2004). This muscle-specific expression profile detected for the ENH family members suggests that besides a possible redundant role in striated muscles, the

four ENH isoforms might play a more specific role in the organization and function of each type of striated muscle.

I-5.7.3 The enigma subfamily: ZASP/cypher/oracle

Z-band alternatively spliced PDZ-motif (ZASP) protein is certainly the best characterized PDZ-LIM protein in striated muscle. It was independently discovered by three different groups. Cypher was first identified and cloned from the mouse as a novel PDZ-LIM protein localized in the Z-disc (Zhou Q et al., 1999). The human orthologue of cypher was at the same time identified and named ZASP (Faulkner G et al., 1999); in addition, cypher was independently cloned from the mouse as oracle (Passier R et al., 2000). ZASP is also known as PDLIM6. Several splicing variants exist in various species, and they are predominantly expressed in skeletal and cardiac muscle. Mouse cypher gene contains 17 exons, which give rise to six splice variants that can be classified into cardiac and skeletal muscle forms (Huang C et al., 2003). Cypher isoforms containing exon 4 are expressed in cardiac muscle (cypher c), whereas the isoforms containing exon 6 are skeletal muscle-specific (cypher s). Notably, exons 4 and 6 encode for the internal motif ZM (Klaavuniemi T et al., 2004). Within each muscle subtype, cypher isoforms can be further subclassified as short (cypher 2c, cypher 2s) or long (cypher 1c, cypher 3c, cypher 1s, cypher 3s), based on the deletion or inclusion of exons encoding the C-terminal LIM domains, respectively. Both cypher 2 short isoforms end with exon 10, whereas exon 11 is differentially spliced to generate cypher 1 (included) or cypher 3 (excluded) variants. Thus, the N-terminal PDZ domain is present in both short and long isoforms and is encoded by exons 1 through 3, whereas only long isoforms contain the three LIM domains, which are encoded by exons 12 to 16 (Vatta M et al., 2003). The human ZASP gene has been mapped to chromosome 10q22.3-23.2 and contains 16 exons (mouse exon 7 is absent). Similarly to mouse, six splicing variants have been reported: ZASP-1, -2, -3, -4, -5, and -6, which are analogous to mouse cypher 2s, 1s, 3s, 2c, 1c, and 3c. In human but not in mouse, it has been demonstrated that skeletal isoforms of ZASP are also expressed in cardiac muscle, whereas cardiac variants are not detected in skeletal muscle. This may explain why mutations in exon 6, an exon predominantly expressed in skeletal muscle, also cause cardiomyopathy in humans (Vatta M et al., 2003). In zebrafish, the gene contains 18 exons and gives rise to at least thirteen splicing variants, only two of which have counterparts in mouse (cypher 2s and cypher 2c). Based on the large number of cypher isoforms in zebrafish, it has been suggested that other

splice variants of cypher may be detected in other species (van der Meer DL et al., 2006).

From now on, the name ZASP will be used indistinctly in the interest of clarity. In muscle, ZASP localizes at the Z-disc, where it binds to the C-terminal EF-hand region of α-actinin by means of its PDZ domain, a feature common to all isoforms (Zhou Q et al., 1999; Faulkner G et al., 1999). More recently, it has been demonstrated that the ZM internal motif of ZASP interacts with the rod central region of α-actinin (Klaavuniemi T, and Ylänne J, 2006). In particular, approximatively 130 residues around the ZM-motif have been shown to be sufficient to colocalize ZASP with α-actinin. Like other members of the enigma family, long isoforms of ZASP containing the LIM domains can directly interact and be phosphorylated by PKC (Zhou Q et al., 1999). ZASP LIM domains bind to all six PKC isoforms (α, β1, γ, ζ, δ and ε). These observations suggest that ZASP may function as an adaptor to couple PKC-mediated signalling, via its LIM domains, to the cytoskeleton by binding α-actinin through its PDZ domain. Interestingly, a mutation in exon 15, which encodes the third LIM domain, has been described in patients suffering of DCM. It has been found that the mutated ZASP has an increased affinity to PKC, thus suggesting that ZASP plays a signalling role in heart (Arimura T et al., 2004). To better understand the role of ZASP in striated muscle, ZASP-null mice were generated (Zhou Q et al., 2001). These mutant mice developed a severe form of congenital myopathy and died from functional failure in multiple striated muscles within one week after birth (Zhou Q et al., 2001). The structure of the Z-disc was analyzed in ZASP-null mice: contracting skeletal and cardiac muscles showed disorganized and fragmented Z-discs, whereas no Z-disc abnormality was detected in the non-contracting embryonic diaphragm muscles. These observations suggested that ZASP is not required for the formation of protein complexes during sarcomerogenesis; however, it is fundamental for maintaining the structural integrity of the Z-disc during muscle contraction (Zhou Q et al., 2001). As a consequence of the lethal phenotype of ZASP knockout mice, an intensive search for ZASP mutations associated with human muscle diseases started. Mutations in exon 4 and exon 6 of ZASP were shown to be associated with isolated non-compaction of the left ventricular myocardium (INVLM) and DCM; whereas mutations in the long isoform-specific exon 10 was associated with a “pure” form of DCM (Vatta M et al., 2003). Other mutations that are localized in the long isoform-specific exons 10, 12 and 13 have also been recently identified in patients with HCM (Theis JL et al., 2006). More recently, ZASP mutations have been identified in skeletal muscle myopathies, which were named zaspopathies (Griggs

R et al., 2007). Mutations in exon 6, also linked to DCM, have been associated to MFM; some of them fall within, or immediately adjacent to, the ZM-motif, which is required for interaction with α-actinin (Selcen D, and Engel AG, 2005).

I-5.7.4 The ALP subfamily: ALP

The actinin-associated LIM protein (ALP) human gene has been mapped to chromosome 4q35; an alternative name for the protein is PDLIM3. Two ALP isoforms are produced as a result of alternative splicing: a 36 kDa protein (smALP) is enriched in cardiac and smooth muscle, whereas a 40 kDa variant (skALP) is found in skeletal muscle (Pomiès P et al., 1999). The two proteins display identical N- and C-termini; they differ only in the central region where 63 aa present in smALP are replaced by 111 aa in skALP. These correspond to the splice variants of the internal ZM-motif containing exons 4 and 6 (Klaavuniemi T et al., 2004). ALP is not found in undifferentiated mouse C2C12 cells, but it is highly induced after fusion of myoblasts to myotubes (Xia H et al., 1997). As its name implies, both ALP isoforms interact directly with α-actinin and are colocalized with this protein at the Z-disc of striated muscle. Two interaction sites have been reported for the binding between ALP and α-actinin in cultured myoblasts: the ALP PDZ domain recognizes the C-terminal portion of α-actinin, whereas the ZM-motif in the internal region of ALP is involved in the interaction with the rod central domain of α-actinin (Klaavuniemi T et al., 2004). It has been demonstrated that the ZM-motif was necessary and sufficient for the localization of ALP to the Z-disc, similarly to ZASP (see par. I-5.7.3). The meaning of this dual interaction might be to keep α-actinin in the anti-parallel crosslinking conformation and, thus, provide mechanical strength to the Z-discs. This hypothesis could be strengthen by the observation that ALP-deficient mouse embryos showed right ventricular (RV) chamber dysmorphogenesis with defective trabeculation, resulting in right ventricular dilation and dysfunction (Pashmforoush M et al., 2001). ALP-null mice were also generated by Jo K and coworkers (Jo K et al., 2001) to test the hypothesis that ALP is responsible of facioscapulohumeral muscular dystrophy (FSHD), since the human ALP gene maps to the FSHD locus. However, the absence of histological abnormalities, a preserved sarcolemma, and an intact cytoskeleton were observed, thus suggesting that ALP does not participate in muscle development and function or another PDZ-LIM protein compensates for the lack of ALP (Jo K et al., 2001).

I-5.7.5 The ALP subfamily: CLP-36

C-terminal LIM domain protein with a molecular weight of 36 kDa (CLP-36) is also known as human 36-kDa carboxyl terminal LIM domain (hCLIM1) protein (Kotaka M et al., 1999), elfin (Kotaka M et al., 2001), and PDLIM1. The protein was first discovered in rat (Wang H et al, 1995), showing high homology to rat RIL (see further); the human gene subsequently has been mapped to chromosome 10q26 (Kotaka M et al., 1999). CLP-36 presents a wide human tissue distribution with a strong expression in the epithelium of lung, liver, intestine, skin and esophagus; moderate expression in spleen and skeletal muscle; and weak expression in testis and brain tissues (Wang H et al, 1995). CLP-36 is also found in heart, and high levels of expression are detected throughout the developing heart (Kotaka M et al., 2001). The PDZ domain of CLP-36 associate with the SLRs of non-muscle α-actinin-1 and 4 in actin stress fibers, suggesting that CLP-36 acts as an adapter between stress fibers and LIM-binding proteins in non-muscle cells (Vallenius T et al., 2000). The CLP-36 colocalizes with α-actinin-2 at the Z-disc, and this interaction seems to be mediated by the LIM domain of CLP-36 on one hand and by the EF-hand region of α-actinin-2 on the other hand (Kotaka M et al., 2000). CLP-36 has been found to interact also with vinculin, a protein needed for anchoring actin and actin-binding proteins at the cell membrane. The two proteins colocalize at the intercalated discs, specialized regions of the sarcolemma that connect cardiomyocites; this colocalization is thought to be mediated via the α-actinin-2 interaction of the two proteins (Kotaka M et al., 2000). Similarly to other PDZ-LIM proteins, it is reported an interaction between the CLP-36 LIM domain and protein kinases. In particular, it has been shown that CLP-36 specifically targets the CLP-36 interacting kinase (Clik1) to actin stress fibers, probably indicating that Clik1 represents a novel regulator of the acto-myosin cytoskeleton in non-muscle cells (Vallenius T, and Mäkelä TP, 2002).

I-5.7.6 The ALP subfamily: RIL

The reversion-induced LIM protein (RIL) was first identified in mouse (Kiess M et al., 1995). The PDZ domain of RIL, ALP and CLP-36 have 58-70% identity, being higher between RIL and CLP-36, whereas the single C-terminal LIM domain of these proteins is 60-67% identical (Vallenius T et al., 2004). RIL, also known as PDLIM4, is expressed in several non-muscle tissues, such as lung, brain, ovary and uterus, and in a variety of cultured cell lines. RIL localizes in

dendritic spines in cultured neurons (Schulz TW et al., 2004) and along stress fibers (Vallenius T et al., 2004). RIL PDZ domain has been shown to associate with the C-terminus of α-actinin (Schulz TW et al., 2004); however, another interaction involving α-actinin SLRs has been reported (Vallenius T et al., 2004). The importance of the RIL-α-actinin interaction relies on the increased ability of α-actinin to interact with actin filaments. This suggests that RIL may be involved in the formation of new actin filaments either by recruiting α-actinin into filaments or by stabilizing existing α-actinin in thin filaments (Vallenius T et al., 2004). RIL has also been implicated in receptors clustering in neurons. Overexpression of RIL in cultured neurons enhances accumulation of α-amino-5-hydroxy-3-methyl-4-isoxazole propionic acid (AMPA) glutamate receptors at dendritic spines by connecting them to the actin cytoskeleton (Schulz TW et al., 2004). The interaction with AMPA receptor is mediated by the RIL LIM domain. It is reported that phosphorylation may regulate RIL function; the LIM domain of RIL can be phosphorylated *in vitro* and *in vivo* and can be dephosphorylated *in vitro* by the PTPase domain of the protein tyrosine phosphatase (PTP-BL) (Cuppen E et al., 1998). An internal binding of RIL PDZ to the RIL LIM domain has been detected (Cuppen E et al., 1998), suggesting that RIL may oligomerize.
Recently, RIL has been found to be highly methylated in patients suffering of acute myelogenous leukemia (AML) and myelodysplastic syndrome (MDS), whereas in normal tissues RIL is not or only poorly methylated. These data lead to the speculation that RIL could be a candidate for a tumor suppressor gene (TSG) silenced by hypermethylation in cancer (Boumber YA et al., 2007).

I-5.7.7 The ALP subfamily: mystique

Mystique is also known as PDZ and LIM domain 2 (PDLIM2), and shows 37%, 39%, and 39% identity with the other family members ALP, CLP-36 and RIL proteins, respectively (Torrado M et al., 2004). Three mystique variants have been found in humans: mystique 1 and 2 are characterized by a N-terminal PDZ domain and a C-terminal LIM domain, whereas mystique 3 is a PDZ only protein (Loughran G et al., 2005). Mystique is expressed in non-muscle cells, such as corneal epithelial cells and lung. Mystique colocalizes with α-actinin in stress fibers (Torrado M et al., 2004), and also with β1-integrin and α-actinin at focal contacts (Loughran G et al., 2005). Silencing of mystique expression with siRNA had a dramatic effect on cell attachment and migration, suggesting that the protein is essential in cell adhesion and motility of epithelial cells. Mutation of the PDZ

domain alone was sufficient to abolish cell attachment, indicating that the LIM domain of mystique is not required for cell adhesion (Loughran G et al., 2005).

I-5.8 The MARP family

As mentioned earlier in the text, a recent and intriguing observation is that a large number of Z-disc associated proteins have a dynamic distribution in muscle and may shuttle between the Z-disc and other subcellular locations, such as the nucleus, to transmit signals. Consequently, the Z-disc can be considered not simply the structural border of the sarcomere but it may play an important role in cell signalling.

The muscle ankyrin repeat protein (MARP) family constitutes an example of sarcomeric proteins that may be involved in the regulation of gene expression in response to muscle stress. The family is composed by the three homologous members cardiac ankyrin repeat protein (CARP), ankyrin repeat domain 2 (ANKRD2) and diabetes-associated ankyrin repeat protein (DARP) (Miller MK et al., 2003). All of these proteins contain four ankyrin-repeat motifs and are expressed mainly in striated muscle. MARPs expression is upregulated upon injury and hypertrophy for CARP (Kuo H et al., 1999; Aihara Y et al., 2000), stretch or denervation for ANKRD2 (Kemp TJ et al., 2000), and during recovery following starvation for DARP (Ikeda K et al., 2003). MARP proteins also interact with the I-band portion of titin forming a complex together with myopalladin and calpain protease p94. These observations suggest that MARPs may act as molecular linkers between myofibrillar stretch-induced signalling pathways and muscle gene expression (Miller MK et al., 2003). In the following, I will give you a brief description of the two best characterized members of the family, CARP and ANKRD2.

I-5.8.1 CARP

CARP has been identified independently by several groups as a cytokine inducible protein, called C-193 (Chu W et al., 1995), or as a doxorubicin-inducible protein, named cardiac adriamycin-responsive protein (CARP) (Jeyaseelan R et al., 1997). CARP is also known as ANKRD1 (Torrado M et al., 2005) or MARP (Miller MK et al., 2003). The protein is predominantly expressed in heart and to a lesser extent in skeletal muscle. CARP is downregulated during heart development but is activated early in hypertrophy; its overexpression results in the regulation of cardiac gene expression (Aihara Y et al., 2000). Indeed, the

CARP gene product is a nuclear protein, and it is believed that CARP is a gene regulator since its interaction with the ubiquitous transcription factor YB-1 (Zou Y et al., 1997), and its negative effect on the expression of specific cardiac genes, including those encoding the myosin light chain-2 (MLC-2v), ANF and troponin C (Nakada C et al., 2003). Interestingly, it has been reported that CARP is localized not only in the nucleus but also in the sarcomeric I-band of cardiomyocytes, where it interacts with the N-terminal region of myopalladin (Bang ML et al., 2001). The interaction of CARP with myopalladin appears to be critical for sarcomeric integrity of cardiomyocytes.

I-5.8.2 ANKRD2

ANKRD2 was first discovered as a protein upregulated during the mechanical stretch response in mouse skeletal muscle (Kemp TJ et al., 2000). The protein is also called ankyrin-repeat protein with a PEST motif and a proline-rich region (Arpp) (Moriyama M et al., 2001). The human ANKRD2 gene was subsequently characterized and it was mapped to chromosome 10q23.31-23.32, the same mapping position of CARP (Pallavicini A et al., 2001). The amino acids sequence of ANKRD2 shows high homology with those of CARP and DARP, being 52% and 36% respectively (Moriyama M et al., 2001; Ikeda K et al., 2003). In addition to the four ankyrin-repeat domains in its central portion, ANKRD2 is characterized by the presence of a nuclear localization signal (NLS), a protein-destabilizing (PEST) motif in its N-terminal region, and a proline-rich region towards the C-terminus (Moriyama M et al., 2001). ANKRD2 is expressed in skeletal muscle, predominantly in type I fibers, and at a lower level in heart. Furthermore, the expression level in both muscles is very low in fetus but high in adult, suggesting that ANKRD2 expression in humans may be upregulated during development (Moriyama M et al., 2001). Interestingly, denervation of slow muscle (e.g. soleus) decreases the level of ANKRD2 below the detection limit in 4 weeks, whereas denervation of fast muscle (e.g. gastrocnemius) increases its expression (Mckoy G et al., 2005). Immunohistochemical analysis revealed that ANKRD2 is localized mainly in the I-band of striated muscle (Tsukamoto Y et al., 2002); nevertheless, it can interact with nuclear proteins. In a recent study it has been found that ANKRD2 accumulates in the nuclei of damaged myofibers after muscle injury, and that the protein tends to be localized in euchromatin, where many genes are transcriptionally active (Tsukamoto Y et al., 2008). Indeed, it has previously been reported that ANKRD2 can bind directly to transcription factors, including p53, YB-1, and premyelocytic leukemia protein (PML), *in vitro*.

In addition, ANKRD2 has also been shown to enhance p53 activation of the p21 promoter during early myogenesis (Kojic S et al. 2004). Another interaction was detected between ANKRD2 and the Z-disc protein telethonin (Kojic S et al. 2004). These findings together suggest that ANKRD2, similarly to its homologue CARP, may translocate from the I-band to the nucleus in response to muscle damage and participate in the regulation of gene expression.

I-6 The PDZ domain

PDZ domains were originally recognized as regions of sequence homology found in diverse signalling proteins (Cho KO et al., 1992). The name PDZ refers to the first three proteins in which this domain was identified: PSD-95 (a 95 kDa protein involved in signalling at the post-synaptic density), Dlg (the *Drosophila melanogaster* Discs large protein), and ZO-1 (the zonula occludens 1 protein involved in maintenance of epithelial polarity) (Harris BZ, and Lim WA, 2001). PDZ domains are also known as discs-large homology regions (DHRs) or GLGF repeats since there are four highly conserved residues (glycine-leucine-glycine-phenylalanine) within the domain. PDZ domains are built of 80-100 aa residues and are involved in protein-protein interactions normally binding the C-terminal sequences (last 4 to 6 aa) of partner proteins; in some cases, PDZ domains are able to bind to internal regions that may structurally resemble C-termini (van Ham M, and Hendriks W, 2003). PDZ domains have been found in a variety of organisms, and they represent 0.2-0.5% of open reading frames in three currently sequenced metazoans genomes (*Caenorhabditis elegans*, *Drosophila melanogaster*, and *Homo sapiens*). Simple modular architecture research tool (SMART) database lists 1163 PDZ domains in 484 human proteins, 259 domains in 153 *D. melanogaster* proteins, and 130 PDZ domains in 95 *C. elegans* proteins. PDZ domains are scarce in yeast and bacteria, and quite rare in plants (Schultz J et al., 1998). PDZ domains can occur as a single copy within the protein or as multiple copies; indeed, 18% of the human PDZ-containing proteins have three or more PDZ domains within the same polypeptide, the highest number being in the multi-PDZ domain protein 1 (MUPP1) that contains 13 PDZ domains (Harris BZ, and Lim WA, 2001). It is thought that the multiplicity of PDZ domains in a single protein can serve as a "glue" to combine different proteins, thus forming macromolecular complexes involved in cell signalling and protein targeting (Jeleń F et al., 2003).

I-6.1 PDZ domain structure and specificity in ligand recognition

The structures of different PDZ domains were solved by x-ray crystallography and/or NMR. The first structure solved was that of the third PDZ domain of PSD-95 (Doyle DA et al., 1996), followed by other PDZ structures such as the second PDZ domain of PSD-95, the single PDZ domain of calcium/calmodulin-dependent serine protein kinase (CASK), syntrophin, neuronal nitric-oxide synthase (nNOS), PDZ2 domain of human phosphatase hPTP1E, and PDZ1 of InaD (Hung AY, and Sheng M, 2002). To date, all described PDZ domains consist of six β-strands (βA-βF) and two α-helices (αA-αB) that are folded as a six-stranded sandwich. The N- and C-termini of PDZ domains are close to one another in this folded structure, which makes these domains highly modular. This arrangement is common to other protein interaction modules, and would probably facilitate the incorporation of the domain as a functional unit between proteins and the preservation of the ligand-binding site (Harris BZ, and Lim WA, 2001). The structures of several PDZ domains complexed with their peptide ligands have also been determined, thus providing the basis for PDZ specificity in the ligand recognition (Harris BZ, and Lim WA, 2001). The strand βB and the helix αB of the PDZ domain form a groove in which the C-terminal ligand protein bind as an anti-parallel β sheet by a mechanism known as β-strand addition (Harrison SC, 1996) (Figure 4).

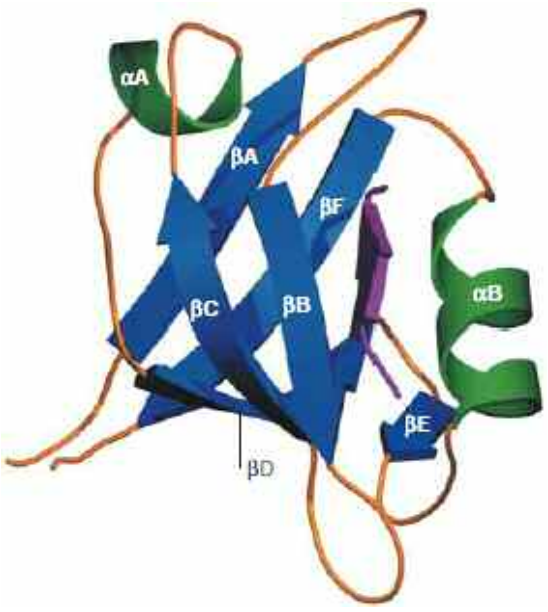

Figure 4. Ribbon representation of the third PDZ domain of PSD-95 (α-helices in green, β-strands in blue) complexed with its target C-terminal peptide (in purple) forming an anti-parallel β sheet with βB-strand (Kim E, and Sheng M, 2004).

Structural analysis of PDZ3 domain of PSD-95 in the presence or absence of the ligand peptide showed that both forms were almost identical, indicating that the

PDZ domain structure does not change significantly upon ligand binding (Doyle DA et al., 1996). In addition, the βA and βB sheets are connected to each other through a loop that contains the well-conserved sequence motif GLGF, creating a hydrophobic cavity surrounding the C-terminus of binding protein. This loop is called carboxylate-binding loop and, together with a highly conserved positively charged arginine or lysine residue three-four amino acids upstream, is involved in the hydrogen bond formation with the terminal carboxylate group. In some PDZ domains, the first glycine of the GLGF motif can be substituted by proline, threonine or serine, whereas the second glycine is highly conserved (Jeleń F et al., 2003) (Figure 5).

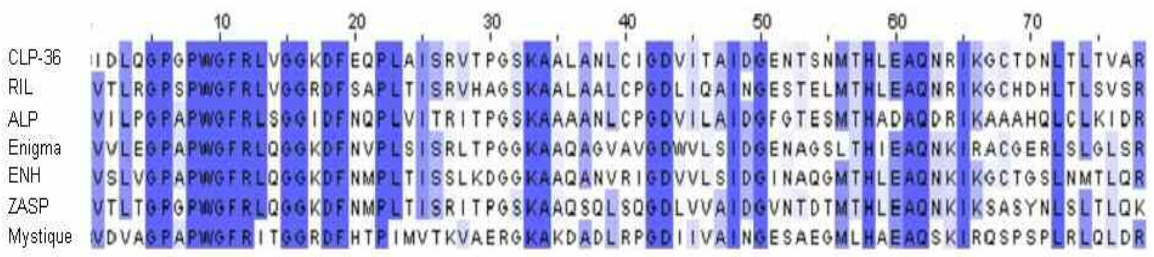

Figure 5. Diagram showing the sequence alignment of the amino acids of the PDZ domains of the enigma family of proteins. The sequence similarity between the PDZ domains is showed with a blue scale. The residues 8-11 represent the carboxylate binding loop GLGF; these are present in the enigma family as PWGF (proline-tryptophan-glycine-phenylalanine) (alignment obtained with ClustalW: http://www.ebi.ac.uk/Tools/clustalw2/index.html).

Therefore, the side chain of the C-terminal residue (by convention the C-terminal residue is referred to as the P_0 residue; subsequent residues towards the N-terminus are termed P_{-1}, P_{-2}, P_{-3}, etc) projects into a hydrophobic pocket, and this explains the preference of various PDZ domains to bind to sequences ending with a hydrophobic residue (such as valine, leucine, or isoleucine) (Songyang Z et al., 1997). On the contrary, the residue at the position P_{-1} is of minor importance for the PDZ binding specificity since its side chain is exposed from the binding surface and does not participate in the formation of hydrogen bonds (Doyle DA et al., 1996). Apart from the position P_0, also the nature of the residue in the position P_{-2} is crucial for the interaction with PDZ domains. The side chain of this residue interacts with the first residue of the αB helix; this interaction plays an essential role in the classification of PDZ domains (discussed below). Most of the PDZ C-terminal ligands contain a serine or threonine residue in the position P_{-2} (Figure 6), another group possesses a hydrophobic residue in the same position, and a third group exposes a negatively charged residue (van Ham M, and Hendriks W, 2003). Crystallographic studies revealed that also the residue in the position P_{-3} is

involved in PDZ binding specificity; in particular, it contacts the βB and βC strands of the PDZ domain. In addition, it has been demonstrated that other residues in the C-terminal region of the interacting protein, up to position P_{-8}, are also important for the PDZ domain binding (van Ham M, and Hendriks W, 2003).

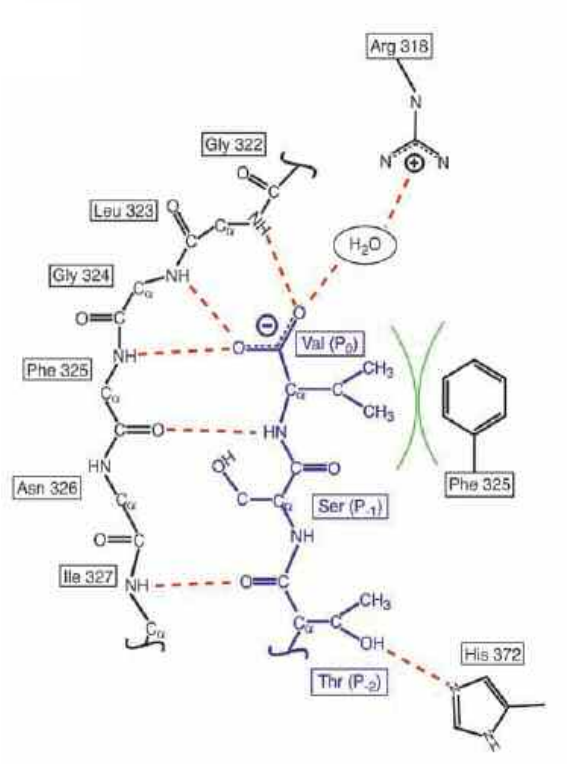

Figure 6. Diagram of the peptide binding pocket. Residues in the PDZ domain binding pocket are shown in black; the peptide is in blue. Hydrogen bonds are drawn as red dotted lines, and hydrophobic packing is indicated by green arcs (Harris BZ, and Lim WA, 2001).

I-6.2 Classification of PDZ domains

PDZ domains can be classified according two different approaches. The first type of classification relies on the C-terminal sequence of the binding protein, with particular consideration of the P_0 and P_{-2} residues. Using this approach, three different classes are defined (Songyang Z et al., 1997). Class I PDZ domains recognize the motif X-[S/T]-X-Φ, where Φ is a hydrophobic amino acid and X is any amino acid. The hydroxyl side chain of the serine or threonine residue at the ligand position P_{-2} forms a hydrogen bond with the amide-3 nitrogen of the histidine residue at position αB1 on the PDZ domain. Class II PDZ domains recognize the motif X-Φ-X-Φ, characterized by hydrophobic residues occupying both the position P_{-2} of the partner protein and the position αB1 of the PDZ domain. Class III PDZ domain recognize the motif X-[D/E/K/R]-X-Φ, where the residue in the position P_{-2} is preferentially negatively charged and a tyrosine residue is found at the position αB1 of the PDZ domain. The hydrogen bond between the tyrosine hydroxyl group from the PDZ domain and the carboxylate

side chain of the P_{-2} ligand residue confers the specificity of this binding. Nevertheless, few other PDZ domains do not fall into any of these specific classes; it is an example the PDZ domain of the nNOS protein (Harris BZ, and Lim WA, 2001). In some cases, PDZ domains are able to bind to different classes of ligands, indicating that the described classification is far from being perfect. For example, the syntenin protein, which interacts with many cell membrane receptors, contains two PDZ domains: PDZ1 binds to peptides from classes I and III, while PDZ2 interacts with classes I and II (Kang BS et al., 2003).

Also the classification used by the eukaryotic linear motif (ELM) resource for predicting functional sites in eukaryotic proteins relies on the C-terminal sequence in the ligand protein (Puntervoll P et al., 2003). However, this classification is more precise in defining the last four residues of the PDZ binding peptide: X-[S/T]-X-[V/I/L], X-[V/Y/F]-X-[V/I/L], and X-[D/E]-X-[V/I/L] correspond to class I, class II, and class III PDZ domains, respectively.

The second approach of classification is based on the nature of amino acids in two critical positions of the PDZ domain, which are the two contact positions of the binding pocket. The first position (Pos1) immediately follows the βB-strand, whereas the second one (Pos2) occupies the first position in the αB helix. Residues in Pos1 and Pos2 positions were grouped into five groups, considering the amino acids polarity and/or bulkiness (Bezprozvanny I, and Maximov A, 2001). The amino acids in Pos1 were divided into five groups as follows: G (glycine), n (negative), Sp (small and polar), Lh (large and hydrophobic), a (aromatic). The amino acids in Pos2 were divided into these five groups: H (histidine), n (negative), p (polar), h (hydrophobic), a (aromatic). Based on this approach, PDZ domains represented in the SMART database were classified into 25 groups. However, according to Vaccaro P and Dente L (Vaccaro P, and Dente L, 2002) the classification of PDZ domains exclusively based on the two conserved positions in the hydrophobic pocket is not sufficient to predict the specificity of binding. The first group (G,H) covers PDZ domains that bind class I peptides, and the remaining groups are less clearly determined. Two of them do not correspond to any known PDZ domains, 14 are not correlated with any ligand sequence, 9 other groups can be unified into class II domains, and 1 corresponds to the PDZ domains having a dual specificity (Bezprozvanny I, and Maximov A, 2001). In addition, Vaccaro P and Dente L demonstrated that the substitution of the histidine at the crucial position αB1 of hINADL-7 (a class I binding PDZ) is not sufficient to change its binding specificity and ligand preference (Vaccaro P, and Dente L, 2002). Thus, in order to better classify PDZ domains it would be

important to consider all the positions in the hydrophobic pocket and also the ligand sequence.

I-6.3 Regulation of PDZ domain-ligand interaction

PDZ-ligand binding can be regulated at different levels. First of all, coexpression of PDZ domain-containing proteins and their ligands in specific cell types and their subcellular localization allows supporting or excluding a possible interaction. Secondly, at the transcript level alternative splicing may determine alternative binding properties. For example, the human serine protease omi is subject to alternative splicing; one of the variants lacks part of the PDZ domain and thus is unable to associate to its known partner, mxi2 (Faccio L et al., 2000). Thirdly, different post-translational modifications can influence subcellular distribution and/or binding affinities (van Ham M, and Hendriks W, 2003). Proteolysis is one of the possible mechanisms; in the case of interleukin-16 (IL-16) precursor, its caspase-dependent cleavage determines the secretion of the mature IL-16 harboring a single PDZ domain. On the contrary, the N-terminal prodomain containing the other two PDZ domains is translocated to the nucleus and functions as a scaffolding protein (Zhang Y et al., 2001). Phosphorylation is another mechanism capable of regulating the interaction of PDZ domains with the C-termini of binding partners. Indeed, most of the PDZ domain ligands contain a serine, threonine or tyrosine residue at the position P_{-2}, which is critical for the interaction with the binding pocket of PDZ domain, as mentioned above. The phosphorylation of the amino acid in this position can affect the binding both positively or negatively. For example, serine phosphorylation at P_{-2} in the inward rectifier K^+ channel Kir2.3 by protein kinase A disrupts binding to PSD-95 PDZ domain (Cohen NA et al., 1996). On the other hand, it has been demonstrated that phosphorylation can also increase the strength of an interaction. Phosphorylation of the serine in the C-terminus of the mitochondrial ribosomal protein (MRP2) increases its binding to three different PDZ domain-containing proteins (Hegedüs T et al., 2003).

I-6.4 The multiplicity and function of PDZ domains

As mentioned earlier in the text, PDZ domain-containing proteins often possess multiple PDZ domains. It has been reported that multiple domains can cooperate to enhance binding to target ligands, as in the case of syntenin. This protein contains two PDZ domains, the second one being able to bind to the C-termini of

several proteins only with the help of the PDZ1 or another copy of PDZ2 (Grootjans JJ et al., 2000). Another study reports that one PDZ domain may influence the folding of an adjacent PDZ domain. This is the case of glutamate receptor-interacting protein (GRIP) PDZ5 domain, which is unstructured and unable to bind GluR2 when alone. However, after its covalently connection with the PDZ4, PDZ5 becomes highly structured and capable of binding GluR2 (Zhang Q et al., 2001). PDZ domains are also found in proteins with other known interaction or signalling domains. For example, the membrane-associated guanylate kinase (MAGUK) proteins are characterized by one or more PDZ domains, a SH_3 domain, and a catalytically inactive guanylate kinase-like (GuK) domain. Other PDZ domain-containing proteins occur in combination with a wide range of interaction modules, such as WW, LIM, calcium/calmodulin-dependent protein kinase (CaMK) domain as well as ankyrin and leucine-rich repeats (Jeleń F et al., 2003). A detailed description of PDZ-LIM proteins and their interaction partners in muscle is reported earlier in the Introduction since some of them were the main object of my study. In general, the multidomain structure of PDZ-containing proteins enables them to interact with several binding partners at the same time, thereby assembling larger protein complexes. In light of what described up to now, it is clear that PDZ domain proteins play an important role in targeting proteins to specific cellular compartments, and consequently in the regulation of their activity. The ability to bind to short C-terminal motifs facilitates the interaction of PDZ proteins with target proteins without disrupting their overall structure and function (Hung AY, and Sheng M, 2002). Key questions remain to be answered; for example, it would be important to define the spatio-temporal regulation of PDZ-mediated interactions in the cell. Furthermore, studies on interaction strength and competition experiments may elucidate the hierarchy of different partner proteins in PDZ domain association. The importance of studying PDZ domain-containing proteins is highlighted by the correlation with the onset of several disorders in humans.

II AIM OF THE STUDY

The Z-disc of striated muscle contains many proteins, such as α-actinin, titin, γ-filamin, nebulin, MLP, and some of them (FATZ, ZASP, telethonin and ANKRD2) were discovered in my laboratory. The main goal of my project was to understand the complex network of protein-protein interactions occurring at Z-disc of skeletal and cardiac muscle. My interest has been focused on muscular PDZ-LIM proteins, in particular on ZASP, ALP and CLP-36. These proteins belong to the enigma family and are characterized by a single N-terminal PDZ domain and one to three C-terminal LIM domains. ZASP, ALP and CLP-36 have in common another binding motif called ZM in their internal region (Klaavuniemi T et al., 2004). Both PDZ and LIM domains are protein-protein interaction domains with diverse functions. A feature common to all PDZ-LIM domain family members is their ability to associate with the actin cytoskeleton (Te Velthuis AJ et al., 2007) and it is thought that, in muscle, they act as adaptors in transmitting mechanical stress signals from the Z-disc to the nucleus (Vallenius T et al., 2004). PDZ domains commonly recognize specific short motifs (4 to 6 aa in length) at the C-terminal of interacting proteins. In collaboration with the groups of Dr. G. Faulkner at ICGEB, Trieste, and Prof. O. Carpen at University of Turku, Finland, we noted that there is sequence homology between the terminal five amino acids of FATZ-1, FATZ-2, FATZ-3, myotilin, palladin and myopalladin. The motif present in these Z-disc proteins is E-[S/T]-[D/E]-[D/E]-L.

The first object of my work was to check if the PDZ domain of the enigma family members ZASP, ALP and CLP-36 could interact with proteins of the FATZ family, myotilin, palladin and myopalladin via their C-terminal amino acids. Some of these interactions were already known (i.e. between the FATZ family and ZASP) (Frey N, and Olson EN, 2002), however the specific binding site has not been mapped on the proteins before. Different techniques were used for studying protein-protein interactions *in vitro*: AlphaScreen (Amplified Luminescent Proximity Homogeneous Assay) and TranSignal PDZ Domain Array. AlphaScreen was also adapted to measure competitions between proteins. SPR (Surface Plasmon Resonance) was finally used to evaluate the strength of some of these bindings. SPR experiments were done in the laboratory of Dr. A. Baines at University of Kent, UK.

Taking into account that at the Z-disc many proteins can interact with the same partners, it would be helpful to define the pattern and level of expression of the

individual proteins in different muscle tissues. In order to gain a better understanding of the role these sarcomeric genes play in muscle, a second aim of my work was to measure the abundance of mRNAs of some Z-disc proteins (the FATZ family, myotilin and ZASP with its alternatively spliced isoforms) in different murine muscles using the Real-Time PCR technique.

III MATERIALS AND METHODS

III-1 Buffers, solutions, media and kit components

Protein purification and analysis

Coomassie Brilliant Blue stain	50% v/v methanol, 10% v/v glacial acetic acid, 0.25% w/v CBB G250
1x PBS	120 mM NaCl, 2.7 mM KCl, 10 mM NaH_2PO_4, pH 7.4
Blocking solution	1x PBS with 5% w/v low fat milk
Lysis buffer (*for HIS-tagged protein*)	50 mM NaH_2PO_4, 300 mM NaCl, 10 mM imidazole, pH 8.0
Wash buffer (*for HIS-tagged protein*)	50 mM NaH_2PO_4, 300 mM NaCl, 20 mM imidazole, pH 8.0
Elution buffer (*for HIS-tagged protein*)	50 mM NaH_2PO_4, 300 mM NaCl, 250 mM imidazole, pH 8.0
Lysis buffer (*for GST recombinant protein*)	25 mM HEPES pH 7.6, 300 mM NaCl, 1 mM EDTA, 1 mM DTT, 0.1 mg/mL lysozyme, protease inhibitor cocktail (*Roche*), 0.5% v/v Triton X-100
2x SDS gel-loading buffer	100 mM Tris-HCl pH 6.8, 4% v/v β-mercaptoethanol, 4% w/v SDS, 0.2% w/v bromophenol blue, 20% v/v glycerol
1x Running buffer	25 mM Tris, 192 mM glycine pH 8.3, 0.1% v/v SDS
1x Transfer buffer	25 mM Tris, 19.2 mM glycine pH 8.3, 0.1% v/v SDS, 10% v/v methanol
Strong destain solution	50% v/v methanol, 10% v/v glacial acetic acid
Weak destain solution	10% v/v methanol, 7% v/v glacial acetic acid

AlphaScreen kit components (*PerkinElmer*)

Anti-GST Acceptor beads, Nickel Chelate Acceptor beads, Streptavidin Donor beads	5 mg/mL in 25 mM HEPES,100 mM NaCl, pH 7.4
Biotinylated-GST, Biotinylated-6xHIS	500 nM in 25 mM HEPES, pH 7.4
10x AlphaScreen buffer	250 mM HEPES, 1 M NaCl, pH 7.4

BIAcore buffers

1x BIAcore running buffer	100 mM sodium phosphate, pH 7.0
1x BIAcore sample buffer	25 mM HEPES, 100 mM NaCl, 0.001% v/v surfactant P20, pH 7.4

Media

LB broth	1% w/v bacto tryptone, 0.5% w/v yeast extract, 0.5% w/v NaCl
LB agar plates	LB broth containing 1% w/v agar

III-2 Bacterial strains

The following *E. coli* strains were used for this work:

DH5α strain (F^-, recA1, endA1, hsdR17 (r_k-, m_k+), supE44, λ-, thi-1, gyrA96, relA1) for the propagation of prokaryotic expression vectors.
M15[pREP4] strain (Nal^S, Str^S, Rif^S, Thi^-, Lac^-, Ara^+, Gal^+, Mtl^-, F^-, $RecA^+$, Uvr^+, Lon^+) for the expression and purification of HIS-tagged recombinant proteins.
BL21 Star (DE3)pLysS (*Promega*) strain (F^-, ompT, hsdSB (r_B^-, m_B^-), dcm, rne131, (DE3), pLysS, Cam^R) for the expression and purification of GST recombinant proteins.
BL21-CodonPlus-RIL (*Promega*) strain (*E. coli* B, $F^–$, ompT, hsdS (r_B^-, m_B^-), dcm^+, Tet^R, gal, endA, Hte, [argU ileY leuW Cam^R]) if the protein sequence contains a high percentage of arginine, isoleucine and leucine.
BL21-CodonPlus-RP (*Promega*) strain (*E. coli* B, $F^–$, ompT, hsdS (r_B^-, m_B^-), dcm^+, Tet^R, gal, endA, Hte, [argU proL Cam^R]) if the protein sequence is rich in proline and arginine.

Both the M15 and the BL21 strains allow high levels of expression of recombinant proteins after IPTG induction.

III-3 Bacterial expression vectors

cDNAs for the different human proteins (full-length or truncated forms) were cloned into the BamHI-HindIII restriction sites in the following bacterial vectors:

pQE-30 (*QIAGEN*): contains a N-terminal six histidine (6xHIS) tag (Figure 7).
pGEX-6PH-3: contains a N-terminal GST tag. The vector is a modified form of the pGEX-6P-3 vector (*GE Healthcare*) containing BamHI-HindIII restriction sites (Figure 8).

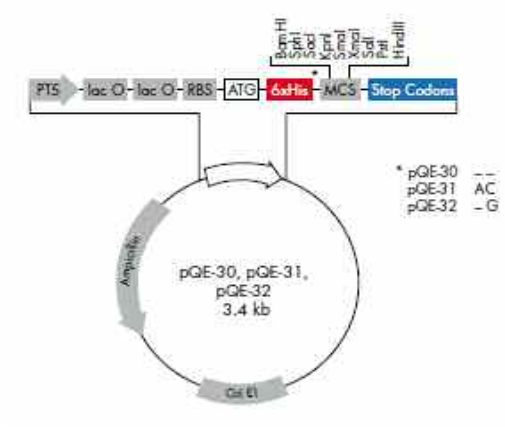

Figure 7. Map of the pQE-30 vector series (*QIAGEN*).

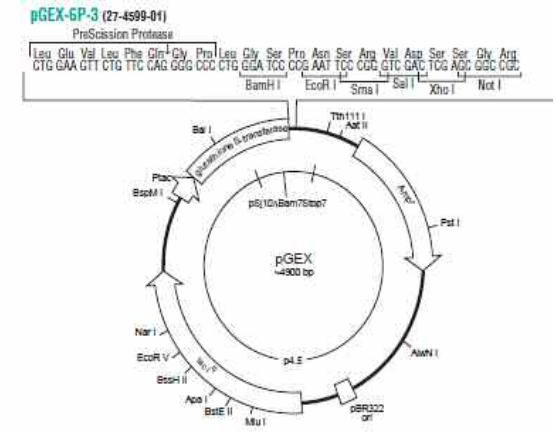

Figure 8. Map of the pGEX-6P-3 vector (*GE Healthcare*).

III-4 Peptides

Peptides were produced in the Protein Structure and Bioinformatics laboratory, ICGEB. The peptides, corresponding to the last five residues of the proteins of the FATZ family, myotilin, palladin, myopalladin and α-actinin-2 were synthesized on solid phase (Fmoc/t-Bu chemistry). The synthesis was automatically performed on a 0.05 mmol scale with a Gilson AspecXl Solid Phase Extraction instrument modified in-house. A linker made up of two GABA units was 12.3 Å in length. Biotin was manually added at the peptide N-terminus as a biotin 4-nitrophenyl ester at the end of the synthesis. After cleavage from the resin the peptides were precipitated with diethyl ether, washed and freeze-dried. The peptides were purified by RP-HPLC on a Zorbax 300SB-C18 column (*Agilent*) using a linear gradient from Eluent A (0.1% v/v trifluoroacetic acid in water) to Eluent B (0.1% v/v trifluoroacetic acid in acetonitrile) using UV monitoring at 214 nm. The

collected fractions were analyzed by ESI-MS on an API150EX single quadrupole mass spectrometer (*Applied Biosystems*), pooled and freeze-dried.

List of peptides synthesized for the project

The following peptides were used for AlphaScreen studies, TranSignal PDZ Domain Array experiments and SPR measurements.

Biotin-GABA-GABA	**-ETEEL**	**-EpTEEL**
	-ESEDL	**-EpSEDL**
	-ESEEL	**-EpSEEL**
	-ESDEL	**-EpSDEL**
	-GESDL	**-GEpSDL**
	-ESEEE	**-EpSEEE**

For competition experiments the same peptides without biotin were used.

III-5 Protein production

III-5.1 Expression and purification of native 6xHIS-tagged proteins

The pQE-30 (*QIAGEN*) vector was used for the expression of HIS-tagged proteins. The *E. coli* strain M15[pREP4] was transformed and after induction colonies were screened for expression of the recombinant HIS tag protein. A fresh colony expressing the protein of interest was inoculated into LB broth (10mL) with ampicillin (100 μg/mL) and kanamycin (30 μg/mL) selection and grown O/N at 37°C with shaking. The next morning, the culture was used to inoculate fresh LB broth (500 mL) supplemented with the appropriate antibiotics and grown at 37°C with shaking until an OD_{600} of 0.6. At this point, IPTG was added to 1 mM and the culture was allowed to continue growing for 4-5 hours at 37°C or at RT with shaking. Then bacteria were harvested by centrifugation at 6,000 rpm for 15 min, the pellet resuspended in 10 mL of lysis buffer (for HIS-tagged protein) and kept at -80°C O/N. The next day, the bacterial suspension was thawed, lysozyme and Triton X-100 were added to 0.1 mg/mL and 0.1% v/v, respectively, and the bacteria were incubated at RT for 20 min. The suspension was then sonicated twice for 1.5 min at high power and centrifuged 10 min at 14,000 rpm to remove cellular debris. The supernatant was transferred to a fresh tube, mixed with 2 mL

of Ni-NTA (*QIAGEN*) resin and incubated for 1 hour at 4°C with gentle mixing. The Ni-NTA resin is a metal chelant adsorbent coupled to Sepharose CL-6B which binds with high affinity to the 6xHIS tag. The mixture was loaded into a column and allowed to flow through it for gravity. The resin was washed twice with 4 mL of wash buffer. The recombinant protein was eluted four times with 0.5 mL of elution buffer.

List of 6xHIS-tagged fusion proteins expressed and purified for the project

These proteins were used for AlphaScreen studies, TranSignal PDZ Domain Array experiments and SPR measurements.

Protein	**Description**
PDZ-ZASP-HIS	Human PDZ domain of ZASP (1-85 aa)
PDZ-CLP-HIS	Human PDZ domain of CLP (1-90 aa)
PDZ-ALP-HIS	Human PDZ domain of ALP (1-87 aa)
C-term FATZ-3-HIS	C-terminal region of human FATZ-3 (81-251 aa)
ACTN2-HIS	Human full-length α-actinin-2 (1-894 aa)

III-5.2 Expression and purification of native GST recombinant proteins

GST recombinant proteins were produced and purified using the Glutathione-S-transferase Gene Fusion System (*GE Healthcare*). The pGEX plasmids are designed for inducible, high-level intracellular expression of genes or gene fragments as GST fusion proteins. The cDNA of different proteins was inserted into pGEX plasmids, these vectors were then transformed in the *E. coli* strain BL21 Star (DE3)pLysS (*Promega*) that is engineered to contain the pLys plasmid encoding the T7 lysozyme. RIL or RP variants of BL21 Star (DE3)pLysS (*Promega*) containing extra codons were used when the protein to be expressed was rich in arginine (R), isoleucine (I), leucine (L) or proline (P). Colonies were screened for the expression of the recombinant protein. A positive colony was grown in LB broth in the presence of ampicillin (100 µg/mL) at 37°C O/N. The next day, this culture was used to inoculate LB broth supplemented with the appropriate antibiotic and grown at 37°C with shaking until an OD_{600} of 0.6. At this point, the GST recombinant protein expression was induced by the addition of 1 mM IPTG and the bacteria were grown for a further 3-4 hours at 37°C or at RT with mixing. Then the cells were collected by centrifugation at 6,000 rpm for 15

min, resuspended in lysis buffer (for GST recombinant protein) and kept on ice for 20 min. The suspension was sonicated and then centrifuged at maximum speed to remove cellular debris. The supernatant was recovered and incubated for 1 hour with Glutathione Sepharose-4B beads (*GE Healthcare*) at 4°C with mixing. During this step the recombinant GST proteins should bind to the glutathione conjugated beads. Then the solution was briefly centrifuged and the recovered resin was washed three times with lysis buffer for 5 min at 4°C with mixing. After a final washing in PBS, the GST recombinant proteins were eluted from the beads by the addition of 200 µL of 20 mM Glutathione (*Sigma*) for 10 min at RT.

List of GST fusion proteins expressed and purified for the project

These proteins were used for AlphaScreen studies.

Protein	**Description**
FATZ-1-GST	Human full length FATZ-1 (1-299 aa)
FATZ-1-5aa-GST	Human FATZ-1 lacking the last five amino acids (1-294 aa)
FATZ-2-GST	Human full length FATZ-2 (1-264 aa)
FATZ-2-5aa-GST	Human FATZ-2 lacking the last five amino acids (1-259 aa)
FATZ-3-GST	Human full-length FATZ-3 (1-251 aa)
FATZ-3-5aa-GST	Human FATZ-3 lacking the last five amino acids (1-246 aa)
Myotilin-GST	Human full length myotilin (1-498 aa)
Myotilin-5aa-GST	Human myotilin lacking the last five amino acids (1-493aa)
ACTN2-GST	Human full-length α-actinin-2 (1-894 aa)

III-6 Protein analysis

Protein levels and purity were checked by SDS-PAGE followed by Coomassie Blue staining, and then blotted onto Immobilon-P transfer membrane (*Millipore*) to perform western blotting.

III-6.1 SDS-PAGE

Protein samples were analyzed by SDS-PAGE using a Mini-PROTEAN 3 Cell apparatus (*Bio-Rad*). Typically, resolving gels were made at 12% of a 29:1 mix of acrylamide/bisacrylamide (*Bio-Rad*) in 375 mM Tris-HCl, pH 8.8, 0.1% v/v SDS, and 0.1% w/v ammonium persulphate (*Bio-Rad*), with 0.04% v/v TEMED (*Bio-Rad*) added for crosslinking. This mix was poured between glass plates in the apparatus. Stacking gels consisting of 5% of the acrylamide mix in 125 mM Tris-HCl, pH 6.8, 0.1% v/v SDS, 0.1% w/v ammonium persulphate, and 0.1 % v/v TEMED were overlaid. Protein samples were diluted with 2x SDS gel-loading buffer and denatured at 94°C for 5 min. Electrophoresis was carried out at 200 V, 40 mA, per gel in running buffer.

III-6.2 Coomassie Blue staining

After polyacrylamide gel electrophoresis, proteins were visualized by staining in Coomassie Brilliant Blue (CBB) stain for 1 hour at RT with slow shaking. The gels were destained in the strong washing solution for 1 hour and subsequently destained in the weak washing solution with 2 or 3 changes until clear. The size of the bands was estimated by comparison with the Precision Plus Protein Standards – Dual color (*Bio-Rad*).

III-6.3 Western blotting

Proteins were transferred to a PVDF membrane using a Mini Trans-Blot Electrophoretic Transfer Cell (*Bio-Rad*) at a current of 100 mA in transfer buffer O/N. The membrane was reversibly stained with Ponceau S stain (*Sigma*) to check for efficient protein transfer, then washed with deionized H_2O and destained with PBS for 15 min. All steps were performed at RT. The membrane was blocked for at least 1 hour in a solution of 5% low fat milk in PBS. The primary antibodies were diluted in 5% low fat milk in PBS and incubated for at least 90 min with gentle mixing. The membrane was rinsed for 10 min in PBS with 0.1% v/v

Tween-20 and 2% w/v NaCl and then blocked again for 1 hour. The secondary antibodies were diluted in 5% low fat milk in PBS and incubated 45 minutes with agitation. The membrane was rinsed as above, then washed three times 15 min (each wash) in PBS with 0.1% v/v Tween-20. Immobilized protein-antibody complexes were visualized by chemiluminescence using ECL Western Blotting Detection Reagents followed by exposure to Hyperfilm (*Amersham*). Molecular weights of the protein bands were estimated by comparison with protein standards as done for Coomassie-stained polyacrylamide gels.

III-7 Gel filtration chromatography

Gel filtration chromatography was used as a further step in protein purification. This method separates proteins, peptides, and oligonucleotides on the basis of size. The chromatographic matrix consists of porous beads, and the size of the bead pores defines the size of macro-molecules that may be fractionated. Those proteins or peptides that are too large to enter the bead pores are excluded, and thus elute from the column first. Smaller macromolecules that enter some, but not all of the pores, are retained slightly longer in the matrix and emerge from the column next. Finally, small molecules filter through most of the pores, and they elute from the column with an even larger elution volume.

The protein sample to be purified was firstly concentrated using the Centricon Centrifugal Filter Device containing Ultracel YM-3 membrane (*Millipore*). An initial sample volume of 1-3 mL was placed in the cellulose membrane support and centrifuged at 4,000 rpm at 10°C until the desired volume was reached. Concentrated samples were centrifuged afterwards to remove any precipitate. The concentrated protein sample (0.2 mL) was applied to a Superose 6 HR 10/30 column (*Amersham*) equilibrated in BIAcore sample buffer (without surfactant P20). The column was run at 0.4 mL/min, calibrated with standard globular proteins obtained from *Amersham* (Thyroglobulin, 669 kDa; Ferritin, 440 kDa; Bovine serum albumin, 67 kDa; Ribonuclease A, 13.7 kDa; Glycyl tyrosin, 238 Da), and the elution profile was monitored at 280 nm. This was done with Waters HPLC System including Waters 600 Quat Pump, Waters 600 Controller, and Waters 2487 Dual lambda Absorbance Detector. The presence of the protein in peak fractions was confirmed by SDS-PAGE.

III-8 Protein biotinylation

For AlphaScreen experiments, biotinylation of one binding protein is generally required. FluoReporter Mini-Biotin-XX Protein Labeling Kit (*Molecular Probes*) provides a method for biotinylating small amounts of proteins. The water soluble biotin-XX sulfosuccinimidyl ester readily reacts with the protein amines to yield a biotin moiety covalently attached via two aminohexanoic chains ("XX").
0.2 mL or 1 mL of the protein solution (0.5-3.0 mg/mL) was transferred to a 2 mL reaction tube containing a stir bar; one-tenth volume of a freshly prepared 1 M sodium bicarbonate solution was then added. The reactive biotin-XX solution was obtained dissolving 200 µL dH_2O to the vial containing the sulfosuccinimidyl ester of biotin-XX. The amount of this solution was added to the tube with the protein solution and sodium bicarbonate according to Table 1. The reaction mixture was then stirred for 1-1.5 hours at RT.

Protein concentration (mg/mL)	**Volume of protein solution (mL)**	**Amount of biotin-XX solution to use (µL)**	**Volume of protein solution (mL)**	**Amount of biotin-XX solution to use (µL)**
0.5	0.2	2	1.0	9
1.0	0.2	3	1.0	12
1.5	0.2	4	1.0	16
2.0	0.2	5	1.0	22
2.5	0.2	6	1.0	26
3.0	0.2	7	1.0	30

Table 1. Amount of reactive biotin-XX solution to be added to different concentrations of protein solution to achieve approximately 3–8 biotin molecules per protein.

For protein volumes of 0.2 mL, the purification of the biotinylated protein from free biotin was achieved using a spin column (containing PBS buffer with 2 mM sodium azide). If protein volumes were larger than 0.5 mL, excess biotinylation reagents were removed dialyzing at 2-8°C for 24 hours in PBS or other desired buffer. Typically, about 70–80% of the protein in the biotinylation reaction was recovered as biotinylated conjugate.

III-9 First-strand cDNA synthesis

Total RNA extracted from different muscle (tibialis, gastrocnemius, soleus and heart) and non-muscle (kidney, liver and brain) tissues was retrotranscribed using Superscript III RNase H^- Reverse Transcriptase according to the manufacturer's specifications (*Invitrogen*). Reactions were done in 1.5 mL tubes in a final volume of 30 µL. The following components were firstly added: 2 µg total RNA, 1.2 µL 100 µM oligo$(dT)_{18}$V, 1.5 µL 10 mM dNTPs, DEPC-treated water to 19.5 µL. The mix was incubated at 65°C for 5 min, then placed on ice for at least 1 min. After a brief centrifugation, the following components were added to the mix: 6 µL 5x First-Strand buffer (250 mM Tris-HCl pH 8.3, 375 mM KCl, 15 mM $MgCl_2$), 1.5 µL 0.1 M DTT, 1.5 µL 40U/µL RNase OUT, 1.5 µL 200U/µL SuperScript III-RT. At this point, the mix was incubated at 45°C for 1 hour and 15 min, then the reaction was inactivated by heating at 70°C for 15 min.

III-10 AlphaScreen

III-10.1 AlphaScreen principles

AlphaScreen is a non-radioactive Amplified Luminescent Proximity Homogeneous Assay, which allows detection of molecular events such as binding. The technique relies on the use of hydrogel coated Donor and Acceptor beads providing functional groups for conjugation to biomolecules. In the AlphaScreen assays, a signal is generated when a Donor and an Acceptor bead are brought into proximity by an interaction between the two conjugated biomolecules. The laser excitation at 680 nm of a photosensitizer (phthalocyanine) present on the Donor bead converts ambient oxygen to a more excited singlet state. The short lifetime of singlet oxygen in aqueous solution (about 4 µs) allows diffusion over a distance up to 200 nm. The singlet oxygen molecules migrate to react with a thioxene derivative in the Acceptor bead generating chemiluminescence at 370 nm that further activates fluorophores contained on the same bead. The fluorophores subsequently emit light at 520−620 nm (Figure 9). In the absence of a specific biological interaction, singlet oxygen produced by the Donor bead falls to ground state without the close proximity of the Acceptor bead. As a result, only a low background signal is produced.

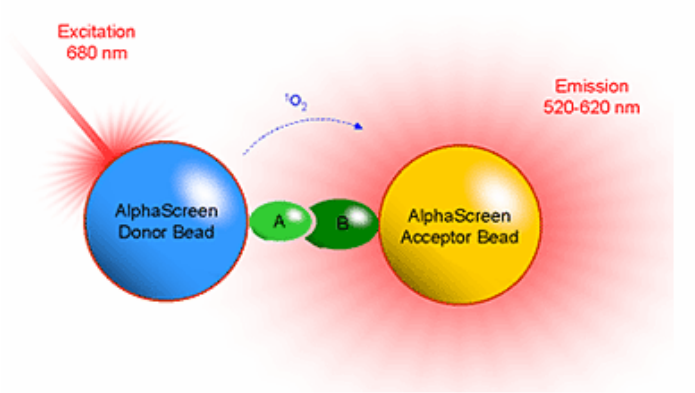

Figure 9. Binding of protein partners brings Donor and Acceptor beads into close proximity (≤ 200 nm) and a fluorescent signal between 520-620 nm is produced (A practical guide to working with AlphaScreen, *PerkinElmer* Inc., 2003).

Donor beads are typically sold as streptavidin conjugates, since biotinylation of one binding partner provides efficient capture onto the Donor bead. Acceptor beads come in a variety of conjugates, primarily linked to antibodies (anti-HIS, anti-GST, etc.); the second binding partner would then need to have the corresponding antigen attached.

The AlphaScreen technique was developed by *PerkinElmer* for analyzing a variety of biological interactions, such as receptor-ligand interactions, enzyme activity or second messenger levels. In my case, the AlphaScreen method was used to evaluate the strength of protein-protein bindings and also to study the interactions occurring when more than one binding partner of a protein is present.

III-10.2 AlphaScreen advantages

The first advantage of the AlphaScreen technique is its sensitivity. Because of the high concentration of photosensitizer, one Donor bead emits up to 60,000 singlet oxygen molecules per second. Also on the Acceptor beads there is a high density of thioxene derivative and fluorophores. This results in amplification of the signal that can be detected down to the femtomolar (10^{-15}) concentration of binding partners.

Another benefit is the low background. The half-life of the decay reaction is 0.3 s, which allows the technology to operate in a time-resolved mode ensuring a reduced background by minimizing the effect of autofluorescence. Also a long excitation wavelength of 680 nm, combined with a shorter emission wavelength of 520−620 nm, reduces interference from biological or assay components.

Another important feature of AlphaScreen is its ability to measure low affinity bindings. This is possible because each Donor bead carries up to 3,000

streptavidin molecules, while each Acceptor bead is coated with up to 300 antibodies. This means that the signal produced by a given Donor/Accpetor bead pair depends not on the binding of one pair of biomolecules, but on dozens, or even hundreds.

III-10.3 AlphaScreen experiments

Alphascreen experiments were performed using HIS-tagged proteins, GST fusion proteins or peptides. Experiments were done in 384-well plates (OptiPlate-384 white opaque, *Packard BioScience*) in a final volume of 25 µL per well. Both the GST detection and the HIS detection Kits for AlphaScreen were used according to the manufacturer's specifications (*PerkinElmer*). The Acceptor and Donor beads were used at a concentration of 0.02 µg/µL (6.5 pM). First, the proteins to be tested were added to the wells and the Acceptor beads were immediately added. The following steps were done in the dark. The plate was incubated for 30 min at RT before adding the Donor beads, then incubated for a further 3 hours after which it was kept for 15 min at 28 °C to equilibrate the temperature. The signal was read at 28°C using a Fusion Alpha Microplate Analyzer (*PerkinElmer*) at 300 ms excitation, 700 ms emission (Figure 10). The instrument is a multidetection microplate reader that can be configured to read fluorescence intensity, time-resolved fluorescence, absorbance, luminescence and AlphaScreen chemistries.

Figure 10. Fusion Alpha Microplate Analyzer (*PerkinElmer*).

III-10.4 AlphaScreen data analysis

When testing a protein for binding it was necessary to titrate it against the partner protein in order to establish the concentration of both proteins that resulted in a significant value for the signal (S) to noise (N) ratio; the S/N is normally used in

the range 8-50. In every experiment negative controls without one or both proteins were used to measure the noise (background) level. Also biotinylated GST (0.5 nM) or biotinylated HIS (1 nM) were used as internal controls to normalize the signal readings. The experiments were repeated at least three times to reduce the possibility of false positives. The ratio (R) was calculated as the mean of the normalized signal divided by the mean of the normalized noise, i.e.:

$$R = \frac{Sm}{Nm}$$

The confidence of the ratio was calculated from the standard deviation of the signal and the noise.

$$\Delta R = R\sqrt{\left(\frac{\delta Sm}{Sm}\right)^2 + \left(\frac{\delta Nm}{Nm}\right)^2}$$

Sm = normalized signal mean
dSm= mean standard deviation of normalized signal
Nm = normalized noise mean
dNm= mean standard deviation of normalized noise

In competition experiments the binding proteins were first added to the wells at a fixed concentration that would result in binding in the absence of a competitor. Then the protein used as possible competitor was added at decreasing concentrations. The result was plotted as the ratio obtained by dividing the signal in the presence of the competitor by that of the signal in the absence of the competitor. The experiments were repeated at least three times and the values for the mean as well as the standard deviation from the mean of the samples were plotted.

III-11 TranSignal PDZ Domain Array

The PDZ array membranes (*Panomics*) were used according to the protocol in the manufacturer's handbook. The array membranes have a notch at the top right-hand corner for orientation purposes. The biotinylated peptides or HIS–tagged purified proteins were used as ligands on the PDZ Domain Array I. When biotinylated peptides were used as ligands, 1.5 µg of the peptide was mixed with 15 µL of Streptavidin-HRP (*Dako*) obtaining a concentration of 0.3 µg/mL, and incubated at 4°C for 30 min. The mix was then added to 5 mL of blocking buffer

(*Panomics*) and kept at 4°C until ready to use. When a HIS–tagged purified protein was used as ligand, it was diluted in blocking buffer to obtain a protein concentration of 15 µg/mL.
The membranes were incubated for 1 hour at RT in blocking buffer and then briefly rinsed with wash buffer (*Panomics*). At this point, the membranes were incubated with gentle shaking for 1-2 hours at RT with the peptide or the purified protein mixes, then washed three times with wash buffer for 10 min (each wash) at RT. When HIS–tagged purified protein was used, the membrane was incubated for a further 1-2 hours at RT with anti-HIS HRP conjugate diluted in wash buffer and then washed three times in wash buffer at RT. After incubation for 5 min at RT with the provided solutions for chemiluminescence, the membranes were exposed to ECL Hyperfilm (*Amersham*).

III-12 Surface Plasmon Resonance (SPR)

III-12.1 SPR general principles

SPR is a technique capable of measuring biomolecular interactions in real-time, without labelling any of the interacting components. There are several SPR-based systems; the most widely used is the BIAcore, produced by *BIAcore AB* (BIAcore International, Uppsala, Sweden). SPR-based instruments use an optical method to measure the refractive index near (within ~300 nm) a sensor surface. In the BIAcore this surface forms the floor of a small flow cell through which an aqueous solution (the *running buffer*) passes under continuous flow (Figure 11).

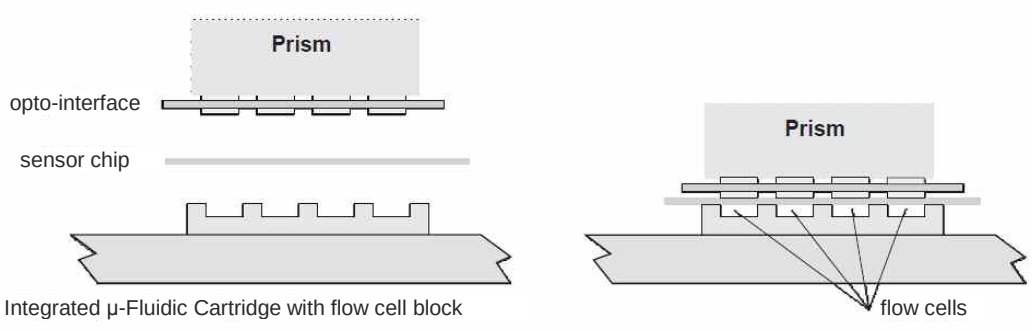

Figure 11. The flow cells are formed by pressing the sensor chip against the integrated µ-fluidic cartridge (IFC) (BIAcore 3000 Instrument Handbook, *BIAcore AB*, 1999).

The technology involves attaching one interacting partner (the *ligand*) to the surface of the sensor chip, and then injecting its binding partner (the *analyte*) in

aqueous solution (the *sample buffer*) through flow cell, also under continuous flow. Association between ligand and analyte results in an increase in the refractive index. This change is proportional to the mass of material bound to the surface, and it increases until equilibrium between binding and release is reached or until the chip surface is saturated with analyte. If the solution containing the analyte is replaced by the running buffer, the complexes formed on the surface decay and the analyte is washed away, resulting again in a gradual refractive index change. These refractive index changes are measured in real-time, and the result plotted as response or resonance units (RUs) versus time, obtaining a *sensorgram* (Figure 12). One RU represents the binding of approximately 1 pg protein/mm^2. Importantly, a response (*background response*) will also be generated if there is a difference in the refractive indices of the running and sample buffers. This background response must be subtracted from the sensorgram to obtain the actual binding response. The background response is recorded by injecting the analyte through a control or reference flow cell, which has no ligand or an irrelevant ligand immobilized to the sensor surface.

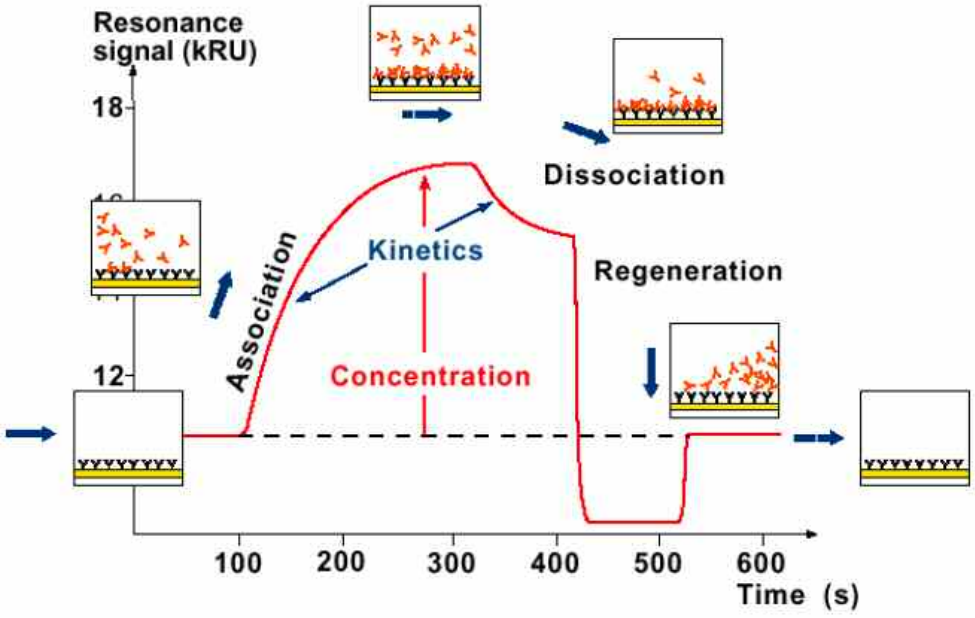

Figure 12. Illustration of a basic BIA sensorgram (Roos H, 2001).

III-12.2 SPR physical principles

SPR is a phenomenon that occurs in thin conducting films at an interface between media of different refractive index. In BIAcore systems, the media are the glass of the sensor chip and the sample solution, and the conducting film is a thin layer of gold on the sensor chip surface.

When light passes through a medium with a high refractive index (the glass) toward a medium with a lower refractive index (the sample solution), part of the light will be reflected from the interface. Above a certain critical angle of incidence, the light is completely reflected (total internal reflection). Nevertheless, an electromagnetic field component (the evanescent wave) penetrates a short distance (about one wavelength of the incident light) into the medium of lower refractive index.

If a thin metal layer is situated at the interface and polarized monochromatic light is used, the intensity of the reflected light is markedly reduced at a specific incident angle, producing a sharp dip (Figure 13). This phenomenon is called *surface plasmon resonance* and the angle at which the dip is produced is the *SPR angle*. Because the SPR angle depends on the refractive index of the lower-density medium, measurement of changes in this angle can be used to assess refractive index changes occurring very close to the metal layer that separates the two media. In biomolecular analysis, such refractive index changes are caused, e.g., by immobilizing a protein on the surface of the metal layer and then allowing a binding partner to interact with the immobilized component. The increase in mass caused by association of the binding partner causes a measurable shift in the SPR angle.

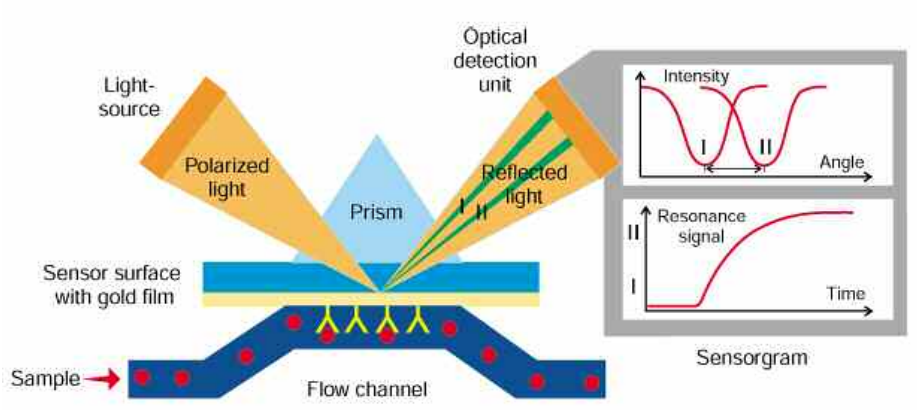

Figure 13. The SPR principle: surface plasmon resonance detects changes in the refractive index of the surface layer of a solution in contact with the sensor chip (Roos H, 2001).

III-12.3 SPR advantages

As mentioned above, the SPR technique generates real-time binding data, making it well suited to the analysis of kinetic measurements. In addition, it is possible to regenerate the sensor chip surface while retaining the immobilized ligand. This

allows a series of separate measurements to be performed on the same sensor chip, contributing to the reproducibility of the data. Another advantage is the rapidity of the analysis: immobilization of interactants on the sensor chip is performed in the instrument and typically takes about 30 min. Real-time interaction analysis takes place in the order of min and also regeneration of the surface is similarly fast.

III-12.4 SPR components

III-12.4.1 Instrument

Biosensor analyses were performed on a BIAcore 2000 instrument (*BIAcore AB*; Figure 14, top). The essential components of a BIAcore system are: the sensor chip where the interaction takes place; the optical system responsible for generation and detection of the SPR signal; a liquid handling system with precision pumps and an integrated µ-fluidic cartridge (IFC) for controlled transport of samples to the sensor surface (Figure 14, bottom).

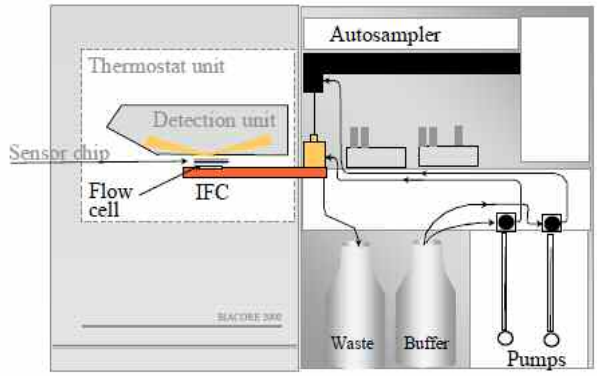

Figure 14. BIAcore 2000 system processing unit and controlling computer (top). Schematic illustration of BIAcore 2000 components (bottom) (Roos H, 2001).

In the table below (Table 2), some of the most relevant technical specifications and working ranges for the BIAcore 2000 instrument are listed.

General	
Automated	yes
Sample recovery	automatic
Fraction collection	automatic
Detection unit	
Light source	LED (Light Emitting Diode)
Wavelength	760 nm
Refractive index change	1.33 – 1.36
Baseline drift	±0.3 RU/min
Temperature control	4 – 40°C
Integrated µ-Fluidic Cartridge (IFC)	
Flow-cell number	4
Flow-cell volume	60 nL
Online subtraction of background response	flow-cells 2-1, 3-1, 4-1
Measuring ranges	
Kinetic measurements	K_a typically $10^3 – 10^7$ M^{-1} s^{-1}
	K_d typically $10^{-1} – 5 \cdot 10^{-6}$ s^{-1}
Affinity measurements at equilibrium	K_A typically $10^4 – 10^{11}$ M^{-1}

Table 2. List of some BIAcore 2000 features.

III-12.4.2 Sensor chip

The sensor chip is the signal transducer in BIAcore technology: it provides the physical conditions necessary to generate the SPR signal, and it is the place where the interaction being studied occurs. The chip is a glass slide with a thin gold layer deposited on one side (Figure 15). Gold is chosen for its chemical inertness and good SPR response. The gold film is in turn covered with a covalently bound matrix on which biomolecules can be immobilized. On most sensor chips (CM-series sensor chips), the matrix consists of carboxymethylated dextran, a flexible linear carbohydrate polymer forming a layer of approximately 100 nm. The carboxymethyl groups enhance the hydrophilicity of the dextran matrix, provide a chemical basis for covalent immobilization of biomolecules, and place negative charges that allow electrostatic concentration of positively charged molecules from the solution.

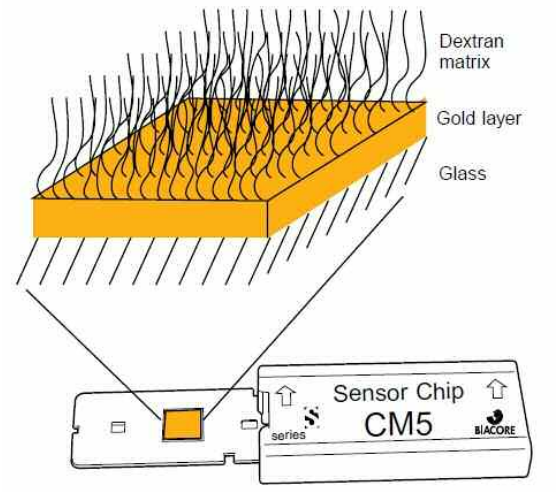

Figure 15. Sensor Chip CM5 (BIAcore Sensor Surface Handbook, *BIAcore AB*, 2003).

III-12.5 SPR experiments

III-12.5.1 Buffers, samples and temperature

All buffers for the BIAcore were degassed using a vacuum chamber and filter-sterilized with 0.22 μm filters at RT. Buffer solutions contained 0.005% surfactant P20 to minimize non-specific adsorption of proteins to the IFC channels.
Samples for analysis were dialyzed or desalted in the BIAcore sample buffer before dilutions were made, to avoid large changes in signal due to refractive index differences. Before placing samples in the sample rack, they were pulsed briefly in a microcentrifuge to dislodge air bubbles from the bottom of the container.
Surface activation, ligand attachment and binding kinetics were performed at 25°C. When running long experiments (e.g. injection of increasing analyte concentrations), samples were kept at 10°C by cooling the sample rack base through a thermoblock. Vials were also capped to prevent sample evaporation.

III-12.5.2 Immobilization of ligand by amine coupling

For all SPR experiments sensor chips CM5 (*GE Healthcare*) were used and ligand was immobilized to the carboxymethylated dextran flow cell surface by standard amine coupling chemistry. Immobilization was either direct, by covalent coupling the protein used as a ligand, or indirect, through capture by a covalently coupled molecule. Neutravidin (*Pierce*) was used for capturing biotinylated peptides. It is

a deglycosylated form of avidin that retains biotin-binding affinity ($K_A = 10^{15}$ M^{-1}), with a more neutral pI (6.3) that minimizes non-specific interactions.

BIAcore running buffer was allowed to run over the flow cell surface at 10 µL/min until the RU baseline was stable. All injections for immobilization were done at 10 µL/min. The surface was activated injecting 70 µL of a freshly prepared NHS/EDC mixture to give reactive succinimide esters (Figure 16). This activation allowed covalent coupling of the ligand via primary amine groups (mainly from lysine residues on the protein) to the flow cell surface. Consequently, buffer components containing primary amine groups and other strong nucleophilic groups (e.g. Tris, sodium azide) were avoided for amine coupling. The optimal concentration of ligand injected over the activated surface was determined empirically. Generally, the ligand was diluted to a final concentration of 10-100 µg/mL in 10 mM sodium acetate buffer and 70 µL of this were injected over the activated flow cell. The pH of acetate buffer for this injection was also determined empirically and is related to the pI of the protein. For all the proteins used, coupling in 10 mM acetate buffer pH 5.0 worked well. This procedure generally produced an increase of 2000-6000 RUs on the chip. The RU increase is proportional to the mass immobilized on the chip surface. The remaining NHS-ester active sites on the surface were then blocked with an injection of 70 µL of 1 M ethanolamine-HCl, pH 8.5.

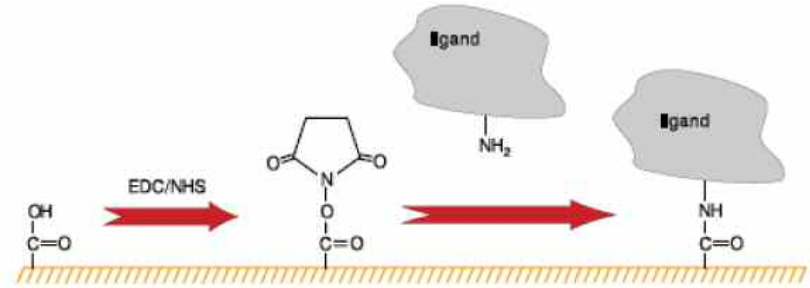

Figure 16. Amine coupling of ligands to the sensor surface: activation of the surface with the EDC/NHS mixture, and immobilization of the ligand (BIAcore Sensor Surface Handbook, *BIAcore AB*, 2003).

III-12.5.3 Binding of analyte

Binding analyses were generally performed at flow rates of 20 µL/min in order to minimize mass transport effects. Analyte injections were generally done at 100 µL/min as it was best flow rate for kinetic determinations. BIAcore sample buffer was allowed to run over the flow cell until a stable baseline was reached. When indirect immobilization of a ligand was the strategy of choice, biotinylated

peptides were captured onto the neutravidin surface before analyte injection. An aliquot of a 10 μM solution of the peptide diluted in the BIAcore sample buffer was injected at 10 μL/min for 1 min, obtaining an increase of 100-200 RUs on the chip surface. Then the protein of interest diluted in the BIAcore sample buffer was injected for 10 or 12.5 min for the association phase. Immediately at the end of the association phase the sample buffer was passed over the chip for the dissociation phase until the response returned to baseline. The association and dissociation phases together represent the sensorgram for the binding event. To maximize reproducibility between analyses, the BIAcore instrument was programmed to perform a series of experiments with increasing concentrations of analyte over the same regenerated surface. Regeneration of the surface was generally not required as the interactions being studied returned to the baseline level during dissociation phase in reasonable time. Typically, at least 5 different analyte concentrations were run, with one of the concentrations in duplicate, at the beginning and at the end of the injection series. A sample with zero analyte concentration was also included (injection of analyte buffer). Ideally, this should be a straight baseline after subtraction of the reference response: however, inclusion of such a sample in the concentration series could facilitate assessment of baseline deviations in the final data.

III-12.6 SPR data analysis

III-12.6.1 Data transformation

Sensorgrams of the interaction generated by the instrument were analyzed using the BIAevaluation 4.1 software (*BIAcore AB*). Signal at the beginning of the sensorgram was zeroed using the mean of the response 20 s before the injection. The reference surface data were subtracted from the reaction surface data to eliminate refractive index changes of the solution and injection noise. The sensorgrams obtained at different analyte concentrations were processed individually and then overlaid so association and dissociation curves could be analyzed simultaneously.

III-12.6.2 Evaluating kinetic data

Kinetic informations obtained from sensorgrams were analyzed to give values for association and dissociation rate constants and/or equilibrium constants. The initial and final 10-20 s of the association phase were excluded from the fitting

procedure to minimize sample dispersion and mass transport effects whereas entire post-injection phase was considered. Data evaluation started with global fitting to the Langmuir model, which is a theoretical model for 1:1 reversible interaction. When a poor fit was obtained using the simplest model, the binding kinetics was considered complex. Then, data from the curves were globally fitted using the set of pre-defined models provided with BIAevaluation: 1:1 binding with drifting baseline, 1:1 binding with mass transfer, bivalent analyte, heterogeneous analyte (competing reactions), heterogeneous ligand (parallel reactions), and two-state reaction (conformation change).

In general, the model data were fitted to the experimental data using the non-linear least-squares fitting processes, available in BIAevaluation software. The evaluation program calculates the best fit of the selected regions of the experimental curves to the theoretical model and provides values for the association rate (K_a) and the dissociaton rate (K_d) constants as well for the affinity constant (K_A). The quality of the data fit was assessed by visually comparing the closeness of the experimental and theoretical curves. Another important parameter considered as an indicator of the validity of the fitting was the residual plot, which represents the difference between observed and calculated data points. The form of the residual plot revealed whether there were systematic deviations between the experimental and the fitted data. The quality of the data was also assessed by looking at the χ^2 value given by the program. The χ^2 value gives a statistical measure of the goodness of fit, with values below 2 being ideal, and values below 10 being generally acceptable according to the manufacturer. An estimate of how sensitive the fitting was to changes in parameters was given by the standard error (SE) values for the data set provided by the program or by T-values (T = X/SE; where X = value of parameter such as dissociation constant). T-values greater than 10 indicated that the value obtained for the parameter was significant.

III-12.6.3 Evaluating affinity data

The affinity constant indicates the strength of binding between two molecules and can be calculated from the K_a and K_d constants ($K_A = K_a/K_d$, measured in 1/M, or its inverse $K_D = K_d/K_a$, measured in M). However, because of the difficulties associated with obtaining reliable kinetic data (i.e. the appropriateness of the model and the quality of the experimental data), equilibrium binding analysis is more accurate. It involves measuring the level of binding at equilibrium after injecting a series of analyte concentrations.

The steady-state binding level (R_{eq}) is related to concentration according to the equation:

$$R_{eq} = \frac{C * R_{max}}{C + K_D}$$

R_{max} = maximum response (total surface binding capacity) (RU)
C = concentration of the injected analyte (M)
R_{eq} values were obtained from report points set on the sensorgrams in the steady-state region of the curve. Rearranging:

$$R_{eq} = -K_D * \frac{R_{eq}}{C} + R_{max}$$

A plot of R_{eq}/C against R_{eq} at different analyte concentrations gives a straight line from which R_{max} and K_D can be calculated.

III-13 REAL-TIME PCR

III-13.1 Real-Time PCR principles

Real-Time PCR can be used for the detection and quantification of mRNA transcript abundance in a sample. Data are collected throughout the PCR process as it occurs, thus combining amplification and detection in a single step. This is achieved using fluorescent probes or dyes that correlate PCR product concentration to fluorescence intensity. Reactions are characterized by the threshold cycle (Ct), the cycle at which fluorescence intensity is greater than background fluorescence. Consequently, the higher the initial amount of the sample, the sooner accumulated product is detected in the PCR process as a significant increase in fluorescence, and the lower the Ct value.

III-13.2 Real-Time PCR experiments

Experiments were performed using the DyNAmo HS SYBR Green qPCR Kit (*FINNZYMES*). The master mix provided by the kit contains an engineered version of *Thermus brockianus* DNA polymerase and SYBR Green I fluorescent dye. The modified polymerase incorporates a non-specific DNA binding domain that confers physical stability to the polymerase-DNA complex. The polymerase is also inactive at RT in order to prevent the extension of non-specifically bound primers during reaction setup and therefore increases PCR specificity. The initial

denaturation step in the PCR protocol reactivates the hot start polymerase. SYBR Green I is specific for double-stranded DNA and fluoresces when bound to the amplified double-stranded PCR product, thereby enabling the direct quantitation of amplified DNA without labeled probes. The passive reference ROX is a dye included in the kit. It does not take part in the PCR reaction and its fluorescence remains constant during the PCR reaction. ROX provides an internal reference to which the signal can be normalized. Normalization is necessary to correct for fluorescent fluctuations due to changes in concentration or volume.

Experiments were done in 96-well plates (Optical Reaction Plate with Barcode and Optical Caps, *Applied Biosystems*) in a final volume of 50 µL per well. The reaction mixture consisted of 25 µL 2x Master Mix (Tbr DNA polymerase, SYBR Green I, buffer, 5 mM $MgCl_2$, dNTP mix including dUTP), 1 µL 50x ROX, 2.5 µL 10 µM primer FOR and REV (each), 5 µL template cDNA, 14 µL H_2O. A GeneAmp 5700 Sequence detection System including a GeneAmp 9600 thermal cycler (*Applied Biosystems*) was used. The final amplification conditions were as follows: 95°C for 15 min; followed by 40 cycles of 95°C for 15 s, 59°C for 30 s, 72°C for 40 s; then 72 °C for 10 min.

List of primers used for the project and the corresponding amplified genes (all primers are shown in 5' to 3' direction)

Gene	Primer FOR sequence	Primer REV sequence	Product length
ZASP E2-4	AGATCAAGTCGGCCAGCTAC	AGGTCTGGGAGAAGGAGGAG	237 bp
ZASP E2-5	AGATCAAGTCGGCCAGCTAC	CATTGGCTGGAGAATTGGCTAC	144 bp
ZASP E16-17	CATCAACCTGTTCAGCACCAAG	GAATGGCTGACCCTCCAGA	145 bp
ZASP E8-10	GCTGTGATCAAAACCCAAAGCA	AACGTGGGCTGTTACGTTC	190 bp
ZASP E8-11	GCTGTGATCAAAACCCAAAGCA	CGGATTCTCCACGGGACTTG	339 bp
ZASP E8-12	GCTGTGATCAAAACCCAAAGCA	GTAGCTGGTATGGGCAGAGG	408/222bp
FATZ-1	GTGGAACTTGGCATTGACCT	CAGGGAATAGGGGTTCGATTGA	227 bp
FATZ-2	TCAAGCCTGAAGGAAAAGCAGA	TGTGATCACGACGGGGATATTC	237 bp
FATZ-3	GGCAGGAGTTCACCAGCTAC	TGAGCAACCCTGTTGAAATTGG	216 bp
myotilin	GACAACGCCGGAAGAGTAAC	GCTGGGAGAGTTTGGATTGGA	151 bp
β-actin	CCTCTATGCCAACACAGTGCT	ACCGATCCACACAGAGTACTT	151 bp
GAPDH	GAACATCATCCCTGCATCCAC	GACAACCTGGTCCTCAGTGTA	235 bp

III-13.3 Real-Time PCR software analysis

At the end of the amplification reactions, the analysis software generates a series of plots containing valuable informations for quantitative analysis.

III-13.3.1 Amplification plot

The amplification plot is the plot of PCR cycle number (x-axis) versus fluorescence signal, R_n (y-axis). R_n is the ratio between the fluorescence intensity of the reporter dye and that of the passive dye. In the linear phase of PCR (the first 10-15 cycles), there is little change in fluorescence signal. Baseline fluorescence is calculated at this time. At the early exponential phase, an increase in fluorescence above the baseline indicates the detection of accumulated PCR product and it defines the threshold line. The point at which the threshold line crosses the amplification plot gives the Ct (Figure 17). The log-linear phase follows during which PCR reaches its optimal amplification period. Finally, the plateau phase is achieved when reaction components become limited and the fluorescence intensity is not longer useful for data analysis (Wong ML, and Medrano ML, 2005).

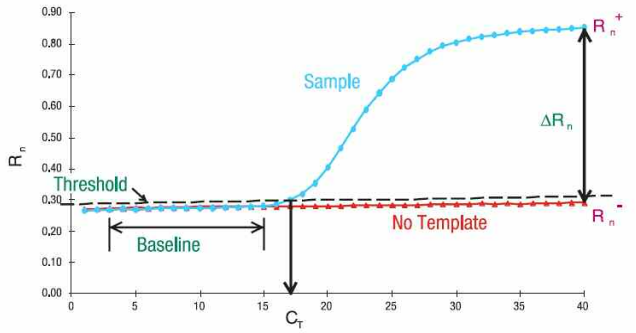

Figure 17. Illustration of an amplification plot.

III-13.3.2 Standard curve

Standard curves for each primer set were produced by running a serial dilution of template. A plot was made by relating the $\log_{10}$[template dilution] (x-axis) against the Ct value obtained for the corresponding dilution (y-axis) (Figure 18). Then, a linear interpolation was done and the slope value of the resulting straight line was used for the calculation of the reaction efficiency (E) (Pfaffl MW, 2001), according to the equation:

$$E = 10^{(-1/slope)}$$

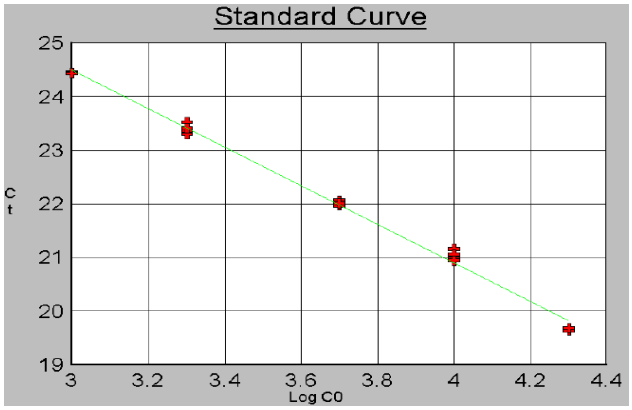

Figure 18. Example of standard curve.

III-13.3.3 Melting curve

The melting curve was used to check the specificity of the PCR product. The temperature was decreased to 60 °C and raised slowly to 95 °C using a temperature transition rate of 0.5°C/30s. By plotting the fluorescence intensity derivative (y-axis) versus the temperature (x-axis), a sharp peak in SYBR Green fluorescence was observed in correspondence of the product melting temperature (Figure 19). Specific products could be distinguished from non-specific products by the difference in their melting temperatures.

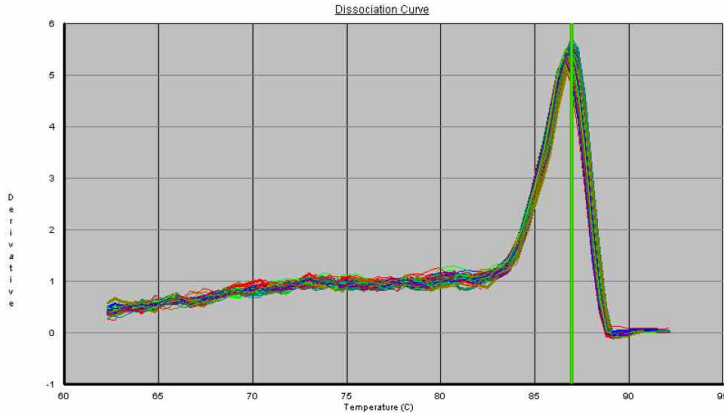

Figure 19. Example of melting curves.

III-13.4 Real-Time PCR data analysis

For the quantification of mRNA transcription the relative method was used. Relative quantification is commonly used to compare the expression levels of a target gene with a reference gene in a specific tissue or the expression levels of a gene in different tissues. When studying gene expression, the quantity of the target gene transcript needs to be normalized against variation in sample quality

and quantity between samples. To ensure identical starting conditions, the relative expression data were normalized by means of reference genes. A gene used as a reference should have a constant expression level independent of the variation in the state of the sample tissue. β-actin and GAPDH were the genes of choice for the project.

Product accumulation during a PCR reaction is represented by the equation (Marino JH et al., 2003):

$$N_t = No * E^{Ct}$$

N_o = *number of amplicons at the beginning of the reaction*
N_t = *number of amplicons at the end of cycle number Ct*
E = efficiency of the reaction. Ideally, it should be 2, indicating that the amount of product exactly doubles with each cycle.

Given two different genes A and B expressed in a specific tissue, the ratio (R) of the initial amplicon abundance between the target gene A and the reference gene B is:

$$R = \frac{N_{o\,(A)}}{N_{o\,(B)}} = \frac{N_{(A)} / E_{(A)}^{\,Ct(A)}}{N_{(B)} / E_{(B)}^{\,Ct(B)}}$$

When the amplicon population growth has reached an identical point in each PCR reaction, i.e. $N_{(A)} = N_{(B)}$, and assuming that the amplification efficiency of the amplicon for the two cDNA populations is equal ($E_{(A)} = E_{(B)}$), the equation becomes:

$$R = E^{Ct(B) - Ct(A)} = E^{\Delta Ct}$$

The R value provides the number of times the target gene A is expressed compared to the reference gene B in the considered tissue.

Three template dilutions in duplicate were made for every gene in every tissue, obtaining six different Ct values. In order to calculate the R ratio, one Ct value for the target gene and one for the reference gene were needed. Usually, it is achieved by averaging the six Ct values. However, a new analysis method was developed,

consisting in the normalization of Ct values. In practice, Ct values obtained at different template dilutions were recalculated by relating them to a reference dilution. In this way, each Ct value can be individually evaluated and excluded from data analysis if not reliable. The normalized Ct value was calculated for each template dilution using the equation:

$$Ct_{norm} = Ct + log_E \frac{C}{C_{ref}}$$

C = sample dilution
C_{ref} = selected reference dilution

For example, a sample diluted eight times compared to a reference dilution would have a $Ct_{norm} = Ct + \log_2 (1/8) = Ct - 3$, assuming 2 the reaction efficiency. It means that three less PCR cycles would have required to reach the same fluorescence signal, if the reaction had started with the reference dilution.

The ΔR error was then calculated according to the propagation error theory, considering an exponential function where the exponent is constituted by the difference between two factors:

$$\Delta R = R * \ln E * \sqrt{(\delta A)^2 + (\delta B)^2}$$

δA =standard deviation of the normalized Ct values for each target gene
δB = error associated to the geometric mean of the normalized Ct values for the reference genes.

IV RESULTS

The Z-disc of striated muscle cells is a highly specialized structure, consisting of dozens of proteins assembled into a multiprotein complex. Several Z-disc proteins, such as telethonin (Valle G et al., 1997), ZASP (Faulkner G et al., 1999), FATZ (Faulkner G et al., 2000), and ANKRD2 (Pallavicini A et al., 2001) were discovered and characterized in the laboratory where I carried out my research, in collaboration with the muscle molecular biology group at ICGEB, Trieste. The main goal of my project was to understand the complex network of protein-protein interactions occurring at Z-disc of skeletal and cardiac muscle. In particular, my work has been focused on two groups of Z-disc proteins: the FATZ and myotilin protein families on one hand, and some proteins belonging to the enigma family on the other hand.

IV-1 The FATZ and myotilin families share high similarity at their extreme C-termini

In collaboration with the groups of Dr. G. Faulkner at ICGEB, Trieste, and Prof. O. Carpen at University of Turku, Finland, we noted that the C-terminal five amino acids of FATZ-1 (ETEEL), FATZ-2 (ESEDL), FATZ-3 (ESEEL), myotilin (ESEEL), palladin (ESEDL) and myopalladin (ESDEL) are highly similar (Figure 20). Interestingly, those of FATZ-2 and palladin (ESEDL) are identical as are those of FATZ-3 and myotilin (ESEEL).

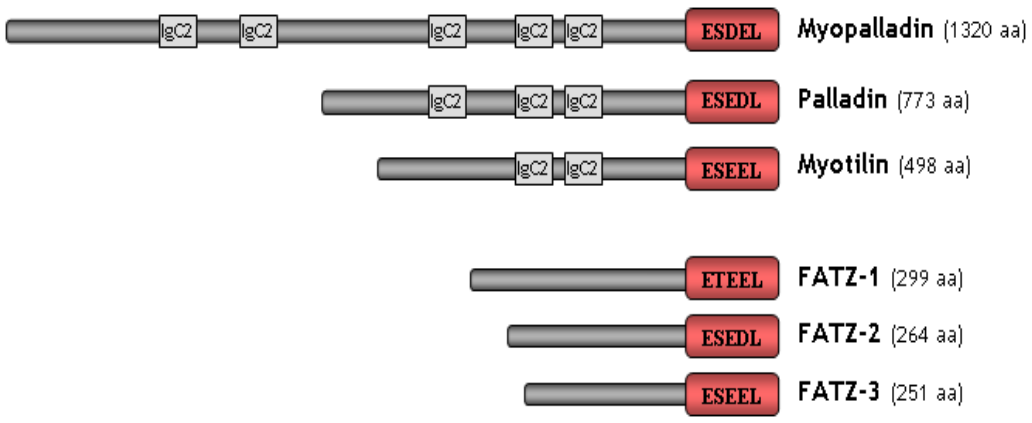

Figure 20. Schematic diagram showing the myotilin family of proteins with their Ig-like domains (IgC2) and the FATZ family of proteins. All these proteins share high similarity at their C-terminal five amino acids.

This high similarity raised the question of whether these proteins could interact via their C-termini with the same protein or proteins, then the possibility that the C-terminal five amino acids in FATZ and myotilin families would represent a new binding motif involved in protein interactions.

First, we wanted to verify if this putative binding motif was shared by other proteins. A program was written by my supervisor Prof. G. Valle, CRIBI, Padova, to extract proteins from any database with the last five amino acids having the motif E-[S/T]-[D/E]-[D/E]-L. The last eight amino acids were considered but only the terminal five amino acids were given the following weights: P_0 [L]=2, P_{-1} [D or E]=1, P_{-2} [D or E]=1, P_{-3} [S or T]=1, P_{-4} [E]=1. The last amino acid had a higher weight since it has previously been shown that the nature of this residue can strongly influence the binding with the PDZ domain (Harris BZ, and Lim WA, 2001). A score of 6 was assigned when all of the criteria were met. The program was used to scan the UniProt Knowledgebase Release 11.3 (UniProtKB/Swiss-Prot Protein Knowledgebase Release 53.3 and UniProtKB/TrEMBL Protein Database Release 36.3 of July 10, 2007). Data are reported in Table 3 only for proteins with a score of 6, corresponding to an exact match for the motif E-[S/T]-[D/E]-[D/E]-L. Notably, the motif was found in Vertebrates to be restricted to the FATZ family of proteins, myotilin, palladin and myopalladin. There is an exception represented by the histidine ammonia-lyase that has its final C-terminal amino acids (ESEDL) identical to those of FATZ-2 and palladin. Proteins of both FATZ and myotilin families are localized in the Z-disc of striated muscle and have a role in muscle or cytoskeletal structure and/or function. The fact that the motif is evolutionary conserved from zebrafish to humans may suggest its importance for the biological function of the proteins containing it.

Score	C-terminal	SwissProt	Protein
6	LDG**ETEEL**	Q9NP98	**MYOZ1_HUMAN FATZ-1 (Myozenin-1/Calsarcin-2)**
6	LDG**ETEEL**	Q1AG03	Q1AG03_CANFA Calsarcin 2 - Canis familiaris (Dog)
6	LDG**ETEEL**	Q8SQ24	MYOZ1_BOVIN Myozenin-1 - Bos taurus (Bovine)
6	LDG**ETEEL**	Q4PS85	MYOZ1_PIG Myozenin-1 - Sus scrofa (Pig)
6	LDG**ETEEL**	Q1AG02	Q1AG02_RABIT Calsarcin 2 - Oryctolagus cuniculus (Rabbit).
6	LDG**ETEEL**	Q9JK37	MYOZ1_MOUSE Myozenin-1 - Mus musculus (Mouse)
6	VDG**ETEEL**	Q6DIU0	Q6DIU0_XENTR Myozenin 1 - Xenopus tropicalis
6	MDG**ETEEL**	Q7SYY0	Q7SYY0_XENLA Myoz1-prov protein - Xenopus laevis
6	FDG**ETDDL**	Q6DHF0	Q6DHF0_DANRE Zgc:92347 - Danio rerio (Zebrafish).
6	SSE**ETDDL**	Q1JQ62	Q1JQ62_DANRE Si:ch211-238e6.5 - Danio rerio (H-L-H protein)
6	FDG**ETDEL**	Q4SQM4	Q4SQM4_TETNG Chromosome 17 SCAF14532, Calsarcin rel.
6	TVP**ESEDL**	Q9NPC6	**MYOZ2_HUMAN FATZ-2 (Myozenin-2/Calsarcin-1)**
6	TVP**ESEDL**	Q5R6I2	MYOZ2_PONPY Myozenin-2 - Pongo pygmaeus (Orangutan)
6	TIP**ESEDL**	Q5E9V3	MYOZ2_BOVIN Myozenin-2 - Bos taurus (Bovine)
6	TIP**ESDDL**	Q1AG08	Q1AG08_PIG Calsarcin 1 - Sus scrofa (Pig)
6	TVP**ESDDL**	Q9JJW5	MYOZ2_MOUSE Myozenin-2 - Mus musculus (Mouse)
6	EIP**ESDDL**	Q8AVF9	Q8AVF9_XENLA Myoz2-prov protein - Xenopus laevis.
6	EIP**ESDDL**	Q5I0T4	Q5I0T4_XENTR Myozenin 2 - Xenopus tropicalis
6	FIP**ESDDL**	Q6P2T2	Q6P2T2_DANRE Myozenin 2 - Danio rerio (Zebrafish)
6	ALV**ESEDL**	Q7L3E0	**Q7L3E0_HUMAN Palladin protein - Homo sapiens**
6	ALV**ESEDL**	Q4R5Y9	Q4R5Y9_MACFA Testis cDNA, clone: QtsA-19723
6	GLV**ESEDL**	Q3MHW8	Q3MHW8_BOVIN PALLD protein - Bos taurus (Bovine)
6	GLV**ESEDL**	Q6DFX7	Q6DFX7_MOUSE Palld protein - Mus musculus (Mouse)
6	GLV**ESDDL**	Q4RKT9	Q4RKT9_TETNG Chromosome 1 SCAF15025, whole genome
6	*KIP**ESEDL***	*Q4VB93*	***Q4VB93_HUMAN Histidine ammonia-lyase - Homo sapiens***
6	*TIP**ESDDL***	*P35492*	*HUTH_MOUSE Histidine ammonia-lyase - Mus musculus*
6	*TIP**ESDDL***	*P21213*	*HUTH_RAT Histidine ammonia-lyase - Rattus norvegicus.*
6	*TIP**ESDDL***	*Q76N86*	*Q76N86_RAT Histidase - Rattus norvegicus (Rat)*
6	SVV**ESDEL**	Q86TC9	**MYPN_HUMAN Myopalladin - Homo sapiens**
6	SVV**ESDEL**	Q5DTJ9	MYPN_MOUSE Myopalladin - Mus musculus (Mouse)
6	SVV**ESDEL**	Q86TC92	MYPN_HUMAN Isoform 2 of Q86TC9 - Homo sapiens (Human)
6	NLP**ESEEL**	Q8TDC0	**MYOZ3_HUMAN FATZ-3 (Myozenin-3/Calsarcin-3)**
6	NLP**ESEEL**	Q8TDC02	MYOZ3_HUMAN Isoform 2 of Q8TDC0 - Homo sapiens
6	NLP**ESEEL**	Q08DI7	Q08DI7_BOVIN Myozenin 3 - Bos taurus (Bovine)
6	NLP**ESEEL**	Q1AG05	Q1AG05_PIG Calsarcin 3 - Sus scrofa (Pig)
6	KLP**ESEEL**	Q8R4E4	MYOZ3_MOUSE Myozenin-3 - Mus musculus (Mouse)
6	KLP**ESEEL**	Q9Z3272	SYNPO_RAT Isoform 2 of Q9Z327 - Rattus norvegicus
6	GLY**ESEEL**	Q9UBF9	**MYOTI_HUMAN Myotilin - Homo sapiens**
6	GLY**ESEEL**	Q0VCX9	Q0VCX9_BOVIN Similar to titin immunoglobulin domain protein
6	GLY**ESEEL**	Q9JIF9	MYOTI_MOUSE Myotilin - Mus musculus (Mouse)

Table 3. Results of the protein database scan for the motif E-[S/T]-[D/E]-[D/E]-L. FATZ-1, FATZ-2, FATZ-3, myotilin, palladin and myopalladin are underlined in yellow. These proteins are members of the FATZ and myotilin families of mainly sarcomeric proteins. Histidine ammonia-lyase is underlined in red as it is not generally not found in muscle.

IV-2 Characterization of the interaction between the FATZ and myotilin families and enigma family proteins using the AlphaScreen technique

As described in the Introduction, proteins of the FATZ family can bind to ZASP. These interactions occurred with both the short ZASP isoforms (having only the N-terminal PDZ domain) and the long ones (including the three C-terminal LIM domains), suggesting that the binding involved the N-terminal region of ZASP. However, the precise binding site has not been mapped on the FATZ proteins before. More recently, in the laboratory of Prof. O. Carpen the result of a two-hybrid experiment revealed an interaction between ZASP and myotilin through its C-terminus and their colocalization at the Z-disc (von Nandelstadh P et al., 2009). On the basis of these data and considering our previous observations, it has been speculated that the last five amino acids of the C-terminal of all myotilin and FATZ family members could have a role in the interaction with ZASP. This hypothesis was further strengthened by informations obtained with the ELM program (Puntervoll P et al., 2003), which predicted that the terminal four amino acids of FATZ-1, FATZ-2, FATZ-3, myotilin, palladin and myopalladin constituted a binding motif for class III PDZ domain proteins. The binding motif is X-[D/E]-X-[V/I/L], where X is any amino acid.

PDZ domains commonly recognize short sequences (4 to 6 aa in length) located at the very C-termini of interacting partners. The AlphaScreen technique (details in Materials and Methods chapter) was used as a quantitative method to measure binding between the PDZ domains of ZASP, ALP and CLP-36 and proteins of the FATZ family and myotilin. ZASP, ALP and CLP-36 belong to the enigma family of proteins together with enigma, ENH, RIL and mystique. These proteins are characterized by a single N-terminal PDZ domain and one to three C-terminal LIM domains. ZASP, ALP and CLP-36 have in common another binding motif called ZM in their internal region. A schematic representation of the enigma family members object of my study is reported in Figure 21. The ZASP-1 isoform lacks the three C-terminal LIM domains. This was the variant used in the experiments of this thesis as it was the form detected by yeast two-hybrid assays to bind to myotilin (von Nandelstadh P et al., 2009). In order to verify if the binding to the PDZ domains could involve the terminal five amino acids of the FATZ proteins and myotilin, both the full-length and the truncated version (lacking the C-terminal five amino acids) of these proteins were produced. All of the native proteins used for AlphaScreen experiments were kindly provided by Dr. G. Faulkner. Since the proteins used in these experiments were expressed in bacteria they were not phosphorylated. Also α-actinin-2 (ACTN2) was introduced

in the study since its C-terminal region has previously been shown to interact with the PDZ domain of ZASP (Zhou Q et al., 1999; Faulkner G et al., 1999) and ALP (Klaavuniemi T et al., 2004). In addition, the four C-terminal residues of α-actinin-2 fits with the consensus ligand sequence of class I PDZ domains, which recognize an X-[S/T]-X-[V/I/L] C-terminal motif according to the ELM program (Puntervoll P et al., 2003).

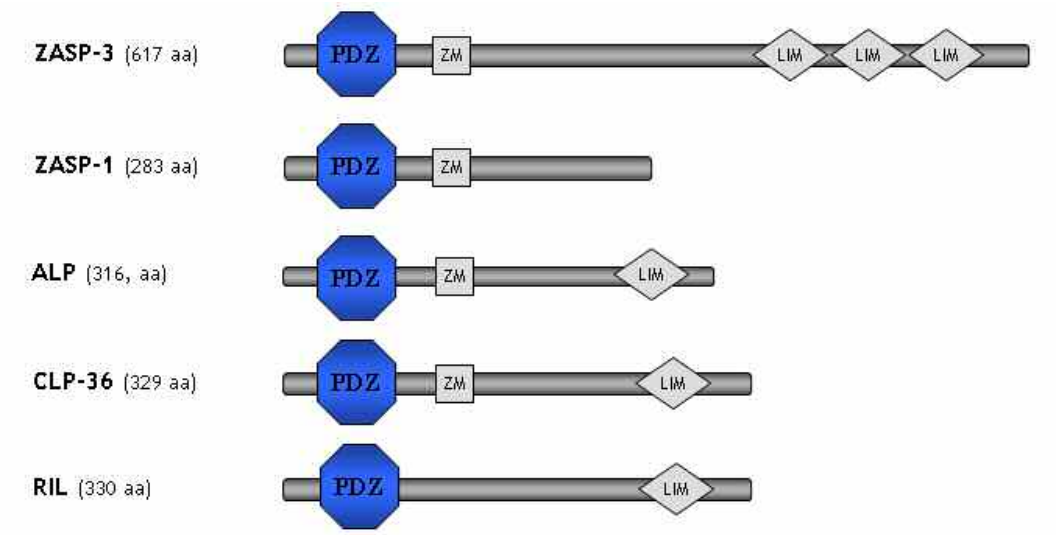

Figure 21. Schematic diagram showing some of the proteins of the enigma family with their different binding domains: ZASP, ALP, CLP-36 and RIL. All these proteins have a N-terminal PDZ domain and C-terminal LIM domains with the exception of the ZASP-1 isoform that has not LIM domains. The ZASP-1 isoform was used in all of the experiments reported in this thesis. ZASP, ALP and CLP-36 contain an additional internal binding motif called ZM.

The biotinylated HIS-tagged PDZ domain proteins ZASP, ALP and CLP-36 were bound to the streptavidin Donor beads, whereas the GST recombinant proteins FATZ-1, FATZ-2, FATZ-3, myotilin and α-actinin-2 were bound to the anti-GST Acceptor beads. The PDZ domains and their ligand proteins were both used at a concentration of 50 nM. The results shown are the mean of nine different experiments and the standard deviations of the means are plotted at the top of each column (Figure 22). As can be seen from the graph, all of the proteins studied (FATZ-1, FATZ-2, FATZ-3, myotilin and α-actinin-2) behaved as ligands for the PDZ domains of the enigma family members ZASP, ALP and CLP-36, even though with some variability depending on ligand and PDZ domain. In general, the PDZ domain of ZASP showed much stronger binding to the ligand proteins than the PDZ domains of ALP or CLP-36 with the exception of α-actinin-2 that had stronger binding to the PDZ domain of CLP-36. The best ligand protein for overall binding was FATZ-2 whereas FATZ-3 bound poorly to the three PDZ

domains studied. On the contrary, all of the truncated proteins did not interact with the PDZ domains of ZASP, ALP and CLP-36. In the interest of clarity, only the result for the truncated FATZ-2 protein is shown in Figure 22, but the C-terminal truncated form was produced and tested for each protein.

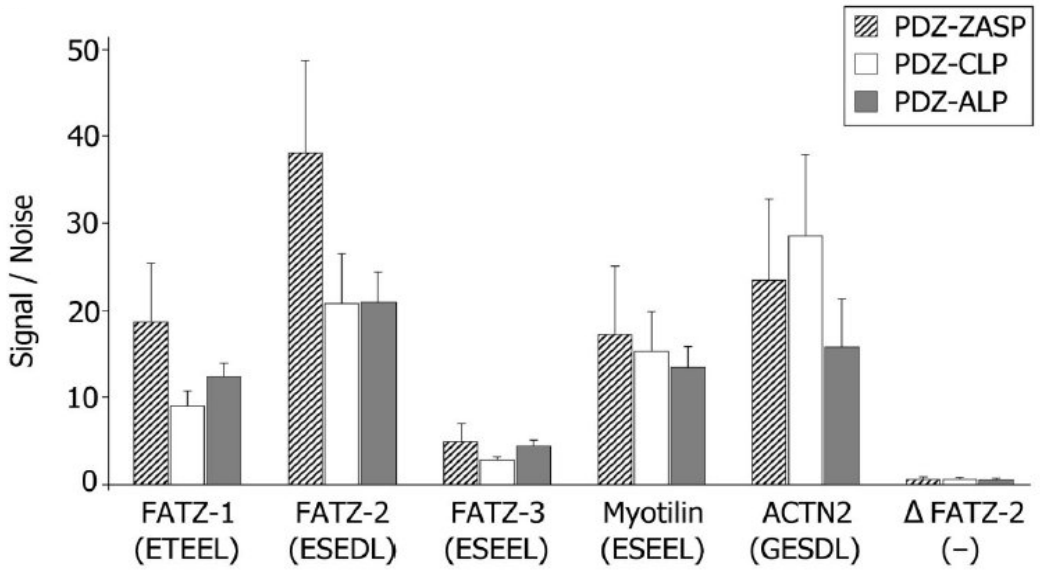

Figure 22. AlphaScreen interaction experiments between the HIS-tagged PDZ domains of ZASP, ALP and CLP-36 and the GST recombinant full-length and truncated (minus the C-terminal five amino acids) forms of FATZ-1, FATZ-2, FATZ-3, myotilin and α-actinin-2. Here, only the result for the truncated FATZ-2 protein is reported in the interest of clarity. The concentration of all the proteins was 50 nM. The experiment was repeated nine times and the standard deviations of the means are shown as bars at the top of the histograms.

IV-3 Peptides corresponding to the C-terminal amino acids of the FATZ and myotilin families bind to the PDZ domains of ZASP, ALP and CLP-36

The result of the database search shown in Table 3 suggested that also palladin and myopalladin share the motif E-[S/T]-[D/E]-[D/E]-L and therefore would be able to interact with the same PDZ domains. In order to demonstrate the specificity of this binding, we designed peptides corresponding to the final five amino acids of FATZ-1 (ETEEL), FATZ-2/palladin (ESEDL), FATZ-3/myotilin (ESEEL) and myopalladin (ESDEL). Also the GESDL peptide was synthesized, corresponding to the final five amino acids of α-actinin-2. Although this motif is different as compared with the other peptides, it is conform to a class of ligands recognized by PDZ domains (Jeleń F et al., 2003). Another peptide was synthesized, named ESEEE, with the final amino acid changed from leucine (L) to

glutamic acid (E). It is known that the type of amino acid at position P_0 is important for the binding between the ligand and the PDZ domain since changing this amino acid can either destroy or alter the binding (Harris BZ, and Lim WA, 2001).

The biotinylated peptides were bound to the streptavidin Donor beads, whereas the HIS-tagged PDZ domains of ZASP, ALP and CLP-36 were bound to the Nickel Chelate Acceptor beads. The PDZ domains were used at a concentration of 50 nM; the ETEEL, ESEDL and ESEEL peptides were used at a concentration of 10 nM, whereas ESDEL, GESDL and ESEEE were used at concentrations of 25 nM, 50 nM and 50 nM, respectively. As a consequence, the binding detected for these peptides, when compared to the others, is even lower than that depicted in Figure 23. The results shown are the mean of at least three different experiments and the standard deviations of the means are plotted at the top of each column (Figure 23).

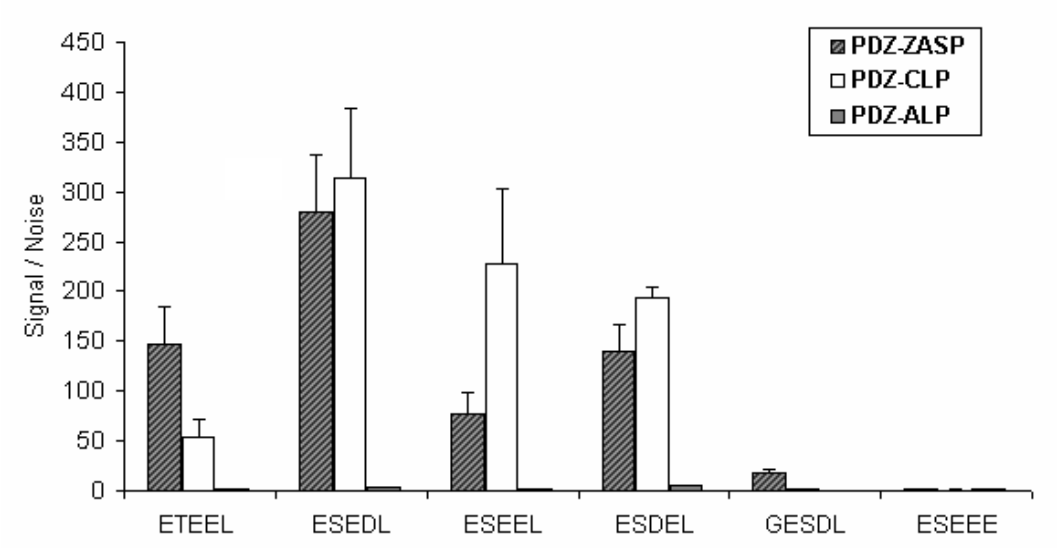

Figure 23. AlphaScreen interaction experiments between the HIS-tagged PDZ domains of ZASP, ALP and CLP-36 and the biotinylated peptides corresponding to the last five amino acids of FATZ-1, FATZ-2/palladin, FATZ-3/myotilin, myopalladin and α-actinin-2. A mutated peptide with the last amino acid changed from L to E was also used. The concentration of the PDZ proteins was 50 nM; the ETEEL, ESEDL and ESEEL peptides were used at 10 nM, ESDEL at 25 nM, GESDL and ESEEE at 50 nM. The experiment was repeated at least three times and the standard deviations of the means are shown as bars at the top of the histograms.

From the results of the AlphaScreen experiments it is clear that all of the peptides bind to the different PDZ domain proteins with the exception of the mutated peptide ESEEE. The FATZ-1 and α-actinin-2 peptides seem to bind better to the PDZ domain of ZASP, the FATZ-2/palladin peptide binds with the same strength

to the PDZ domain of ZASP and CLP-36, whereas the FATZ-3/myotilin and myopalladin peptides both bind better to the PDZ domain of CLP-36. The binding to the ALP-PDZ domain was particularly weak in all cases.

IV-4 Phosphorylation of the C-terminal peptides affects the binding activity to the PDZ domains of ZASP, ALP and CLP-36

As described in the Introduction, the interaction between the PDZ domain and its ligand is often regulated by phosphorylation of the ligand sequence. The C-terminal sequence of the FATZ and myotilin families proteins and that of α-actinin-2 contains a potential phosphorylation site (S or T). To evaluate the effect of phosphorylation on the binding between the peptides and the PDZ domains, we designed peptides phosphorylated on either the serine (EpSEDL, EpSEEL, EpSDEL, GEpSDL) or the threonine (EpTEEL) residues. To test the specificity of the binding, we also designed a phosphopeptide in which the last amino acid was changed from L to E (EpSEEE). We then tested these peptides for the interaction with the PDZ domains of ZASP, ALP and CLP-36 using AlphaScreen (Figure 24).

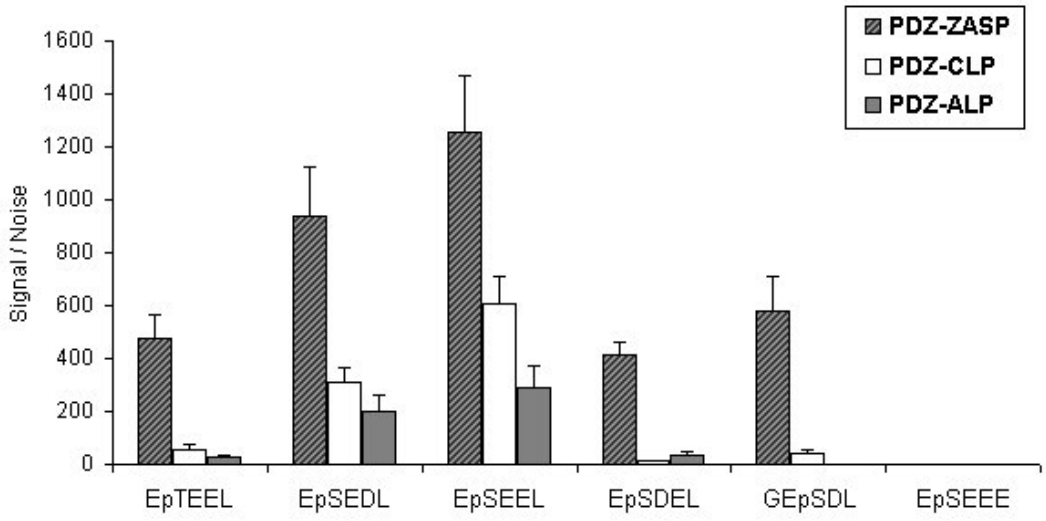

Figure 24. AlphaScreen interaction experiments between the HIS-tagged PDZ domains of ZASP, ALP and CLP-36 and the biotinylated phosphorylated peptides. The concentration of the PDZ proteins was 50 nM; the EpTEEL, EpSEDL and EpSEEL peptides were used at 10 nM, EpSDEL at 25 nM, GEpSDL and EpSEEE at 50 nM. The experiment was repeated at least three times and the standard deviations of the means are shown as bars at the top of the histograms.

The biotinylated phosphorylated peptides were bound to the streptavidin Donor beads, whereas the HIS-tagged PDZ domains of ZASP, ALP and CLP-36 were

bound to the Nickel Chelate Acceptor beads. The concentrations of the PDZ domains and peptides were the same of the previous experiment, and also in this case the results represent the mean of at least three different experiments.
As can be seen from the graph, all of the phosphopeptides showed increased but highly different binding activity to ZASP PDZ domain. The strongest binding being that of the FATZ-3/myotilin peptide followed in order of decreasing strength by that of FATZ-2/palladin, FATZ-1, α-actinin-2 and myopalladin. I would like to remark that the EpSDEL and GEpSDL peptides were used at a higher concentration compared to the other peptides. Only the FATZ-2/palladin and FATZ-3/myotilin peptides showed appreciable binding to the PDZ domain of CLP-36, whereas in the case of ALP PDZ domain the phosphorylated peptide ligands showed better binding although this did not reach the values seen for the other PDZ domains. The mutated peptide EpSEEE did not show any interaction with the three PDZ domains.

IV-5 Overview of the effect of phosphorylation on the binding of the peptide ligands to the PDZ domains

An overview of the changes seen in the strength of binding due to phosphorylation of the ligand is given in Figure 25. Results are shown as Log_2 of the ratio between phosphorylated and non-phosphorylated peptides.

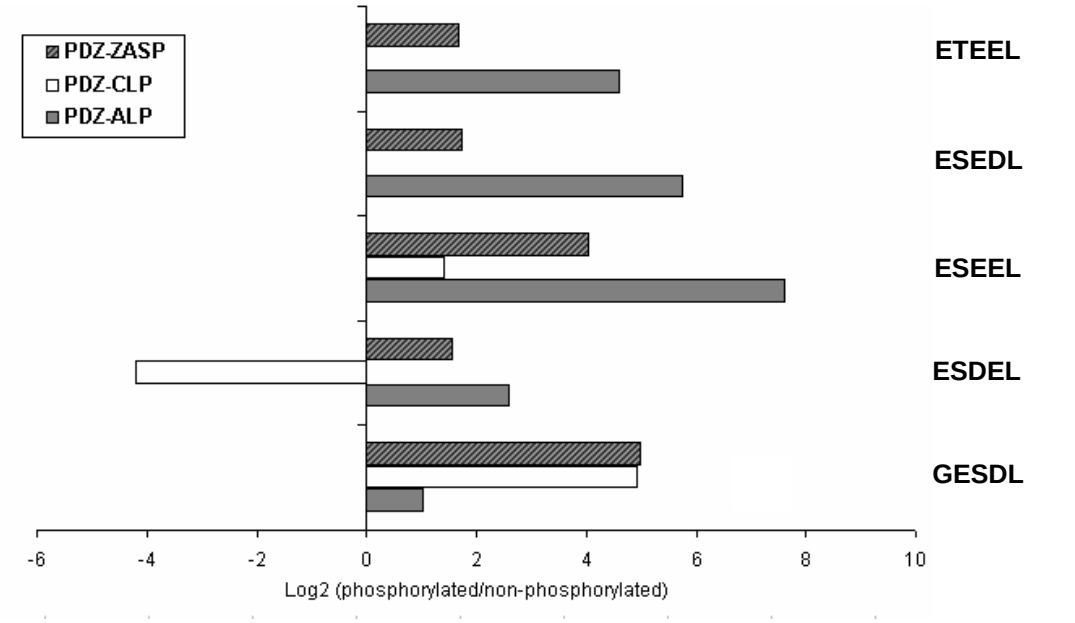

Figure 25. An overview of the effect of phosphorylation of the peptide ligands on the binding to the PDZ domains of ZASP, ALP and CLP-36.

In practical terms, the Log_2 values indicate how many times you have to double, or half if negative, the non-phosphorylated value to obtain that of the phosphorylated. As can be seen from the figure, the strength of the binding interactions varied between the peptides and the PDZ domains considered. The results for the mutated peptide phosphorylated (EpSEEE) or not-phosphorylated (ESEEE) are not reported since they did not show any binding with the PDZ domains of ZASP, ALP and CLP-36. This result agrees with the known literature on PDZ domain interactions, namely that the last amino acid of the ligand protein is crucial for its interaction with the PDZ domain. Therefore, we can conclude that this observation is also true for the binding of the E-[S/T]-[D/E]-[D/E]-L ligand to the three PDZ domains studied. For the FATZ-1 (ETEEL, EpTEEL) and FATZ-2/palladin (ESEDL, EpSEDL) peptides phosphorylation appears to be an advantage for the binding to ZASP and ALP PDZ domains. On the other hand, the binding to CLP-36 PDZ domain was not affected by phosphorylation. For the FATZ-3/myotilin (ESEEL, EpSEEL) and α-actinin-2 (GESDL, GEpSDL) peptides phosphorylation had a positive effect on the interaction with all the three PDZ domains. For the myopalladin (ESDEL, EpSDEL) peptide phosphorylation increased the binding to the PDZ domains of ZASP and ALP, whereas it negatively affected the binding to CLP-36 PDZ domain. These results demonstrate that phosphorylation seems to regulate the binding activity between the PDZ domain and its ligands and that the type of the final amino acid of the ligand is crucial for this interaction.

IV-6 The C-terminal of FATZ-1 competes with the interaction between ZASP-1 and FATZ-3/myotilin peptide ligand

One of the advantages of the AlphaScreen technique is that it can be used for competition studies. In this kind of assays we want to evaluate the effect of a third protein on the binding between two interacting partners (Figure 26).
The C-terminal domain of the FATZ-1 protein (CD2) was used as competitor of the interaction between the ZASP-1 protein and the phosphorylated and non-phosphorylated peptides of FATZ-3/myotilin. CD2 is the C-terminal region of FATZ-1 comprising aa 171-299 (Faulkner G et al., 2000) and therefore it has the ETEEL motif, which is capable of binding the PDZ domain of ZASP. ZASP-1 and peptides were used at fixed concentrations: 100 nM for the protein and 50 nM for the phosphorylated and non-phosphorylated peptides. The FATZ-1-CD2 competitor was then added at increasing concentrations, ranging from 0 to 200 nM (Figure 27). The graphs clearly show that the FATZ-1-CD2 fragment was

able to compete with the interactions between ZASP-1 and both the non-phosphorylated (ESEEL) and phosphorylated (EpSEEL) peptide ligands. However, 10 times less (10 nM instead of 100 nM) FATZ-1-CD2 protein was required to markedly reduce the binding of ZASP-1 to the non-phosphorylated ligand compared to that of the phosphorylated ligand. This result correlates well with our previous finding that the ZASP PDZ domain bound better to phosphorylated than non-phosphorylated FATZ-3/myotilin peptide. This experiment also confirms that AlphaScreen can qualitatively measure the strength of binding and that the ZASP-1 full-length protein behaves in a similar manner to the PDZ domain alone.

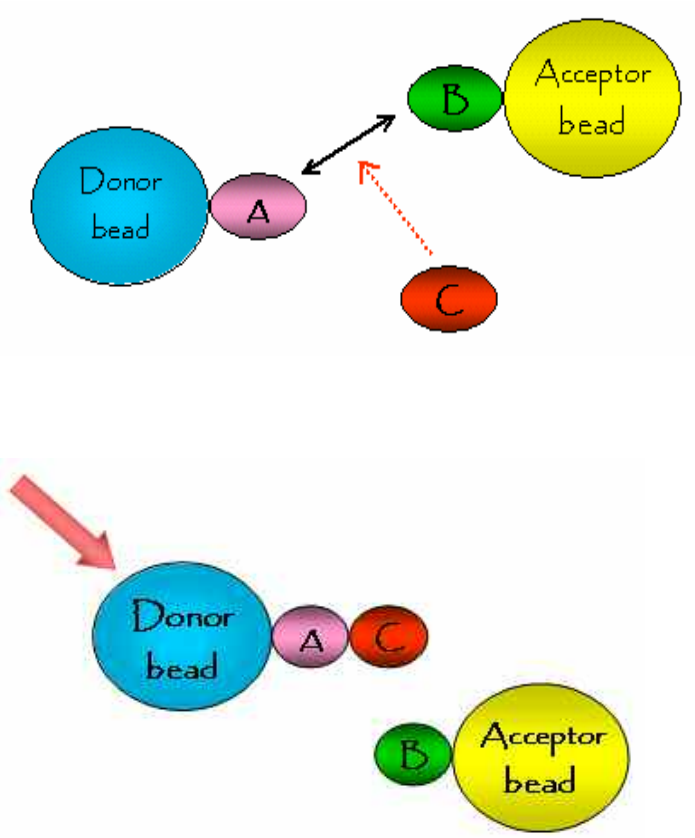

Figure 26. Schematic diagrams showing the effect of a third molecule on the binding between two interacting partners. The two proteins A and B can bind to each other (top). The presence of the third protein C prevents this interaction with the consequence that no AlphaScreen signal is detected (bottom).

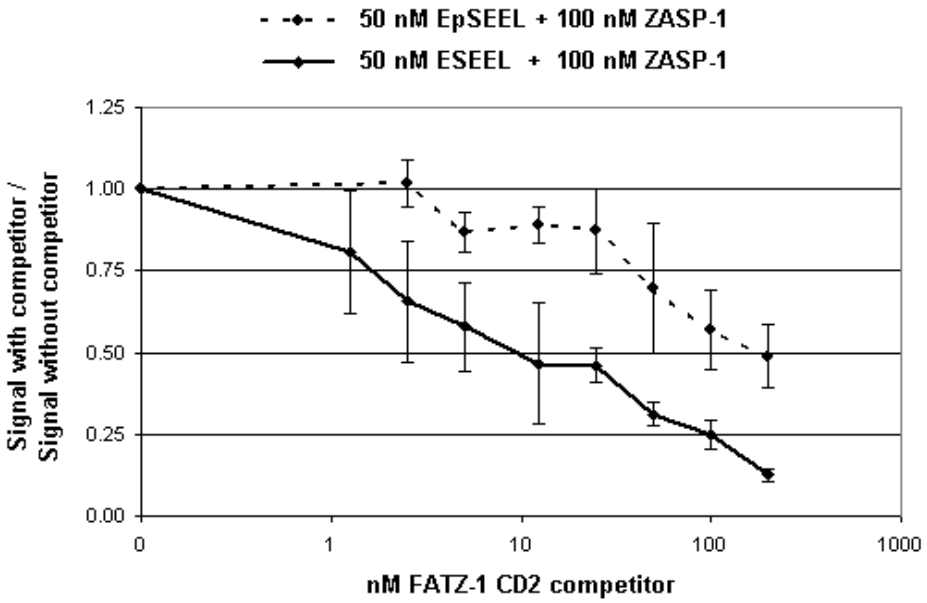

Figure 27. AlphaScreen competition assay. C-terminal FATZ-1 (FATZ-1 CD2) protein competes with the interaction between ZASP-1 (100 nM) and the non-phosphorylated (ESEEL) and phosphorylated (EpSEEL) FATZ3/myotilin peptide ligands (50 nM both). The results shown are the mean of at least three different experiments and the standard deviations of the mean are given for each point. Each point denotes the signal obtained in the presence of the competitor divided by the signal obtained without the competitor.

IV-7 The α-actinin-2 protein competes with the interaction between ZASP-1 and FATZ-3/myotilin peptide ligand

As reported above, α-actinin-2 binds to the PDZ domain of ZASP, ALP and CLP-36 via the final five amino acids of its C-terminal, GESDL. This sequence represents a binding motif for class I PDZ domain proteins. However, the three PDZ domains can also be classified as class III PDZ domains since their interactions with the C-termini of FATZ and myotilin families. Therefore, we wanted to check if α-actinin-2 was capable of competing the binding between the ZASP-1 protein and the phosphorylated and non-phosphorylated peptides of FATZ-3/myotilin. As in the previous competition experiment, ZASP-1 and peptides were used at 100 nM and 50 nM, respectively; then, increasing amounts of α-actinin-2 were added to this interaction (Figure 28). From the graphs we can observe that α-actinin-2 competed better with the interaction between ZASP-1 and the non-phosphorylated peptide (ESEEL). Although the competition was not as striking as that seen using the C-terminal FATZ-1 protein as competitor, α-actinin-2 is capable of interfering with the interaction between a different class of PDZ domain and its ligands.

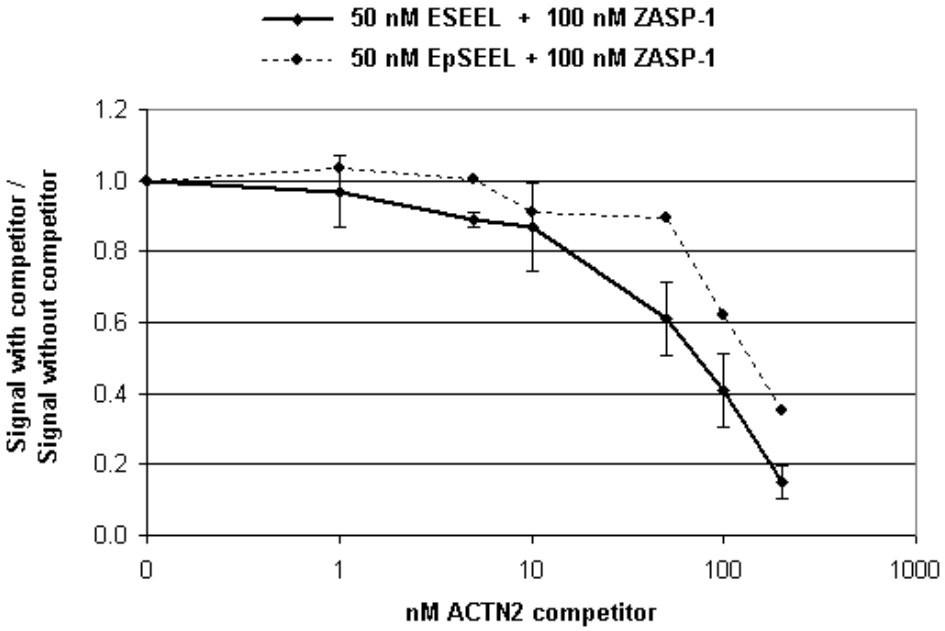

Figure 28. AlphaScreen competition assay. α-actinin-2 protein competes with the interaction between ZASP-1 (100 nM) and the non-phosphorylated (ESEEL) and phosphorylated (EpSEEL) FATZ3/myotilin peptide ligands (50 nM both).

IV-8 PDZ binding specificity of the E-[S/T]-[D/E]-[D/E]-L motif

At this point it was important to know if the E-[S/T]-[D/E]-[D/E]-L motif was specific for a set of PDZ domains or if it bound to any PDZ domains. For this purpose, the TranSignal PDZ Domain Array from *Panomics* was used (Figure 29). It is a commercial array containing 28 different human PDZ domains spotted in duplicate as well as positive and negative control proteins. This array contains the PDZ domain of CLP-36 (hCLIM1) but not those of ZASP and ALP; therefore, only the results for CLP-36 can be directly compared with those of AlphaScreen experiments. However, the membrane possesses the PDZ domain of RIL, another member of the enigma family of proteins.

The PDZ array experiments were done in collaboration with the group of muscle molecular biology at ICGEB. The same biotinylated phosphorylated and non-phosphorylated peptides used for the AlphaScreen assays were employed but at a concentration of 0.3 μg/mL. Also a native HIS-tagged C-terminal FATZ-3 protein (aa 81-251) was used as ligand on the PDZ array at a concentration of 15 μg/mL.

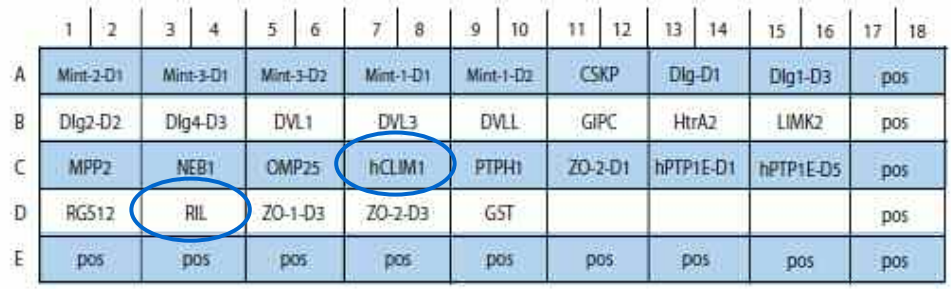

	1 2	3 4	5 6	7 8	9 10	11 12	13 14	15 16	17 18
A	Mint-2-D1	Mint-3-D1	Mint-3-D2	Mint-1-D1	Mint-1-D2	CSKP	Dlg-D1	Dlg1-D3	pos
B	Dlg2-D2	Dlg4-D3	DVL1	DVL3	DVLL	GIPC	HtrA2	LIMK2	pos
C	MPP2	NEB1	OMP25	hCLIM1	PTPH1	ZO-2-D1	hPTP1E-D1	hPTP1E-D5	pos
D	RGS12	RIL	ZO-1-D3	ZO-2-D3	GST				pos
E	pos	pos	pos	pos	pos	pos	pos	pos	pos

POSITION	PDZ DOMAIN	FULL NAME
A1, 2	Mint-2-D1	X11L protein, PDZ domain #1
A3, 4	Mint-3-D1	X11L2 protein, PDZ domain #1
A5, 6	Mint-3-D2	X11L2 protein, PDZ domain #2
A7, 8	Mint-1-D1	X11 protein, PDZ domain #1
A9, 10	Mint-1-D2	X11 protein, PDZ domain #2
A11, 12	CSKP	Calcium/calmodulin-dependent serine protein kinase
A13, 14	Dlg-D1	Synapse-associated protein 97(SAP-97), PDZ domain #1
A15, 16	Dlg1-D3	Synapse-associated protein 97(SAP-97), PDZ domain #3
B1, 2	Dlg2-D2	Channel associated protein of synapse-110 (Chapsyn-110), PDZ domain #2
B3, 4	Dlg4-D3	Human postsynaptic density-95 (PSD-95), PDZ domain #3
B5, 6	DVL1	Dishevelled 1
B7, 8	DVL3	Dishevelled 3
B9, 10	DVLL	Dishevelled-1-like
B11, 12	GIPC	GAIP C-terminus interacting protein GIPC
B13, 14	HtrA2	High temperature requirement protein A2
B15, 16	LIMK2	LIM motif-containing protein kinase-2
C1, 2	MPP2	MAGUK p55 subfamily member 2
C3, 4	NEB1	Neurabin-I
C5, 6	OMP25	Mitochondrial outer membrane protein 25
C7, 8	hCLIM1	Human 36 kDa carboxyl terminal LIMdomain protein
C9, 10	PTPH1	Protein-tyrosine phosphatase H1
C11, 12	ZO-2-D1	Zonula occludens protein 2, PDZ domain #1
C13, 14	hPTP1E-D1	Protein-tyrosine phosphatase 1E, PDZ domain #1
C15, 16	hPTP1E-D5	Protein-tyrosine phosphatase 1E, PDZ domain #5
D1, 2	RGS12	Regulator of G-protein signaling 12
D3, 4	RIL	Reversion-induced LIM protein
D5, 6	ZO-1-D3	Zonula occludens 1 protein, PDZ domain #3
D7, 8	ZO-2-D3	Zonula occludens protein 2, PDZ domain #3
D9, 10	GST	Glutathione-S-Transferase

Figure 29. Schematic diagram of the TranSignal PDZ Domain Array I (top) with the corresponding PDZ Domain list (bottom) (TranSignal PDZ Domain Arrays, *Panomics*). The PDZ proteins on the array are spotted in duplicate at 100 ng. Positive controls (HIS-tagged ligands) are spotted along the row E and the columns 17, 18; a negative control (GST protein) is spotted at the positions D9, 10. The PDZ domains of CLP-36 (hCLIM1) and RIL are circled in blue in both panels.

IV-8.1 FATZ-1 peptides bind to the PDZ domains of CLP-36 and RIL

Both the phosphorylated and the non-phosphorylated FATZ-1 peptides (EpTEEL and ETEEL) were incubated on two different membranes in order to check for interactions with PDZ domain proteins. Interestingly, both the peptides specifically recognized only the PDZ domains of the enigma family of proteins (Figure 30). The phosphorylated peptide showed a stronger binding to the PDZ domain of CLP-36 than the non-phosphorylated peptide; whereas in AlphaScreen experiments a similar binding for the two peptides was seen (Figure 25). Both peptides bound to RIL PDZ domains and, as in case of CLP-36, the binding was stronger for the phosphorylated peptide.

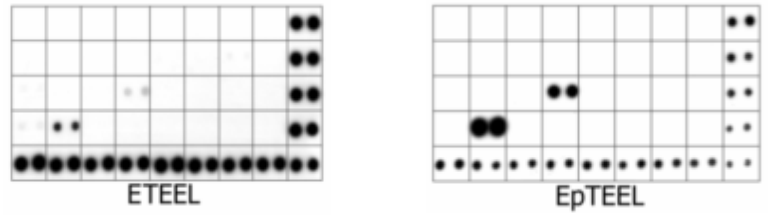

Figure 30. PDZ array blots showing the interactions of the phosphorylated (EpTEEL) and non-phosphorylated (ETEEL) FATZ-1 peptides with the PDZ domain proteins on the blot. The only two PDZ domains positively selected were those of CLP-36 and RIL.

IV-8.2 FATZ-2/palladin peptides bind to the PDZ domains of CLP-36 and RIL

The phosphorylated and the non-phosphorylated FATZ-2/palladin peptides (EpSEDL and ESEDL) were incubated on two different PDZ arrays. Both of them had interactions with the PDZ domains of CLP-36 and RIL although the non-phosphorylated peptide bound better to RIL than the phosphorylated one (Figure 31). Both peptides bound with equal strength to CLP-36, confirming our previous AlphaScreen experiments (Figure 25).

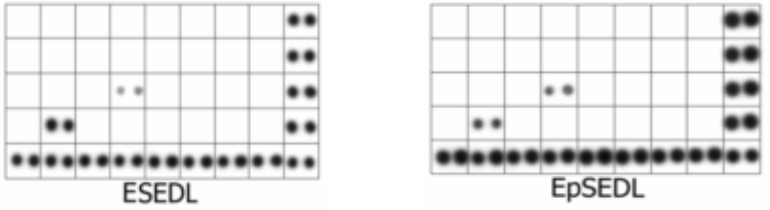

Figure 31. PDZ array blots showing the interactions of the phosphorylated (EpSEDL) and non-phosphorylated (ESEDL) FATZ-2/palladin peptides with the PDZ domains of CLP-36 and RIL.

IV-8.3 FATZ-3/myotilin peptides bind to the PDZ domains of CLP-36 and RIL

The phosphorylated and the non-phosphorylated FATZ-3/myotilin peptides (EpSEEL and ESEEL) were incubated on two different PDZ arrays and both showed binding to the CLP-36 and RIL PDZ domains (Figure 32). However, in this case the non-phosphorylated peptide had a stronger binding to both the PDZ domains. This result is in contradiction with that found using AlphaScreen (Figure 25). A possible explanation is that the amount of protein spotted on the array can vary; therefore the PDZ array is a less precise method than the AlphaScreen where more accurate concentrations of proteins and peptides can be used.

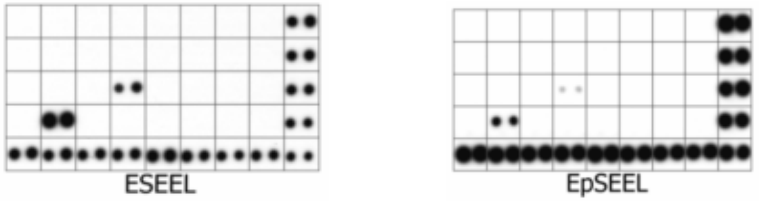

Figure 32. PDZ array blots showing the interactions of the phosphorylated (EpSEEL) and non-phosphorylated (ESEEL) FATZ-3/myotilin peptides with the PDZ domains of CLP-36 and RIL.

IV-8.4 Myopalladin peptides bind to the PDZ domains of CLP-36 and RIL

The phosphorylated and the non-phosphorylated myopalladin peptides (EpSDEL and ESDEL) were incubated on two different arrays. The non-phosphorylated peptide bound stronger to the CLP-36 and RIL PDZ domains than the phosphorylated peptide (Figure 33), confirming what previously found with the AlphaScreen experiments (Figure 25).

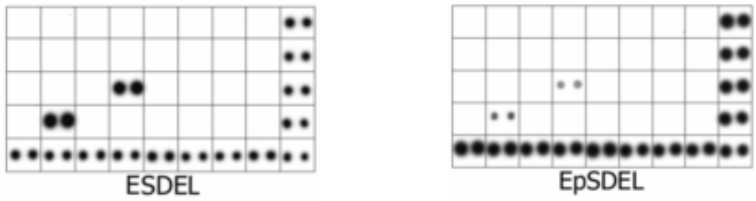

Figure 33. PDZ array blots showing the interactions of the phosphorylated (EpSDEL) and non-phosphorylated (ESDEL) myopalladin peptides with the PDZ domains of CLP-36 and RIL.

IV-8.5 The mutated peptides do not bind to the PDZ domains of CLP-36 and RIL

The phosphorylated and the non-phosphorylated mutated peptides (EpSEEE and ESEEE) were both tested for binding to the PDZ domains on the array. As expected, both of them did not interact with the CLP-36 and RIL PDZ domains. However, the non-phosphorylated peptide showed an interaction with another PDZ domain, the third PDZ domain of PSD-95 (Dlg4-D3). Also in this case the importance of the last residue of the ligand motif is evident.

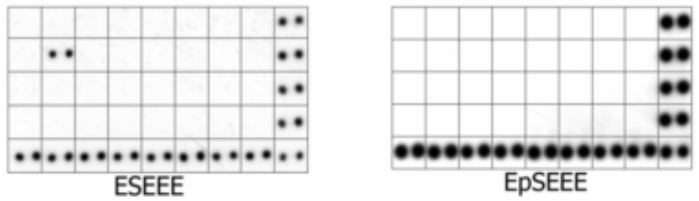

Figure 34. PDZ array blots showing that the phosphorylated (EpSEEE) and non-phosphorylated (ESEEE) mutated peptides did not show interactions with the PDZ domains of CLP-36 and RIL. The non-phosphorylated peptide ESEEE bound to the PDZ domain of the Dlg4-D3 protein.

IV-8.6 The C-terminal FATZ-3 protein behaves as the non-phosphorylated FATZ-3/myotilin peptides

The C-terminal FATZ-3 protein was produced as a native HIS-tagged protein and used in the PDZ array experiments to check if it could show the same binding activity as the non-phosphorylated peptide (ESEEL).

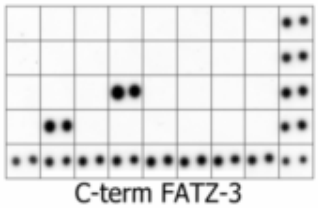

Figure 35. PDZ array blots showing that the native HIS-tagged C-terminal FATZ-3 protein interacts with the PDZ domains of CLP-36 and RIL.

As can be seen in Figure 35, the C-terminal protein bound well to the PDZ domains of CLP-36 and RIL, thus showing the same binding activity of the ESEEL peptide. This result indicates that the non-phosphorylated peptide and the C-terminal FATZ-3 protein behave in a similar manner in binding experiments.

IV-8.7 Overview of the PDZ domain array experiments

A composite figure of the PDZ domain array experiments using the phosphorylated and non-phosphorylated peptides as well as the C-terminal FATZ-3 protein is given in Figure 36. It is clear that all of the peptides bound specifically only to the PDZ domains of CLP-36 (hCLIM1) and RIL, two members of the enigma family of proteins. On the contrary, the mutated peptides ESEEE and EpSEEE did not show any interactions with these two PDZ domains; instead, the non-phosphorylated mutated peptide showed an interaction with the PDZ domain of Dlg4-D3. The FATZ-2/palladin peptides (ESEDL, EpSEDL) bound equally well to the CLP-36 PDZ domain, confirming what found with AlphaScreen. Also the poor binding of the phosphorylated myopalladin peptide (EpSDEL) confirms the AlphaScreen experiments. In contrast, the binding of the FATZ-1 non-phosphorylated peptide (ETEEL) was weaker than that seen with AlphaScreen, where both the phoshorylated (EpTEEL) and non-phosphorylated peptides showed the same binding. Also the result of the phosphorylated FATZ-3/myotilin peptide (EpSEEL) is in contradiction with AlphaScreen experiments since it did not bind well on the PDZ array.
The binding of RIL PDZ domain to peptides corresponding to the last five amino acids of FATZ-1, FATZ-2, FATZ-3, myotilin, palladin and myopalladin was previously unknown; interestingly, it agrees with the fact that RIL belongs to the same family of the ZASP, ALP and CLP-36 proteins.

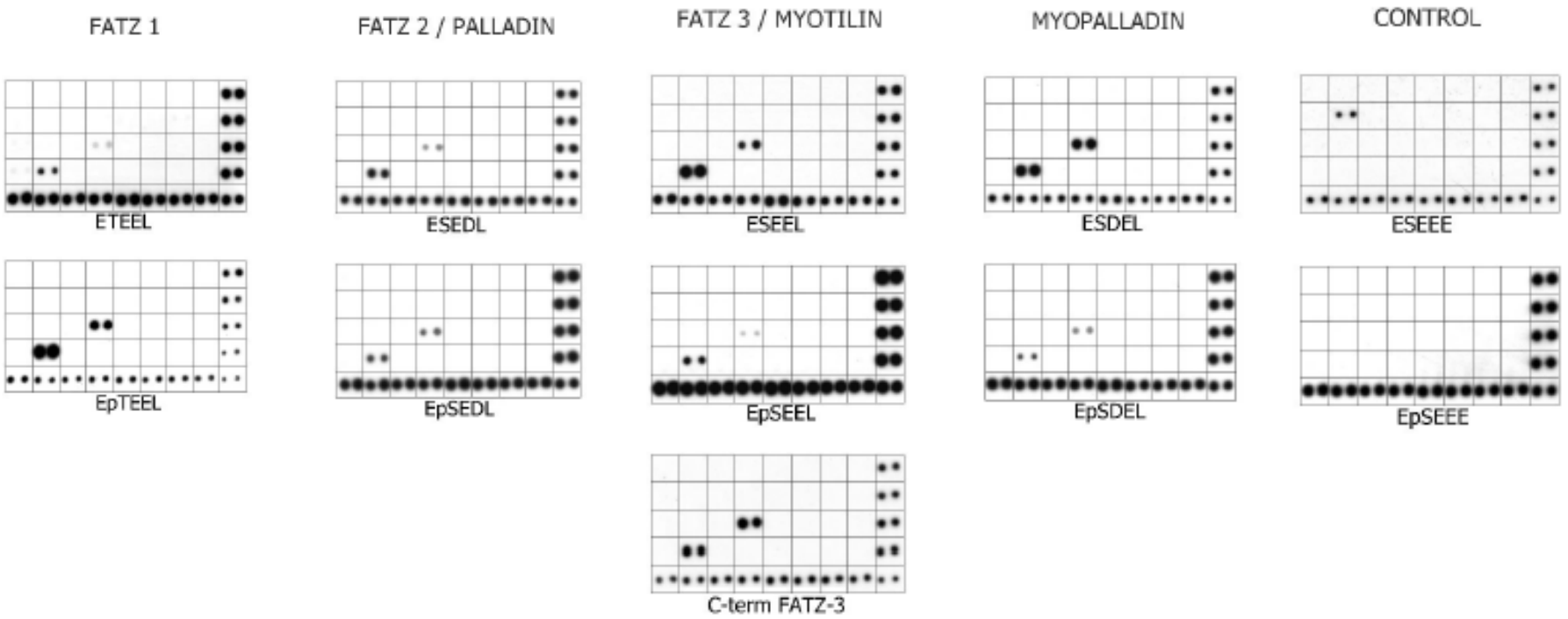

Figure 36. An overview of the PDZ domain array experiments using the phosphorylated and non-phosphorylated peptides. Specific binding was seen with the PDZ domains of CLP-36 (hCLIM1) and RIL. The mutated peptide ESEEE bound only to Dlg4-D3. The intensities of the spots give an indication of the binding affinity of the ligand of interest to the PDZ domains.

IV-9 Characterization of the interactions between the C-terminal peptides of the FATZ and myotilin families and the PDZ domain of ZASP with the SPR technique

To better characterize some of the interactions studied so far, SPR experiments were performed. In fact, the SPR technique is capable of studying biomolecular interactions in real-time, and the subsequent data analysis can give informations about the kinetics and affinity of a particular binding event. SPR experiments were done with the BIAcore 2000 instrument at University of Kent, UK. The major requirement when performing SPR measurements is that the proteins are highly pure. In addition, it is recommended that the sample buffer (the analyte-containing buffer) matches the running buffer as much as possible. In this way, refractive index changes are only related to the binding event. I spent part of the time in the laboratory of Dr. A. Baines at University of Kent in setting up the best conditions for the expression and purification of different proteins. When necessary, proteins were further purified with gel filtration chromatography. The SDS-PAGE native gel relative to the purification of the ZASP HIS-tagged PDZ domain is only given as an example in Figure 37.

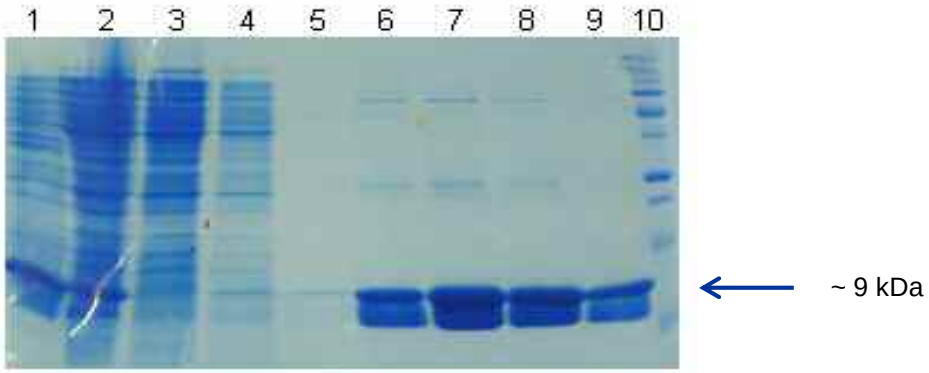

Figure 37. 15% SDS-PAGE gel stained with Coomassie Brilliant blue showing the purification of the ZASP HIS-tagged PDZ domain. Lane 1: after induction with IPTG; lane 2: lysate (soluble proteins); lane 3: after binding to the Ni-NTA resin; lane 4-5: first and second washes; lane 6-7-8-9: first, second, third and fourth elutions (250 mM imidazole); lane 10: Precision Plus Protein Standards – Dual color (*Bio-Rad*).

Most of the experiments were done using the peptides as ligand and the ZASP PDZ domain as analyte. Biotinylated peptides were captured on the sensor surface by neutravidin molecules. The experimental design of a typical interaction measurement with BIAcore is described in Figure 38.

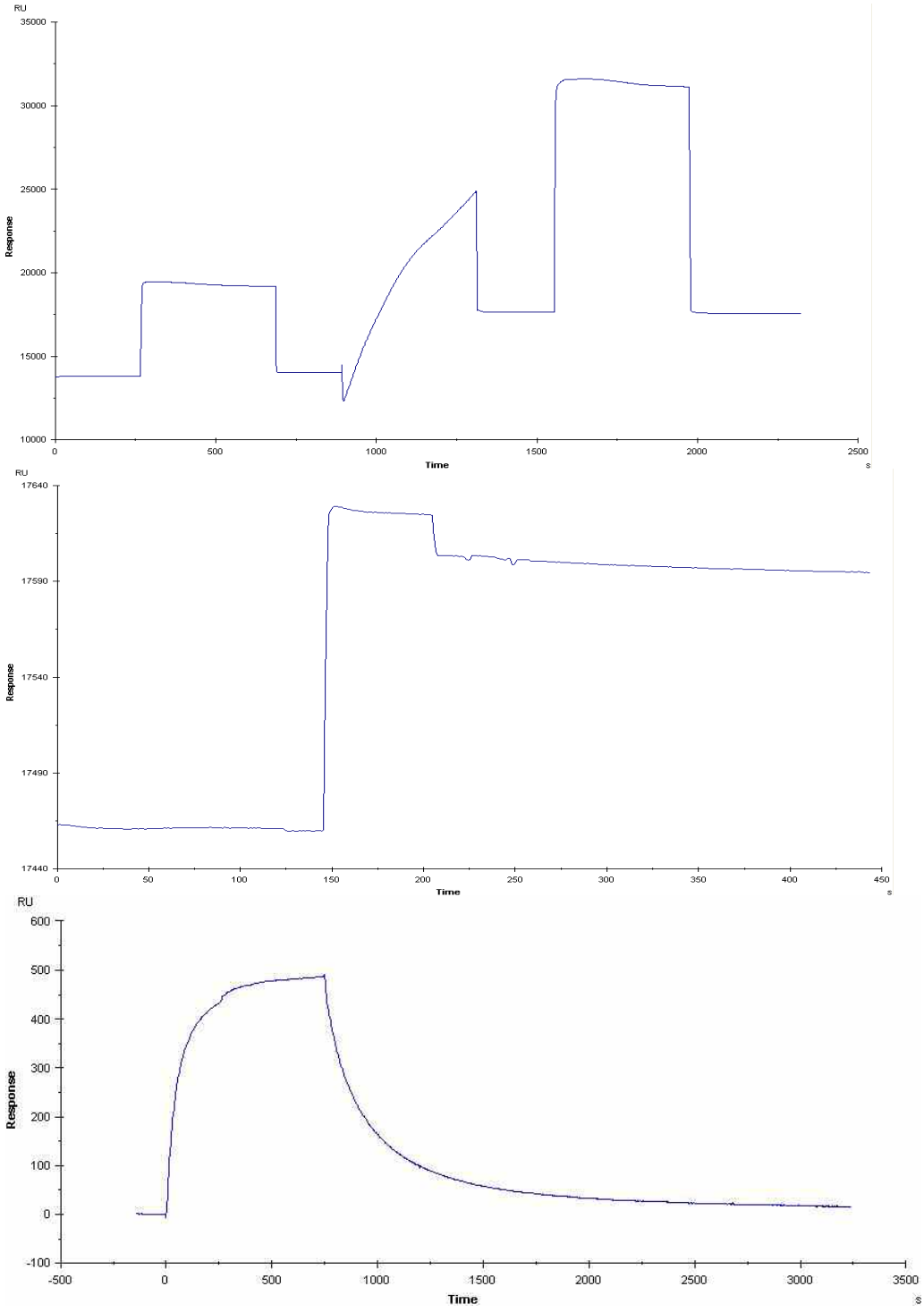

Figure 38. Experimental design for the study of interactions using BIAcore. Neutravidin-coated surface was created on CM5 sensor chips using amine coupling chemistry (top panel). Biotinylated peptides were captured onto the neutravidin surface in different flow cells at 100-200 RU (middle panel). PDZ domain-analyte solutions were injected, and binding was followed as an increase in the response during the association phase and a decrease in the response during the dissociation of the complex (bottom panel). Sensorgram is shown for 320 nM solution of ZASP HIS-tagged PDZ domain at 20 μL/min over an EpSEEL-coated surface.

Binding analyses were generally performed at flow rates of 20 µL/min for 12.5 min at 25°C, and the BIAcore instrument was programmed to perform a series of experiments with increasing concentrations of analyte over the same regenerated surface to maximize reproducibility between analyses. Different analyte concentrations were run on the peptide-coated surface after intervals of 40 min to allow spontaneous dissociation of bound proteins. Sensor chip CM5 contained four flow cells, and sensorgrams were usually obtained for all of the cells simultaneously. Three of these cells were immobilized with a different ligand, while the remaining cell served as a negative control. Sensorgrams obtained with the control cell were subtracted from those obtained with the analyte cell prior to start analysis.

IV-9.1 Interaction between the PDZ domain of ZASP and FATZ-3/myotilin peptides

In order to compare the strength of the binding of a phosphorylated and non-phosphorylated peptide to the PDZ domain of ZASP, the FATZ-3/myotilin peptides were used for SPR experiments. Figure 39 shows the time course of the non-phosphorylated peptide (ESEEL) binding to five different concentrations of ZASP HIS-tagged PDZ domain (10-40-80-160-320 nM), whereas Figure 40 represents the binding of six different concentrations (10-20-40-80-160-320 nM) of the same PDZ domain to an EpSEEL-coated surface. In both cases, the data were analyzed by GlobalFit in the BIAevaluation program. The model used for the fitting was that of heterogeneous analyte. Calculated curves fitted to the data (shown in black) are superimposed on the observed data (shown in colour). The bottom panel of each figure shows the residual plots, which indicate the difference between experimental and fitted data points. As can be seen from the graph, the residuals are acceptable for both the experiments.

The dissociation constants (K_D) for the EpSEEL/ZASP-PDZ and ESEEL/ZASP-PDZ interactions were calculated as described in the Materials and Methods chapter. K_D is determined as the concentration of analyte at which the fraction bound is 50% of the total analyte; this resulted to be 113.68 ± 0.27 nM and 351.77 ± 0.86 nM, respectively for the phosphorylated and the non-phosphorylated peptide. A lower K_D indicates a higher affinity of the ligand for the analyte, since a low concentration of analyte is necessary to bind half the ligands. The result is in agreement with previous AlphaScreen experiments, where a higher signal was obtained for the binding between the ZASP PDZ domain and the phosphorylated peptide EpSEEL.

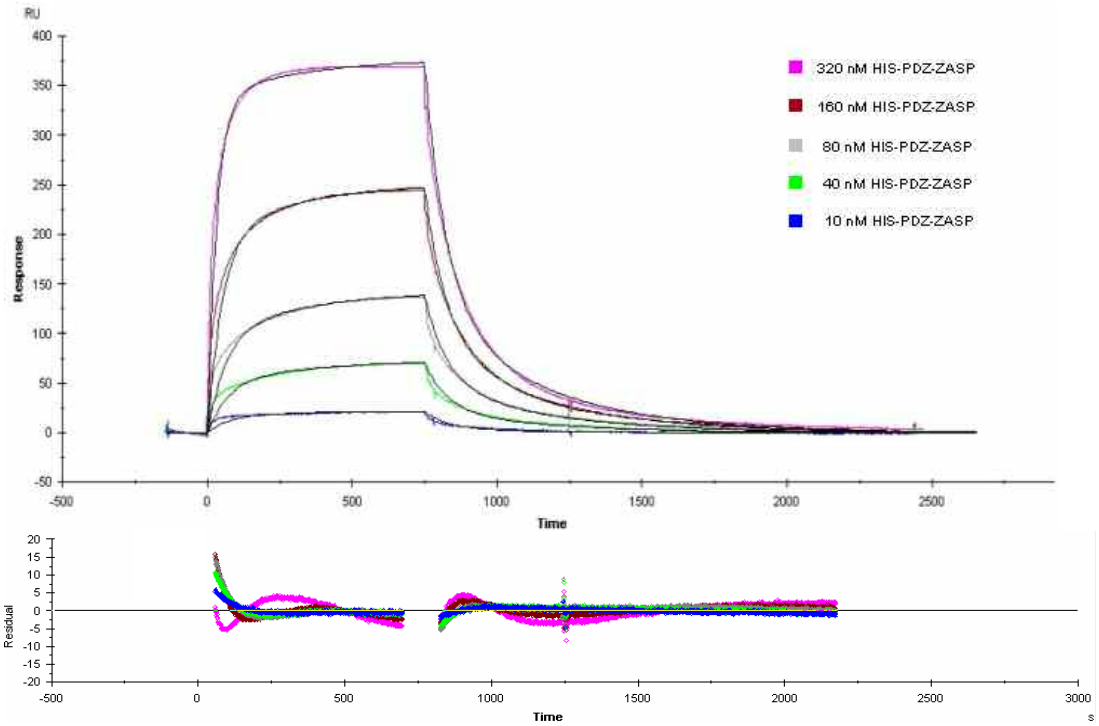

Figure 39. ZASP PDZ domain at five different concentrations was injected at 20 µL/min over an ESEEL surface in the BIAcore 2000 instrument. Sensorgrams were globally fitted to a heterogeneous analyte interaction model; the fitted curves (in black) superimpose the experimental curves (in colour) (top panel). The relative residual for each curve was calculated (bottom panel).

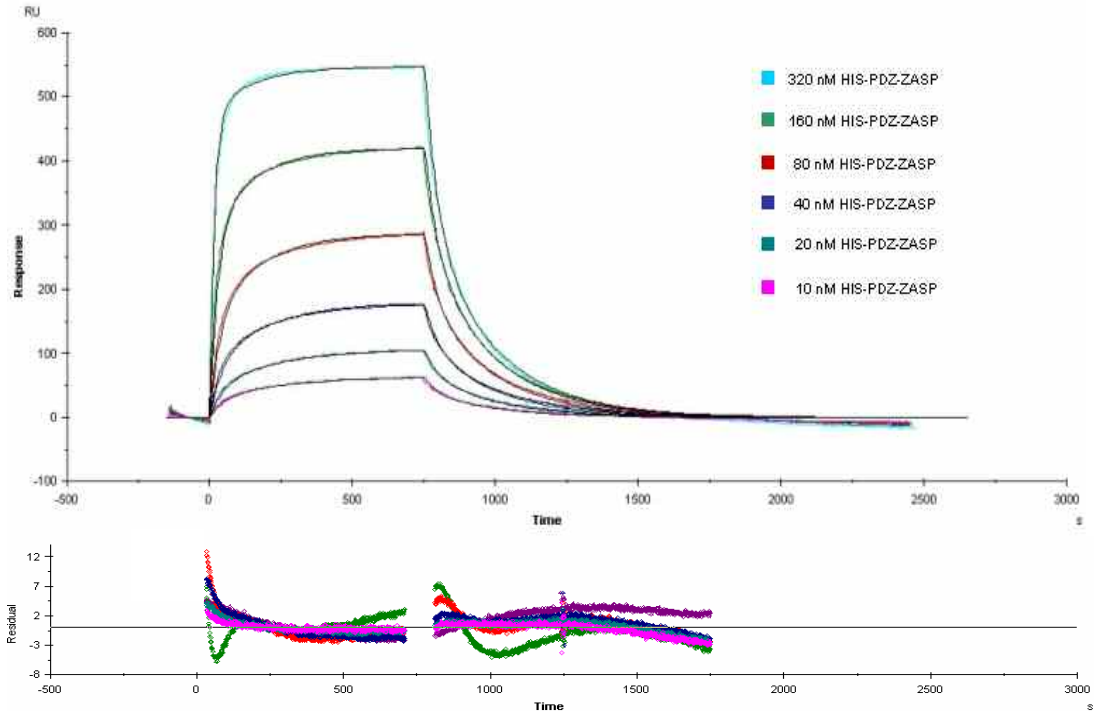

Figure 40. ZASP PDZ domain at six different concentrations was injected at 20 µL/min over an EpSEEL surface in the BIAcore 2000 instrument. Sensorgrams were globally fitted to a heterogeneous analyte interaction model; the fitted curves (in black) superimpose the experimental curves (in colour) (top panel). The relative residual for each curve was calculated (bottom panel).

IV-9.2 Interaction between the PDZ domain of ZASP and FATZ-2/palladin and myopalladin peptides

SPR experiments were repeated as described earlier but using the FATZ-2/palladin (EpSEDL) and myopalladin (EpSDEL) phosphorylated peptides as ligand and the ZASP PDZ domain as analyte. Bindings resulted to have dissociation constants of 149.27 ± 0.27 nM and 452.65 ± 1.74 nM, respectively for the EpSEDL and EpSDEL peptides. The K_D of the binding between EpSEDL and ZASP PDZ domain was somewhat similar to that of the interaction of the EpSEEL peptide with the same PDZ domain. On the contrary, the strength of the interaction seemed to decrease in the binding between EpSDEL and ZASP PDZ domain. Also in this case the result correlates with the AlphaScreen experiments, where a good interaction signal with ZASP PDZ domain was possible only doubling the concentration of the EpSDEL peptide compared to that used for the EpSEEL and EpSEDL peptides.

The experiment performed with the non-phosphorylated myopalladin peptide (ESDEL) and the PDZ domain of ZASP was characterized by a constant negative drift (Figure 41). This phenomenon, probably due to loss of material from the sensor chip surface, complicated the interpretation of our results and did not allow an estimation of affinity constants.

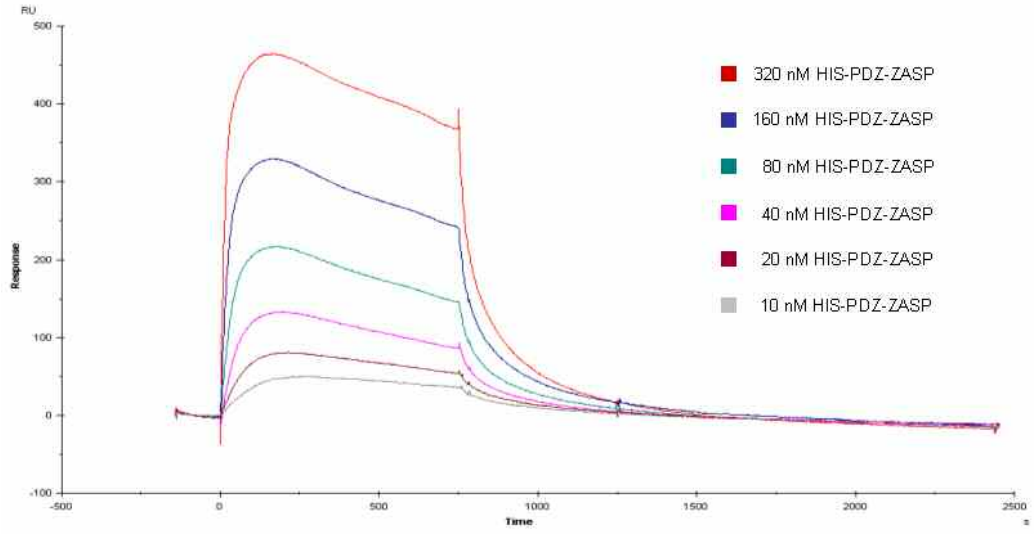

Figure 41. ZASP PDZ domain at six different concentrations was injected at 20 µL/min over an ESDEL surface in the BIAcore 2000 instrument. All the experimental curves displayed a negative drift; therefore, they were not used for the estimation of affinity constants.

IV-9.3 Interaction between the PDZ domain of ZASP and the mutated peptide ESEEE

SPR assays were also performed with the mutated peptide ESEEE. Absence of interaction resulted in the experiment between the ESEEE peptide and the PDZ domain of ZASP, thus validating AlphaScreen and PDZ array experiments and confirming the importance of the last residue of the motif in the binding with the PDZ domain.

IV-9.4 Interaction between the PDZ domain of ZASP and α-actinin-2

Further SPR experiments were made using the α-actinin-2 protein as ligand and the PDZ domain of ZASP as analyte. First, α-actinin-2 was covalently bound by means of its amino groups to the sensor chip surface. Then, the BIAcore 2000 instrument was programmed to perform a series of experiments with increasing concentrations of ZASP PDZ domain (20-40-80-160 nM) over the same regenerated α-actinin-2 surface (Figure 42). The PDZ domain of ZASP was injected at 20 µL/min for 10 min at 25°C. Sensorgrams were fitted using the heterogeneous analyte interaction model. This experiment demonstrated the binding between α-actinin-2 and the ZASP PDZ domain, and the dissociation constant for the interaction resulted to be 83.59 ± 0.39 nM.

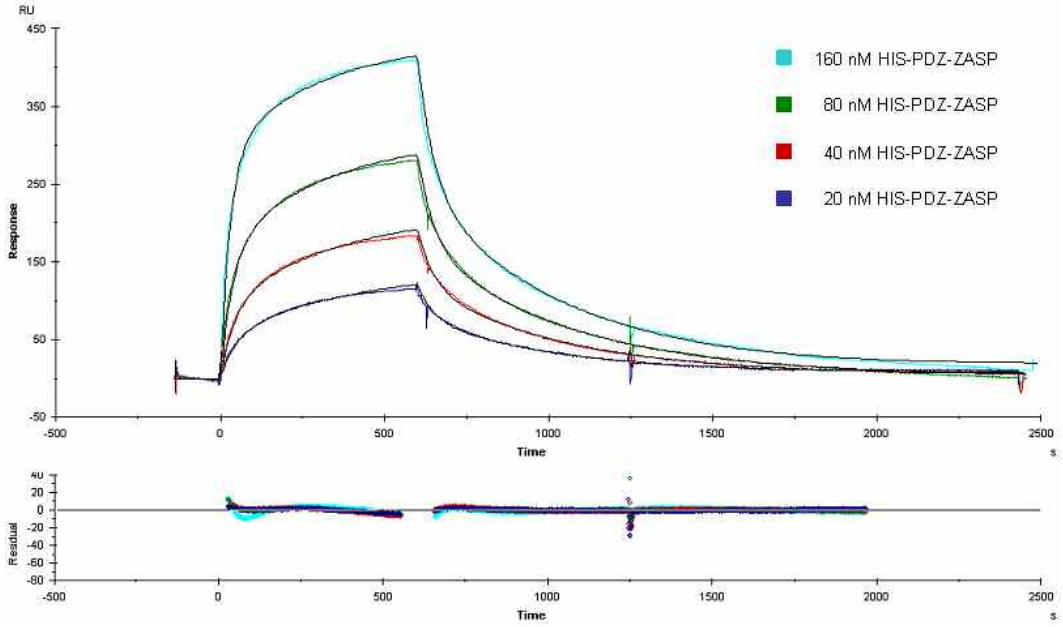

Figure 42. ZASP PDZ domain at four different concentrations was injected at 20 µL/min over a α-actinin-2 surface in the BIAcore 2000 instrument. Sensorgrams were globally fitted to a heterogeneous analyte interaction model; the fitted curves (in black) superimpose the experimental curves (in colour) (top panel). The relative residual for each curve was calculated (bottom panel).

IV-9.5 Interaction between the PDZ domain of ZASP and ANKRD2

Last SPR experiments employed the ANKRD2 protein as ligand. ANKRD2 was directly bound to the surface of the sensor chip, and the ZASP PDZ domain was injected at four different concentrations (20-40-80-160 nM) at 20 µL/min for 10 min at 25°C over the chip surface (Figure 43). Sensorgrams, which were globally fitted to a heterogeneous analyte model, demonstrated an interaction between ANKRD2 and ZASP PDZ domain. Also in this case, the strength of the binding was in the nM range and in particular a K_D of 170.73 ± 0.74 nM was calculated. This was a completely new indication about the binding between the PDZ domain of ZASP and ANKRD2; our collaborators in Trieste have recently found by coimmunoprecipitation experiments an interaction involving the ZASP full-length protein and ANKRD2 (personal communication, data not shown).

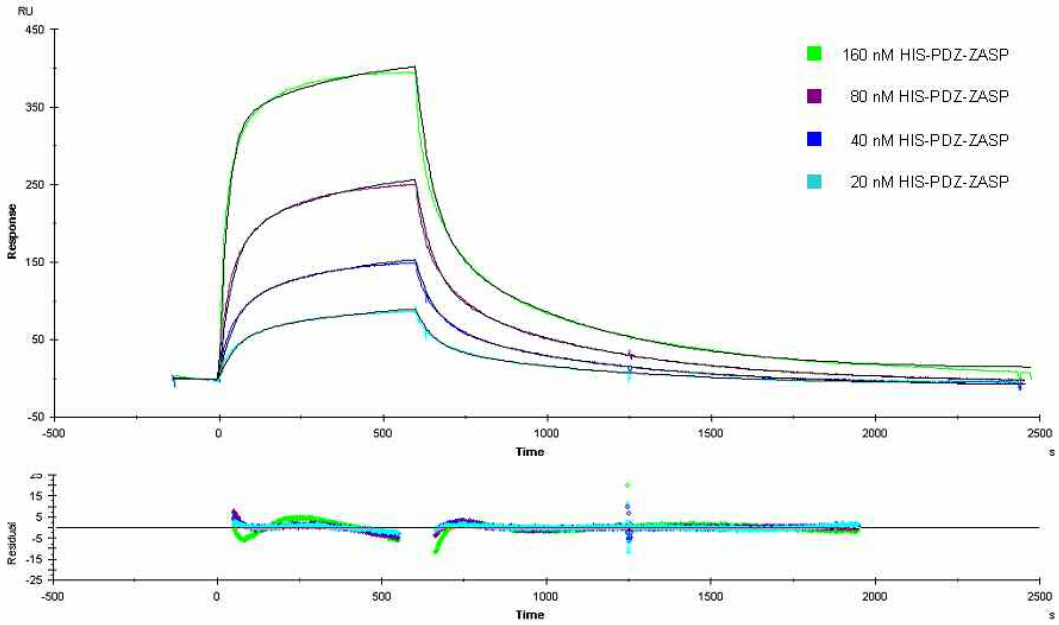

Figure 43. ZASP PDZ domain at four different concentrations was injected at 20 µL/min over an ANKRD2 surface in the BIAcore 2000 instrument. Sensorgrams were globally fitted to a heterogeneous analyte interaction model; the fitted curves (in black) superimpose the experimental curves (in colour) (top panel). The relative residual for each curve was calculated (bottom panel).

IV-10 Expression studies of murine sarcomeric genes using Real-Time PCR

Taking into account that PDZ domain-containing proteins can interact with the same C-terminal motif-containing partners, their coexpression in specific cell types could allow us to support or exclude a possible interaction at the Z-disc.

Real-Time PCR was used to determine the transcript abundance of products of the FATZ family, myotilin and ZASP genes in different murine striated muscles: soleus (a slow-twitch muscle), tibialis (a fast-twitch muscle), gastrocnemius (a muscle with mixed fibers) and cardiac muscle (here referred to as heart). Liver, kidney and brain were used as negative controls.
Three template dilutions were replicated for every gene in every tissue, and the dilutions were as follows: 1:5, 1:10 and 1:20 for the amplification of low expressed isoforms; 1:10, 1:20 and 1:40 for the forms expressed at intermediate levels; 1:25, 1:50 and 1:100 for the abundant variants. β-actin cDNA was diluted to final concentrations of 1:50, 1:100 and 1:200, whereas for the GAPDH gene the dilutions 1:500, 1:1000 and 1:2000 were used. All these dilutions were chosen on the basis of preliminary PCR reactions. Data analysis was performed after normalization of the Ct values; the 1:50 dilution was selected as reference dilution. For each gene an amplification efficiency of 2 resulted from the standard curves analysis. The R value was then calculated as described in the Materials and Methods chapter, by considering the mean of the normalized Ct values of each gene and the geometric mean of the normalized Ct values of the reference genes. The ΔR error associated to each R value is also reported.

IV-10.1 Expression of ZASP alternatively spliced isoforms

In order to evaluate the expression and distribution in different murine muscles of the six ZASP variants identified so far (Huang C et al., 2003), six primer pairs were designed. The primer pair ZASP E2-E4 amplified the region comprised between exons 2 and 4. Since exon 4 is specific for the cardiac muscle forms, it did not amplify the skeletal muscle variants. On the contrary, ZASP E2-E5 primers were designed to amplify only the skeletal muscle forms. In both cases, all the short and long isoforms were amplified. Cardiac and skeletal short ZASP forms were discriminated by the primer pair ZASP E8-E10, whereas the long variants were amplified by the primers ZASP E16-E17. Within the long ZASP isoforms, the primer pair ZASP E8-E12 amplified both the variants including exon 11 and without exon 11; the primers ZASP E8-E11 were specific for the long ZASP with exon 11 only (Figure 44). As reference genes, β-actin and GAPDH were selected. Two distinct genes were chosen, in order to compensate for possible small gene expression differences in the considered tissues.

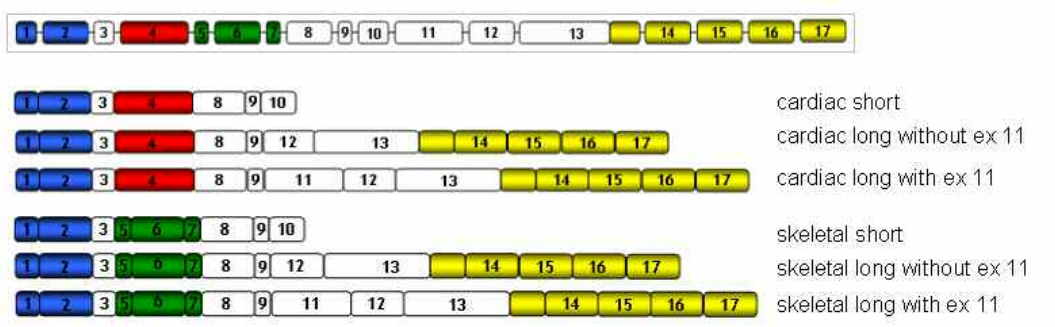

Figure 44. Schematic diagram showing the ZASP gene organization with its 17 exons (top) and the corresponding six splicing variants (bottom) in mouse.

Table 4 shows the R values relative to the expression of the different ZASP variants in the four murine muscles considered; the same values are graphically reported in Figures 45 and 46.

ZASP isofoms (primer pair)	**Gastrocnemius**	**Tibialis**	**Soleus**	**Heart**
Long ZASP (ZASP E16-E17)	0.088. ± 0.013	0.065. ± 0.020	0.142. ± 0.019	0.069. ±0.039
Short ZASP (ZASP E8-E10)	0.179. ± 0.027	0.189. ± 0.043	0.345. ± 0.055	0.100. ± 0.012
Long ZASP (with exon 11 and without exon 11) (ZASP E8-E12)	0.037± 0.007	0.035 ± 0.010	0.071 ± 0.010	0.068 ± 0.014
Long ZASP with exon 11 (ZASP E8-E11)	0.0020 ± 0.0003	0.005 ± 0.002	0.014 ± 0.003	0.028 ± 0.007
Skeletal muscle ZASP (ZASP E2-E5)	0.128 ± 0.021	0.200 ± 0.067	0.193 ± 0.033	0.0030 ± 0.0007
Cardiac ZASP (ZASP E2-E4)	-	-	-	0.243 ± 0.039

Table 4. R values and ΔR errors relative to the expression of the different ZASP isoforms in gastrocnemius (muscle with mixed fibers), tibialis (fast-twitch muscle), soleus (slow-twitch muscle) and heart. The expression of long ZASP (first row) and long ZASP (with exon 11 and without exon 11) (third row) should be the same. In fact, all the long isoforms are amplified in both cases. However, it is known that the retrotranscription efficiency is higher near the 3' end and decreases towards the 5' end of a gene. The primer pair ZASP E16-E17 amplifies a region of the gene closer to the 3' end compared to the primers ZASP E8-E12. Nevertheless, the primer pair ZASP E8-E12 was used in order to compare the expression of the long ZASP with exon 11 and long ZASP without exon 11.

Our results showed a higher level of expression of the short isoforms of ZASP compared to that of the long proteins in both skeletal and cardiac muscles (Figure 45). Among these, the long variants lacking exon 11 were more expressed than the isoforms with exon 11 in all the four muscle tissues considered (Figure 46). However, the expression of the ZASP long variant containing exon 11 was significant in soleus and heart compared to the tibialis and gastrocnemius muscles. From our results seemed that the overall ZASP expression was higher in skeletal muscle than in heart.

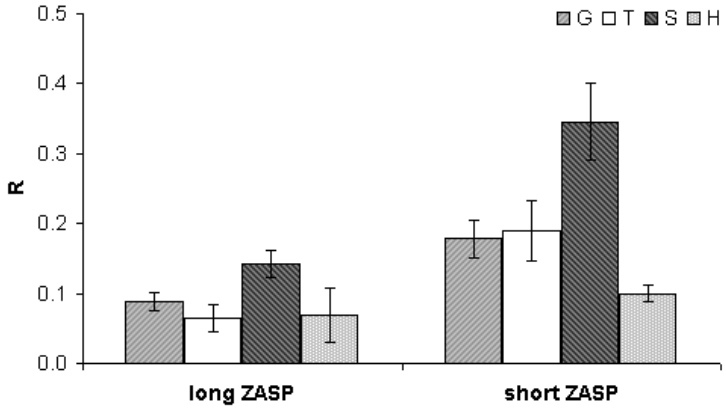

Figure 45. Expression values for the long and short ZASP isoforms after normalization with reference genes in gastrocnemius (G), tibialis (T), soleus (S) and heart (H).

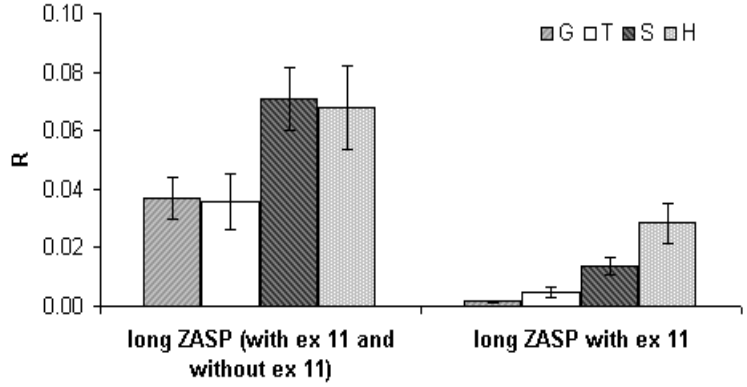

Figure 46. Expression values for the long ZASP isoforms (with exon 11 and without exon 11) and long ZASP isoforms with exon 11 after normalization with reference genes in gastrocnemius (G), tibialis (T), soleus (S) and heart (H). The difference between the expression of long ZASP (with exon 11 and without exon 11) and long ZASP with exon 11 should represent the real expression of long ZASP without exon 11.

IV-10.2 Expression of the FATZ family of proteins and myotilin

The R values relative to the expression of the FATZ family of proteins and myotilin in the four murine muscles considered are shown in Table 5; the same values are graphically reported in Figure 47.

Protein	Gastrocnemius	Tibialis	Soleus	Heart
FATZ-1	0.656 ± 0.079	0.679 ± 0.169	0.283 ± 0.055	0.001 ± 0.001
FATZ-2	0.068 ± 0.010	0.067 ± 0.027	1.030 ± 0.236	0.497 ± 0.080
FATZ-3	0.055 ± 0.013	0.020 ± 0.006	0.022 ± 0.003	0.0001.± 0.0001
myotilin	0.166 ± 0.034	0.265 ± 0.075	0.541 ± 0.092	0.020 ± 0.004

Table 5. R values and ΔR errors relative to the expression of FATZ-1, FATZ-2, FATZ-3 and myotilin in gastrocnemius (muscle with mixed fibers), tibialis (fast-twitch muscle), soleus (slow-twitch muscle) and heart.

FATZ-1 was preferentially expressed in fast-twitch fiber type (tibialis and gastrocnemius) and to a lesser extent in slow-twitch fiber type (soleus); no expression was found in heart. FATZ-3 behaved similarly to FATZ-1 although its expression was overall lower in all of the tissues analyzed. On the contrary, FATZ-2 seemed to be expressed predominantly in soleus and in heart, which shares several molecular features with slow-twitch fiber type.
As expected, the expression of myotilin was preferentially restricted to skeletal muscle tissues and no expression was found in heart.

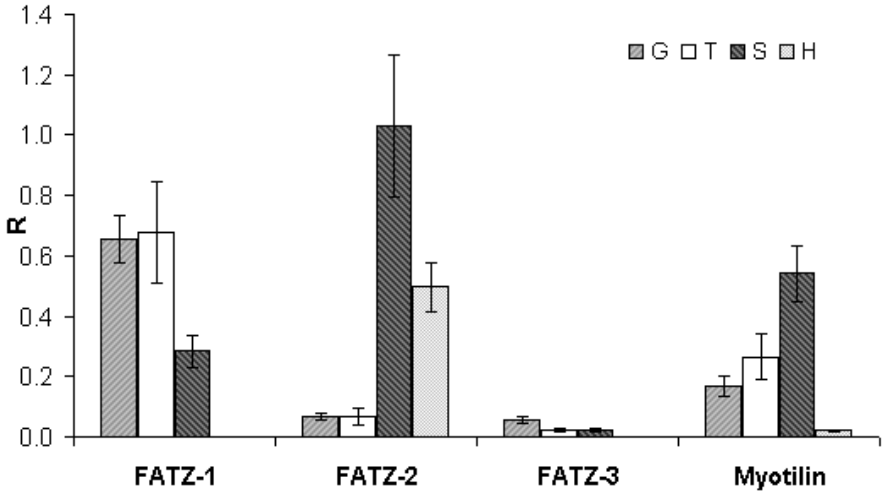

Figure 47. Expression values for FATZ-1, FATZ-2, FATZ-3 and myotilin after normalization with reference genes in gastrocnemius (G), tibialis (T), soleus (S) and heart (H).

V DISCUSSION

The sarcomere is the functional unit of striated muscle. Its organization represents a unique example of biological system wherein several dozens of proteins are assembled into a highly specialized structure, which is able to convert the molecular interactions produced by actin and myosin proteins into the efficient macroscopic motion of contraction. The essential component that confers to the sarcomere this ability is represented by the Z-disc. The Z-disc defines the lateral boundaries of the sarcomere where thin filaments are anchored. It acts by keeping the structure of the sarcomere in register and transmitting tension during muscle contraction. Over the past few years, the perception of the Z-disc in muscle has undergone significant changes. Beyond a well-defined structural function, it is now emerging the hypothesis that Z-disc could have a role in signal transduction both in skeletal and cardiac muscles (Frank D et al., 2006). Indeed, numerous signalling molecules have shown to interact with Z-disc proteins, and some of them can shuttle between the Z-disc and other cellular compartments, such as the nucleus, thus underlining the dynamic nature of Z-disc components. Alterations of the tightly regulated interactions between Z-disc proteins can lead to disruption and malfunction of the contractile apparatus, resulting in myopathies and/or muscular dystrophies. Although several Z-disc proteins have recently been identified, the complex molecular architecture of Z-disc and the mechanism of its assembly and adaptation are mostly unknown. Therefore, a better knowledge of Z-disc proteins and their interactions is essential for understanding their role in the structure and function of muscle. The work of this thesis, which was part of a wider project involving the groups coordinated by Dr. G. Faulkner at ICGEB, Trieste, and Prof. O. Carpen at University of Turku, Finland, has led to the identification of a binding motif common to the C-terminus of FATZ and myotilin families of proteins. We have found that this C-terminal motif specifically interacts with the PDZ domain of the enigma family members ZASP, ALP, CLP-36 and RIL. These interactions were identified with different *in vitro* methods such as the AlphaScreen (Amplified Luminescent Proximity Homogeneous Assay) technique and the TranSignal PDZ Domain Array. The SPR (Surface Plasmon Resonance) technique was finally used to evaluate and compare the strength of some of these bindings.

FATZ and myotilin families constitute two groups of mainly sarcomeric proteins. The FATZ family is composed by FATZ-1, FATZ-2 and FATZ-3. These proteins share high homology at their N- and C-termini but are less conserved in the intervening region. All of the three members localize at the Z-disc where they interact with several proteins; γ-filamin, α-actinin, telethonin, ZASP, myotilin and calcineurin are the binding partners shared by the FATZ family of proteins. On the contrary, the myotilin family comprises proteins with a wider range of distribution; myotilin and myopalladin are predominantly expressed in skeletal and cardiac muscles, whereas palladin is present in a variety of tissues. Together with our collaborators, we noted that the C-terminal five amino acids of FATZ-1 (ETEEL), FATZ-2 (ESEDL), FATZ-3 (ESEEL), myotilin (ESEEL), palladin (ESEDL) and myopalladin (ESDEL) are highly similar. Notably, those of FATZ-2 and palladin are identical as are those of FATZ-3 and myotilin. This high similarity raised the question of whether these proteins could interact via their C-termini with the same protein or proteins, then the possibility that the C-terminal five amino acids in FATZ and myotilin families would represent a new binding motif involved in protein interactions.

In order to find out if other proteins contained the putative binding motif E-[S/T]-[D/E]-[D/E]-L, a program was written by my supervisor Prof. G. Valle, CRIBI, Padova. This program was used to scan the UniProt Knowledgebase Release 11.3 (UniProtKB/Swiss-Prot Protein Knowledgebase Release 53.3 and UniProtKB/TrEMBL Protein Database Release 36.3 of July 10, 2007). The result of the database scan interestingly revealed that the motif is restricted in Vertebrates to the FATZ and myotilin families with the exception of histidine ammonia-lyase that has its final C-terminal amino acids (ESEDL) identical to those of FATZ-2 and palladin (Table 3). Histidine ammonia-lyase is a cytosolic enzyme catalyzing the first reaction in histidine catabolism, the non-oxidative deamination of L-histidine to trans-urocanic acid. Genetic deficiency of the enzyme, transmitted as an autosomal recessive trait, causes histidinaemia, which is characterized by elevated histidine and histamine as well as decreased urocanic acid in body fluids. Although there is a report of histidine ammonia-lyase in the sarcoplasm of the muscle (Krishnamoorthy RV, 1977), normally it is not found in muscle. It is probable that hystidine ammonia-lyase can bind to the same proteins as the FATZ and myotilin families but whether it really does so would depend on its localization. On the contrary, the FATZ family, myotilin, palladin and myopalladin are mainly located at the Z-disc of striated muscle where they can interact with the same set of proteins.

It is now well-established that the phenomenon of binding to C-terminal sequences of other proteins is the canonical binding mode of PDZ domain-containing proteins (van Ham M, and Hendriks W, 2003). Furthermore, PDZ domains are classified considering the C-terminal sequence of the interacting protein, with particular attention to the residues P_0 and P_{-2} (Songyang Z et al., 1997). Also the classification used by the ELM program is based on the C-terminal sequence of the ligand but with a more precise definition of the four C-terminal ligand residues (Puntervoll P et al., 2003). To date, three classes of PDZ domains are defined: class I is represented by the motif X-[S/T]-X-[V/I/L], class II by the motif X-[V/Y/F]-X-[V/I/L], and class III by the motif X-[D/E]-X-[V/I/L] (Figure 48, top panel). Based on this classification the terminal four amino acids of FATZ-1, FATZ-2, FATZ-3, myotilin, palladin and myopalladin were considered a probable binding motif for class III PDZ domain proteins (Figure 48, middle panel). As can be noted, the canonical PDZ ligand motif is usually four amino acids in length; nevertheless, we consider that also E at the position P_{-4} of the motif is important as it is conserved from zebrafish to humans in both the FATZ and myotilin families.

Starting from the knowledge that ZASP can bind to the FATZ family of proteins via its N-terminal PDZ domain (Frey N, and Olson EN, 2002), that the interaction between ZASP and myotilin is mediated by the C-termini of myotilin (preliminary results of our Finnish collaborators), and considering our previous observations, we wanted to determine if the last C-terminal five amino acids of all the FATZ and myotilin members could have a role in the interaction with ZASP and other enigma proteins.

Proteins of the enigma family are characterized by the presence of a single N-terminal PDZ domain and one to three C-terminal LIM domains. The enigma family is formed by seven members grouped into two subfamilies based on the number of LIM domains. The enigma subfamily (three LIM domains) includes enigma, ENH and ZASP; the ALP subfamily (one LIM domain) is composed by ALP, CLP-36, RIL and mystique. ZASP, ALP and CLP-36 have also in common a conserved stretch of 26-27 residues called ZM in their internal region. PDZ domains are globular 80-100 aa interaction modules found in proteins with diverse functions. They usually recognize short sequences (4 to 6 aa in length) located at the very C-termini of interacting proteins. The binding occurs in a groove between the strand βB and the helix αB of the PDZ domain, whereas the connecting loop between βA and βB is involved in the interaction with the C-terminal carboxylate group of the ligand sequence. This loop is referred to as the carboxylate-binding loop and it usually contains the residues GLGF (glycine-

leucine-glycine-phenilalanine); instead, the PDZ domains of the enigma family members possess the sequence PWGF (proline-tryptophan-glycine-phenylalanine). It is possible that this sequence accounts for the binding specificity of the PDZ domains of the enigma family members for the C-terminal motif of the FATZ and myotilin families of proteins. However, it has to be reminded that RIL is mainly found in non-muscle tissues; consequently, its interaction with the FATZ family, myotilin and myopalladin is unlikely to occur at least at the Z-disc. In the same way, palladin is primarily localized in smooth muscle and non-muscle tissues and it could interact with the PDZ domain of CLP-36 that presents a wider tissue distribution compared to the other enigma members.

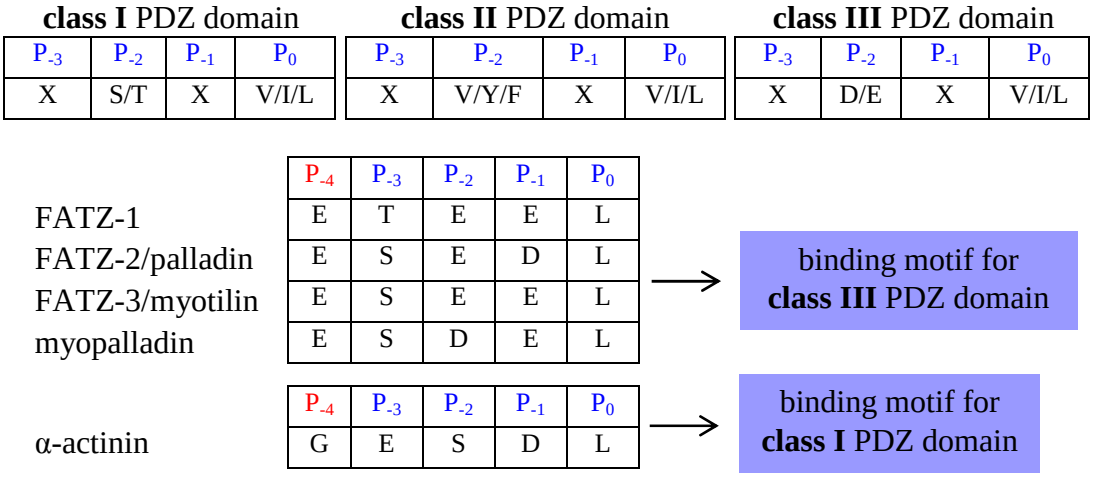

Figure 48. The three classes of PDZ domains as classified by the ELM program considering the last four amino acids of the ligand motif (top panel). According to this classification (but also including the residue at position P_{-4}) the C-terminus of the FATZ and myotilin families of proteins is classified as a binding motif for class III PDZ domains (middle panel), whereas the C-terminus of α-actinin is classified as a binding motif for class I PDZ domains (bottom panel).

AlphaScreen experiments performed using the PDZ domains of ZASP, ALP and CLP-36 revealed an interaction with the full-length FATZ-1, FATZ-2, FATZ-3 and myotilin proteins (Figure 22). This interaction seemed to be mediated by the last five amino acids of these proteins as the truncated version of the FATZ proteins and myotilin did not show any binding to the same PDZ domains. The strength of the binding varied depending on ligand and PDZ domain. All of the ligand proteins bound to the three PDZ domains although the FATZ-3 protein did not bind as well as myotilin, with which shares the C-terminal motif. However, it is important to remember that both the PDZ domains and the ligand proteins were expressed in bacteria and therefore not phosphorylated. Phosphorylation could

represent one of the mechanisms able to influence such an interaction. Also α-actinin-2 was included in this study; its C-terminus has previously been shown to interact with the PDZ domains of ZASP and ALP (Zhou Q et al., 1999; Faulkner G et al., 1999; Klaavuniemi T et al., 2004). AlphaScreen experiments effectively confirmed the interaction of ZASP and ALP PDZ domains with α-actinin-2. As described in the Introduction, CLP-36 is able to interact with α-actinin-2 via its LIM domain (Kotaka M et al., 2000); here, an interaction between the PDZ domain of CLP-36 and α-actinin-2 also emerged. The C-terminus of α-actinin-2 contains the sequence GESDL, which fits with the consensus ligand sequence of class I PDZ domains (Figure 48, bottom panel). These findings together would suggest that the PDZ domains of ZASP, ALP and CLP-36 are both class I and class III PDZ domains. They do not represent the sole examples of PDZ domain with a dual specificity of binding. Indeed, the syntenin protein contains two PDZ domains that are able to interact with peptides from different classes: PDZ1 binds to peptides from classes I and III, while PDZ2 interacts with classes I and II (Kang BS et al., 2003). This would indicate that PDZ domain classification is far from being definitive and needs further improvements in order to predict with sufficient confidence the putative targets of any PDZ domain.

The specificity of the binding between the PDZ domains of ZASP, ALP and CLP-36 and the C-terminal motif of the FATZ and myotilin families was demonstrated by further AlphaScreen experiments. Synthetic peptides corresponding to the last five amino acids of FATZ-1, FATZ-2/palladin, FATZ-3/myotilin, myopalladin and α-actinin-2 behaved as ligands for the PDZ domains of ZASP, ALP and CLP-36 (Figure 23). Also in this case there was some variability in the strength of the binding, and generally all of the peptides bound poorly to the ALP PDZ domain. These data are in contrast with those obtained using the full-length proteins where good interaction signals with the ALP PDZ domain were detected. AlphaScreen interaction assays also confirmed the importance of the last residue of the motif for the PDZ domain recognition. Indeed, the binding to the three PDZ domains was completely destroyed after changing the last amino acid of the ligand sequence from leucine (L) to glutamic acid (E).

The interaction between PDZ domain and its ligands can be regulated by phosphorylation of the ligand sequence. The C-terminal motif of the FATZ and myotilin families of proteins and α-actinin-2 contains a potential phosphorylation site. Synthetic phopshorylated peptides were used in AlphaScreen experiments and all of them showed binding to the PDZ domains of ZASP, ALP and CLP-36 (Figure 24). However, the effect of phosphorylation on binding varied depending on the PDZ domain and the ligand (Figure 25). In fact, phosphorylation greatly

increased binding of all the FATZ and myotilin families peptides with ZASP PDZ domain. In the same way, the FATZ-3/myotilin and α-actinin-2 peptides bound better to the PDZ domain of CLP-36 when phoshorylated, whereas the binding to the FATZ-1 and FATZ-2/palladin peptides did not change upon phosphorylation. In contrast, phosphorylation of the C-terminal myopalladin peptide led to disruption of binding to the PDZ domain of CLP-36. This is the most common effect of phosphorylation of the C-terminal PDZ-binding motif (Kim E, and Sheng M, 2004). The ALP PDZ domain behaved similarly to ZASP in that phosphorylation strongly increased the binding to all the FATZ, myotilin and α-actinin-2 ligand peptides. However, it has to be reminded that binding of the PDZ domain of ALP to peptides did not reach the values registered for the other peptides. In conclusion, we can say that phosphorylation seems to modulate the ability of the FATZ and myotilin peptides to bind to the PDZ domains of enigma family members. An important finding from our collaborators is the fact that different kinases phosphorylate the C-terminal amino acids of the group of ligand proteins (von Nandelstadh P et al., 2009). CaMKII (calcium/calmodulin-dependent protein kinase II) can phosphorylate *in vitro* FATZ-3 and myotilin, which share the last five amino acids; on the contrary, PKA (protein kinase A) can phosphorylate *in vitro* FATZ-1 and FATZ-2 but not FATZ-3 and myotilin. This is not casual and the use of different kinases for phosphorylation could be another factor that decides which protein binds to its target when there are potential several partners available.

As the number of proteins known to interact with each other increases, it would be important to understand what happens when they meet at the same time. For this purpose, some competition experiments using the AlphaScreen technique were performed. We looked at the competition in the binding between the ZASP-1 protein and the FATZ-3/myotilin peptide ligands. The C-terminal of FATZ-1 (FATZ-1 CD2) can compete with the interaction between ZASP-1 and the FATZ-3/myotilin ligand both phosphorylated and not (Figure 27). This means that a PDZ class III interaction could be competed by the addition of another class III ligand. There was also competition when the α-actinin-2 protein was used as competitor but in this case much higher concentrations of the protein were needed to obtain the same effect as the C-terminal of FATZ-1 (Figure 28). The C-terminal ligand of α-actinin-2 is a class I PDZ binding ligand therefore it may not be able to compete as well as a type III ligand.

Another important result of this work concerned the specificity of the interaction between the PDZ domain of enigma proteins and the FATZ and myotilin families. In fact, only a restricted number of PDZ domains was selectively bound by the peptide ligands in the TranSignal PDZ Domain Array experiments. Interestingly, these PDZ domains corresponded to the only two enigma family members on the array, CLP-36 (hCLIM1) and RIL (Figure 29). Unfortunately, ZASP and ALP PDZ domains were not represented on the array; therefore it was not possible to completely compare the results of PDZ arrays with those of AlphaScreen experiments. However, in agreement with the AlphaScreen results the phosphorylated myopalladin peptide bound poorly to the PDZ domain of CLP-36 (Figure 36). Also the FATZ-2/palladin peptides behaved similarly in both systems used. The main contrast between the AlphaScreen results and the arrays was the binding with the FATZ-3/myotilin peptides since in the arrays the phosphorylated peptide did not bind well. Another discrepancy concerned the binding of the FATZ-1 non-phosphorylated peptide that did not show the same binding of the phoshorylated peptide as detected in the AlphaScreen assays. The differences observed in AlphaScreen and PDZ array experiments could be explained by the variability in the amount of protein spotted, which could vary from array to array. On the contrary, the AlphaScreen technique allows a more precise monitoring of the concentrations used for proteins and peptides. Another explanation could be based on the difference of the PDZ domains used in the two systems: HIS-tagged PDZ domains in solution for AlphaScreen experiments, and GST recombinant PDZ domains immobilized onto membranes for PDZ array experiments. As mentioned earlier, PDZ arrays allowed the identification of a previously unknown interaction between the PDZ domain of RIL and the C-terminal region of the FATZ and myotilin families of proteins. These interactions are likely to occur since RIL belongs to the same protein family as ZASP, ALP and CLP-36. Another important confirmation given by the PDZ array experiments was about the nature of the last residue of the motif in PDZ-ligand recognition. Indeed, both the mutated peptides, phosphorylated and not, did not bind to the PDZ domains of the enigma proteins CLP-36 and RIL; furthermore, the ESEEE peptide showed binding to the PDZ domain of another protein, Dlg4-D3. These experiments confirmed the importance of the leucine at the position P_0 for specificity of binding.

To quantify the strength of binding between the PDZ domains of enigma family and the FATZ and myotilin ligand peptides, the SPR technique was used. Although many examples of PDZ-peptide ligand interactions have now been

identified, uncertainty exists about the binding affinities of PDZ domains for their peptide ligands (Harris BZ, and Lim WA, 2001). Estimates of dissociation constants (K_D), measured using a variety of techniques, have ranged from low nM to high μM. Much of this confusion may result from the methods used: solid-phase assays such as SPR or ELISA (enzyme-linked immunosorbent assays), which involve immobilization of one binding partner on a solid support, measured affinities in the 10-100 nM range. The results of my SPR experiments effectively match with the nM affinities reported in literature. On the other hand, in-solution measurements such as fluorescence polarization detected lower affinities of PDZ binding to their ligands, being in the μM range (1-10 μM). Such moderate values are suitable for regulatory functions, since binding can be reversible and dependent on intracellular conditions. However, it is possible that *in vivo* binding affinity is much higher due to the presence of many PDZ domains within a single protein or simultaneous interactions of other protein-protein interaction modules. For example, it is known that both ZASP and ALP have two interaction sites with α-actinin; the ZM-motif on ZASP and ALP binds to the rod central region of α-actinin, whereas the PDZ domain of these proteins interacts with the α-actinin C-terminal portion (Klaavuniemi T et al., 2004; Klaavuniemi T, and Ylänne J, 2006). It is possible that the PDZ domain-mediated binding may occur only after the colocalization of ZASP and ALP with α-actinin at the Z-disc mediated by their ZM-motifs.

SPR experiments were performed in the laboratory of Dr. A. Baines at the University of Kent, UK, using the BIAcore 2000 instrument. As a general observation, all of the experimental curves obtained for the PDZ-peptide or PDZ-protein interactions were fitted with good accuracy using the heterogeneous analyte model, indicating that more than one process might be involved. Such a model implies the presence of two different species in the analyte sample, the PDZ domain solution in my experiments. However, it has been suggested that other factors can contribute to this multiphase kinetics (Edwards PR, and Leatherbarrow RJ, 1997). One contributory effect is steric hindrance, where initial binding causes physical occlusion of some binding sites within the three-dimensional carboxymethyldextran matrix of the sensor chip. Binding to the less accessible sites then either requires dissociation of already-bound material followed by rearrangement and rebinding, and is slower due to restricted access to these sites. Thus, the kinetics for this kind of interaction is characterized by two different rate constants; the faster rate has been found to correspond most closely to the rate constant for the interaction in solution. However, it is very important in evaluating kinetic data to accept the simplest model which fits the data within the

limits of the experiment. A more complex model may fit the data better, but the crucial question is whether the improvement is biologically or experimentally significant. For this reason, I decided to evaluate the binding affinities considering the steady-state response at equilibrium obtained at different analyte concentrations.

Experiments done with the FATZ-3/myotilin phosphorylated and non-phosphorylated peptides confirmed the interaction with the PDZ domain of ZASP. The dissociation constant was lower in the binding of ZASP PDZ domain to the phosphorylated peptide (EpSEEL) compared to that of the non-phosphorylated peptide (ESEEL). These results suggest that the binding between EpSEEL and ZASP PDZ domain is stronger if related to the interaction of the same PDZ domain with the corresponding non-phosphorylated peptide. The dissociation constant of the binding between the FATZ-2/palladin phosphorylated peptide (EpSEDL) and ZASP PDZ domain was similar to that of the interaction of the EpSEEL peptide with the same PDZ domain. On the contrary, the strength of the interaction seemed to decrease in the binding between the myopalladin phosphorylated peptide (EpSDEL) and ZASP PDZ domain. These results, as the previous, are in agreement with the AlphaScreen studies, where a good interaction signal with the PDZ domain of ZASP was possible only doubling the concentration of the peptide EpSDEL compared to that used for the EpSEEL and EpSEDL peptides. SPR experiments also confirmed the interaction between the ZASP PDZ domain and α-actinin-2.

An important finding of the SPR experiments concerned the identification of an unknown interaction between the PDZ domain of ZASP and ANKRD2. The ANKRD2 protein is present in the nucleus of undifferentiated striated muscle cells and in the cytoplasm of adult cells. As described in the Introduction, the ANKRD2 gene is significantly upregulated in response to prolonged mechanical induced stretch. Recently, it has been found that ANKRD2 accumulates in the nuclei of damaged myofibers after muscle injury, and it tends to be localized in euchromatin, where many genes are transcriptionally active (Tsukamoto Y et al., 2008). In effect, ANKRD2 has previously been shown to bind to YB-1, PML and p53 transcription factors, suggesting its role in signalling. ANKRD2 is also able to interact with Z-disc proteins such as telethonin (Kojic S et al., 2004). SPR experiments revealed an interaction between ANKRD2 and the PDZ domain of ZASP, with a dissociation constant for the binding in the nM range. This result seems to be supported by a recent finding from our collaborators in Trieste, where an interaction between the ZASP full-length protein and ANKRD2 has been demonstrated by means of coimmunoprecipitation experiments (personal

communication). Several interesting questions are now opened and this result could represent the starting point for better investigating the role of ANKRD2 in muscle.

As already emphasized in this thesis, the fact that multiple binding partners for a protein is the rule rather than the exception, it would be very helpful to define if and where all of these proteins could bind in reality. Therefore, a period of my PhD project was dedicated to expression studies using the Real-Time PCR technique; mRNAs from different muscles of adult mice were used as starting material. Particular attention was focused on ZASP, for which several alternatively spliced isoforms have been reported (Huang C et al., 2003). In mouse the gene contains 17 exons and gives rise to six splice variants, three cardiac isoforms and three skeletal one. Within each muscle subtype, ZASP isoforms can be further subclassified as short or long, based on the deletion or inclusion of exons encoding the C-terminal LIM domains, respectively. Among the ZASP long isoforms, there is a further distinction in those containing or lacking exon 11. Our results revealed that the short isoforms are more expressed than the long proteins in both skeletal and cardiac adult muscles. In effect, it is known from the literature that the short isoform expression is barely detectable during embryogenesis but it increases post-birth, suggesting an important role in mature muscle (Huang C et al., 2003). Regarding the ZASP long isoforms, Huang C and colleagues reported that in skeletal muscle ZASP with exon 11 is the predominant long isoform during embryogenesis and in neonatal muscle, but is gradually replaced by the long isoform lacking exon 11 with progressive aging. Our experiments showed a higher expression of the ZASP long variant lacking exon 11 in adult murine muscles, thus confirming what already known. However, ZASP long variant containing exon 11 was more expressed in soleus (slow-twitch muscle) compared to tibialis (fast-twitch muscle) and gastrocnemius (muscle with mixed fibers). Also in cardiac muscle the long isoform of ZASP with exon 11 showed a significant expression although the long isoform without exon 11 was the mainly expressed variant. This would probably indicate a more important function of the ZASP long isoform with exon 11 in soleus and cardiac muscle, which also reflect a higher similarity between these two muscles compared with tibialis and gastrocnemius.

Regarding the FATZ family of proteins, Real-Time PCR experiments confirmed what previously known (Frey N, and Olson EN, 2002). FATZ-1 is preferentially expressed in fast-twitch fiber type (tibialis and gastrocnemius) and to a lesser extent in slow-twitch fiber type (soleus); no expression is found in heart. FATZ-3

behaves similarly to FATZ-1 although its overall expression is greatly reduced in all of the tissues analyzed. In contrast, FATZ-2 is predominantly expressed in soleus and heart, which shares several molecular features with the slow-twitch muscle. As expected, the expression of myotilin is preferentially restricted to skeletal muscle tissues (tibialis, gastrocnemius and soleus), whereas no expression is found in heart. Unfortunately, ALP and CLP-36 were not included in the Real-Time PCR experiments; however it would be useful to extend this study to them in order to have an overview of the real expression of these proteins in muscle.

VI CONCLUSIONS

The main finding of this thesis is the identification of a binding motif common to the C-terminus of the FATZ and myotilin families of sarcomeric proteins that specifically interacts with the PDZ domains of the enigma family members ZASP, ALP, CLP-36 and RIL. The E-[S/T]-[D/E]-[D/E]-L C-terminal motif is found in Vertebrates to be restricted to the FATZ and myotilin families, and it can be considered a novel type of class III PDZ binding motif specific for the PDZ domains of enigma proteins. These interactions were identified by different *in vitro* binding techniques such as AlphaScreen, PDZ Domain Array and SPR. The work of this thesis was part of a wider project done in collaboration with the groups of Dr. G. Faulkner, ICGEB, Trieste, and Prof. O. Carpen, University of Turku, Finland.

AlphaScreen experiments show that the interaction between the PDZ domains of ZASP, ALP and CLP-36 is mediated by the last five amino acids of the FATZ family of proteins and myotilin. The specific binding site on these proteins was demonstrated by absence of interaction when using the truncated version (lacking the terminal five amino acids) of the FATZ proteins and myotilin. Biotinylated peptides corresponding to the last five amino acids of FATZ-1 (ETEEL), FATZ-2/palladin (ESEDL), FATZ-3/myotilin (ESEEL) and myopalladin (ESDEL) behave as ligands for the PDZ domains of ZASP, ALP and CLP-36, confirming that binding to PDZ domains occurs via the C-terminal region of these proteins. The very last amino acid of the ligand motif (L in FATZ and myotilin families of proteins) is fundamental for the PDZ recognition as the interaction with the three PDZ domains is completely destroyed after changing the last amino acid from leucine to glutamic acid. AlphaScreen experiments also confirm the already known interactions of ZASP and ALP PDZ domains with α-actinin-2 (Zhou Q et al., 1999; Faulkner G et al., 1999; Klaavuniemi T et al., 2004) and demonstrate an interaction between the PDZ domain of CLP-36 and α-actinin-2. The interactions between ZASP, ALP and CLP-36 PDZ domains and α-actinin-2 involve the last five amino of this protein as verified by AlphaScreen experiments done with the C-terminal peptide ligand of α-actinin-2. Unlike FATZ and myotilin families, the C-terminus of α-actinin-2 (GESDL) is considered a class I PDZ binding motif. These results together would indicate that ZASP, ALP and CLP-36 PDZ domains have a dual specificity of binding as they can interact with both class I and class III PDZ binding motifs. Phosphorylation of the ligand sequence seems to be an

important factor in modulating the binding activity between the PDZ domains of enigma proteins and the FATZ and myotilin families. AlphaScreen interaction experiments were done with the same biotinylated peptides but phosphorylated on the serine or threonine residue. The most common effect of phosphorylation is the disruption of the binding between PDZ and its ligand (Kim E, and Sheng M, 2004). We noted a negative effect in a single situation (i.e. between CLP-36 PDZ domain and myopalladin peptide). In some cases binding was not affected by phosphorylation of the ligand sequence (e.g. between CLP-36 PDZ domain and FATZ-1 and FATZ-2/palladin peptides), but in most cases phosphorylation even increased the strength of the interaction (e.g. between CLP-36 PDZ domain and FATZ-3/myotilin and α-actinin-2 peptides).

The interaction of the FATZ and myotilin families with the enigma family members is highly specific as demonstrated by the restricted number of PDZ domains bound by the peptide ligands in PDZ array experiments. Interestingly, these PDZ domains correspond to the only two enigma family members on the array, CLP-36 (hCLIM1) and RIL. Based on the results of the PDZ arrays, RIL would seem another binding partner for proteins of the FATZ family, myotilin, palladin and myopalladin. However, it has to be noted that RIL is mainly found in non-muscle tissues; consequently, its interaction with the FATZ and myotilin families needs further investigations.

Important questions remain to be answered; for example, it would be helpful to understand what happens when several proteins, able to interact with the same partners, meet at the same time. Interesting results were obtained from AlphaScreen competitions studies. Such experiments demonstrate that a PDZ class III interaction (between the ZASP-1 protein and the FATZ-3/myotilin peptides) can be competed by the addition of another class III ligand (the C-terminal region of FATZ-1), as expected. On the contrary, a class I PDZ binding ligand (α-actinin-2) is not able to compete as well as a type III ligand in the same interaction. Also expression studies would be useful in this sense, since they could provide indications about the level and pattern of distribution of the single proteins in different muscles. Real-Time PCR experiments show that the FATZ family of proteins, myotilin and ZASP (with its alternatively spliced isoforms) are differently distributed in various muscles. For example, FATZ-1 and FATZ-3 are mainly found in fast-twitch muscles (tibialis and gastrocnemius), whereas FATZ-2 is expressed in slow-twitch muscle (soleus) and heart. On the contrary, myotilin is only found in skeletal muscle, while expression of ZASP long isoforms characterized by the presence of exon 11 is more significant in soleus and heart than in tibialis and gastrocnemius. As demonstrated by our interaction

experiments, all of these proteins can effectively bind with each other, but the relevance of their interactions should also consider the pattern and level of expression of each protein in a given muscle.

The strength of the bindings between the PDZ domain of ZASP and some of the peptides was evaluated with SPR experiments done in the laboratory of Dr. A. Baines at University of Kent, UK. The affinities of the interactions are in the nM range, but they vary depending on the ligand considered. SPR results indicate that phosphorylation may be a mechanism able to influence the interactions between the enigma members and the FATZ and myotilin families of proteins. The unknown interaction of ZASP PDZ domain with ANKRD2, a protein involved in muscle stress response pathways and interacting with several transcription factors, is undoubtedly relevant. In fact, it would provide an indication of the further role of the Z-disc as a coordinator of intracellular signalling.

The function of PDZ domain-containing proteins as adaptors in recruiting signalling molecules to the actin cytoskeleton is now well-established. In muscle, it is thought that they are able to transmit mechanical stress signals from the Z-disc to the nucleus (Vallenius T et al., 2004). This is based on the ability of some PDZ proteins to associate with cytoskeletal structures via the PDZ domain, and also on the capacity of several PDZ-LIM proteins (such as the enigma family proteins) to bind to kinases by means of their LIM domains. Thus, it is possible that enigma family members link proteins of the FATZ and myotilin families to signalling events such as PKC phosphorylation. However, it is important to realize that the results presented in this thesis are based on *in vitro* binding techniques. They provide evidence that the interactions occur, but they might not always reflect the *in vivo* situation. It would be of great interest to verify these results with *in vivo* models. In this way, it would be also possible to better define if and where all of the proteins studied could bind in reality, and if phosphorylation effectively modulates the strength of these interactions.

VII REFERENCES

Aihara Y, Kurabayashi M, Saito Y, Ohyama Y, Tanaka T, Takeda S, Tomaru K, Sekiguchi K, Arai M, Nakamura T, Nagai R (2000). Cardiac ankyrin repeat protein is a novel marker of cardiac hypertrophy: role of M-CAT element within the promoter. *Hypertension*. 36(1):48-53.

Arber S, Hunter JJ, Ross J Jr, Hongo M, Sansig G, Borg J, Perriard JC, Chien KR, Caroni P (1997). MLP-deficient mice exhibit a disruption of cardiac cytoarchitectural organization, dilated cardiomyopathy, and heart failure. *Cell*. 88(3):393-403.

Arimura T, Hayashi T, Terada H, Lee SY, Zhou Q, Takahashi M, Ueda K, Nouchi T, Hohda S, Shibutani M, Hirose M, Chen J, Park JE, Yasunami M, Hayashi H, Kimura A (2004). A Cypher/ZASP mutation associated with dilated cardiomyopathy alters the binding affinity to protein kinase C. *J Biol Chem*. 279(8):6746-52.

Arola AM, Sanchez X, Murphy RT, Hasle E, Li H, Elliott PM, McKenna WJ, Towbin JA, Bowles NE (2007). Mutations in PDLIM3 and MYOZ1 encoding myocyte Z line proteins are infrequently found in idiopathic dilated cardiomyopathy. *Mol Genet Metab*. 90(4):435-40.

Au Y (2004). The muscle ultrastructure: a structural perspective of the sarcomere. *Cell Mol Life Sci*. 61(24):3016-33.

Bang ML, Mudry RE, McElhinny AS, Trombitás K, Geach AJ, Yamasaki R, Sorimachi H, Granzier H, Gregorio CC, Labeit S (2001). Myopalladin, a novel 145-kilodalton sarcomeric protein with multiple roles in Z-disc and I-band protein assemblies. *J Cell Biol*. 153(2):413-27.

Barrès R, Gonzalez T, Le Marchand-Brustel Y, Tanti JF (2005). The interaction between the adaptor protein APS and Enigma is involved in actin organisation. *Exp Cell Res*. 308(2):334-44.

Bartoloni L, Horrigan SK, Viles KD, Gilchrist JM, Stajich JM, Vance JM, Yamaoka LH, Pericak-Vance MA, Westbrook CA, Speer MC (1998). Use of a CEPH meiotic breakpoint panel to refine the locus of limb-girdle muscular dystrophy type 1A (LGMD1A) to a 2-Mb interval on 5q31. *Genomics*. 54(2):250-5.

Beggs AH, Byers TJ, Knoll JH, Boyce FM, Bruns GA, Kunkel LM (1992). Cloning and characterization of two human skeletal muscle alpha-actinin genes located on chromosomes 1 and 11. *J Biol Chem*. 267(13):9281-8.

Berchtold MW, Brinkmeier H, Müntener M (2000). Calcium ion in skeletal muscle: its crucial role for muscle function, plasticity, and disease. *Physiol Rev*. 80(3):1215-65.

Bezprozvanny I, and Maximov A (2001). Classification of PDZ domains. *FEBS Lett*. 509(3):457-62.

Bond M, and Somlyo AV (1982). Dense bodies and actin polarity in vertebrate smooth muscle. *J Cell Biol*. 95(2 Pt 1):403-13.

Borrello MG, Mercalli E, Perego C, Degl'Innocenti D, Ghizzoni S, Arighi E, Eroini B, Rizzetti MG, Pierotti MA (2002). Differential interaction of Enigma protein with the two RET isoforms. *Biochem Biophys Res Commun*. 296(3):515-22.

Bottinelli R, and Reggiani C (2000). Human skeletal muscle fibres: molecular and functional diversity. *Prog Biophys Mol Biol*. 73(2-4):195-262.

Boukhelifa M, Parast MM, Bear JE, Gertler FB, Otey CA (2004). Palladin is a novel binding partner for Ena/VASP family members. *Cell Motil Cytoskeleton*. 58(1):17-29.

Boumber YA, Kondo Y, Chen X, Shen L, Gharibyan V, Konishi K, Estey E, Kantarjian H, Garcia-Manero G, Issa JP (2007). RIL, a LIM gene on 5q31, is silenced by methylation in cancer and sensitizes cancer cells to apoptosis. *Cancer Res*. 67(5):1997-200.

Burkitt HG, Young B, Heath JW, Deakin PJ (1993). Wheater's functional histology: a text and colour atlas. Edinburgh, Churchill Livingstone.

Cazorla O, Wu Y, Irving TC, Granzier H (2001). Titin-based modulation of calcium sensitivity of active tension in mouse skinned cardiac myocytes. *Circ Res*. 88(10):1028-35.

Cho KO, Hunt CA, Kennedy MB (1992). The rat brain postsynaptic density fraction contains a homolog of the Drosophila discs-large tumor suppressor protein. *Neuron*. 9(5):929-42.

Chu W, Burns DK, Swerlick RA, Presky DH (1995). Identification and characterization of a novel cytokine-inducible nuclear protein from human endothelial cells. *J Biol Chem*. 270(17):10236-45.

Clark KA, McElhinny AS, Beckerle MC, Gregorio CC (2002). Striated muscle cytoarchitecture: an intricate web of form and function. *Annu Rev Cell Dev Biol*. 18:637-706.

Cohen NA, Brenman JE, Snyder SH, Bredt DS (1996). Binding of the inward rectifier K+ channel Kir 2.3 to PSD-95 is regulated by protein kinase A phosphorylation. *Neuron*. 17(4):759-67.

Cuppen E, Gerrits H, Pepers B, Wieringa B, Hendriks W (1998). PDZ motifs in PTP-BL and RIL bind to internal protein segments in the LIM domain protein RIL. *Mol Biol Cell*. 9(3):671-83.

Dempsey EC, Newton AC, Mochly-Rosen D, Fields AP, Reyland ME, Insel PA, Messing RO (2000). Protein kinase C isozymes and the regulation of diverse cell responses. *Am J Physiol Lung Cell Mol Physiol*. 279(3):L429-38.

Djinovic-Carugo K, Gautel M, Ylänne J, Young P (2002). The spectrin repeat: a structural platform for cytoskeletal protein assemblies. *FEBS Lett*. 513(1):119-23.

Doyle DA, Lee A, Lewis J, Kim E, Sheng M, MacKinnon R (1996). Crystal structures of a complexed and peptide-free membrane protein-binding domain: molecular basis of peptide recognition by PDZ. *Cell*. 85(7):1067-76.

Duboscq-Bidot L, Xu P, Charron P, Neyroud N, Dilanian G, Millaire A, Bors V, Komajda M, Villard E (2008). Mutations in the Z-band protein myopalladin gene and idiopathic dilated cardiomyopathy. *Cardiovasc Res*. 77(1):118-25.

Durick K, Gill GN, Taylor SS (1998). Shc and Enigma are both required for mitogenic signaling by Ret/ptc2. *Mol Cell Biol*. 18(4):2298-308.

Ecarnot-Laubriet A, De Luca K, Vandroux D, Moisant M, Bernard C, Assem M, Rochette L, Teyssier JR (2000). Downregulation and nuclear relocation of MLP during the progression of right ventricular hypertrophy induced by chronic pressure overload. *J Mol Cell Cardiol*. 32(12):2385-95.

Edwards PR, and Leatherbarrow RJ (1997). Determination of association rate constants by an optical biosensor using initial rate analysis. *Anal Biochem*. 246(1):1-6.

Ehler E, Horowits R, Zuppinger C, Price RL, Perriard E, Leu M, Caroni P, Sussman M, Eppenberger HM, Perriard JC (2001). Alterations at the intercalated disk associated with the absence of muscle LIM protein. *J Cell Biol*. 153(4):763-72.

Faccio L, Fusco C, Viel A, Zervos AS (2000). Tissue-specific splicing of Omi stress-regulated endoprotease leads to an inactive protease with a modified PDZ motif. *Genomics*. 68(3):343-7.

Faulkner G, Pallavicini A, Formentin E, Comelli A, Ievolella C, Trevisan S, Bortoletto G, Scannapieco P, Salamon M, Mouly V, Valle G, Lanfranchi G (1999). ZASP: a new Z-band alternatively spliced PDZ-motif protein. *J Cell Biol*. 146(2):465-75.

Faulkner G, Pallavicini A, Comelli A, Salamon M, Bortoletto G, Ievolella C, Trevisan S, Kojic S, Dalla Vecchia F, Laveder P, Valle G, Lanfranchi G (2000). FATZ, a filamin-, actinin-, and telethonin-binding protein of the Z-disc of skeletal muscle. *J Biol Chem*. 275(52):41234-42.

Feit H, Silbergleit A, Schneider LB, Gutierrez JA, Fitoussi RP, Réyès C, Rouleau GA, Brais B, Jackson CE, Beckmann JS, Seboun E (1998). Vocal cord and pharyngeal weakness with autosomal dominant distal myopathy: clinical description and gene localization to 5q31. *Am J Hum Genet*. 63(6):1732-42.

Frank D, Kuhn C, Katus HA, Frey N (2006). The sarcomeric Z-disc: a nodal point in signalling and disease. *J Mol Med*. 84(6):446-68.

Frey N, Richardson JA, Olson EN (2000). Calsarcins, a novel family of sarcomeric calcineurin-binding proteins. *Proc Natl Acad Sci U S A*. 97(26):14632-7.

Frey N, and Olson EN (2002). Calsarcin-3, a novel skeletal muscle-specific member of the calsarcin family, interacts with multiple Z-disc proteins. *J Biol Chem*. 277(16):13998-4004.

Frey N, Barrientos T, Shelton JM, Frank D, Rütten H, Gehring D, Kuhn C, Lutz M, Rothermel B, Bassel-Duby R, Richardson JA, Katus HA, Hill JA, Olson EN (2004). Mice lacking calsarcin-1 are sensitized to calcineurin signaling and show accelerated cardiomyopathy in response to pathological biomechanical stress. *Nat Med*. 10(12):1336-43.

Furukawa T, Ono Y, Tsuchiya H, Katayama Y, Bang ML, Labeit D, Labeit S, Inagaki N, Gregorio CC (2001). Specific interaction of the potassium channel beta-subunit minK with the sarcomeric protein T-cap suggests a T-tubule-myofibril linking system. *J Mol Biol*. 313(4):775-84.

Gautel M, Goulding D, Bullard B, Weber K, Fürst DO (1996). The central Z-disk region of titin is assembled from a novel repeat in variable copy numbers. *J Cell Sci*. 109:2747-54.

Gimona M, Djinovic-Carugo K, Kranewitter WJ, Winder SJ (2002). Functional plasticity of CH domains. *FEBS Lett*. 513(1):98-106.

Gontier Y, Taivainen A, Fontao L, Sonnenberg A, van der Flier A, Carpen O, Faulkner G, Borradori L (2005). The Z-disc proteins myotilin and FATZ-1 interact with each other and are connected to the sarcolemma via muscle-specific filamins. *J Cell Sci*. 118(Pt 16):3739-49.

Granzier HL, Labeit S (2004). The giant protein titin: a major player in myocardial mechanics, signaling, and disease. *Circ Res*. 94(3):284-95.

Gregorio CC, Trombitás K, Centner T, Kolmerer B, Stier G, Kunke K, Suzuki K, Obermayr F, Herrmann B, Granzier H, Sorimachi H, Labeit S (1998). The NH2 terminus of titin spans the Z-disc: its interaction with a novel 19-kD ligand (T-cap) is required for sarcomeric integrity. *J Cell Biol*. 143(4):1013-27.

Gregorio CC, Granzier H, Sorimachi H, Labeit S (1999). Muscle assembly: a titanic achievement? *Curr Opin Cell Biol*. 11(1):18-25.

Griggs R, Vihola A, Hackman P, Talvinen K, Haravuori H, Faulkner G, Eymard B, Richard I, Selcen D, Engel A, Carpen O, Udd B (2007). Zaspopathy in a large classic late-onset distal myopathy family. *Brain*. 130(Pt 6):1477-84.

Grootjans JJ, Reekmans G, Ceulemans H, David G (2000). Syntenin-syndecan binding requires syndecan-synteny and the co-operation of both PDZ domains of syntenin. *J Biol Chem*. 275(26):19933-41.

Guy PM, Kenny DA, Gill GN (1999). The PDZ domain of the LIM protein enigma binds to beta-tropomyosin. *Mol Biol Cell*. 10(6):1973-84.

Guyon JR, Kudryashova E, Potts A, Dalkilic I, Brosius MA, Thompson TG, Beckmann JS, Kunkel LM, Spencer MJ (2003). Calpain 3 cleaves filamin C and regulates its ability to interact with gamma- and delta-sarcoglycans. *Muscle Nerve*. 28(4):472-83.

Harper BD, Beckerle MC, Pomiès P (2000). Fine mapping of the alpha-actinin binding site within cysteine-rich protein. *Biochem J*. 350:269-74.

Harris BZ, and Lim WA (2001). Mechanism and role of PDZ domains in signaling complex assembly. *J Cell Sci*. 114(Pt 18):3219-31.

Harrison SC (1996). Peptide-surface association: the case of PDZ and PTB domains. *Cell*. 86(3):341-3.

Hauser MA, Horrigan SK, Salmikangas P, Torian UM, Viles KD, Dancel R, Tim RW, Taivainen A, Bartoloni L, Gilchrist JM, Stajich JM, Gaskell PC, Gilbert JR, Vance JM, Pericak-Vance MA, Carpen O, Westbrook CA, Speer MC (2000). Myotilin is mutated in limb girdle muscular dystrophy 1A. *Hum Mol Genet*. 9(14):2141-7.

Hayashi T, Arimura T, Itoh-Satoh M, Ueda K, Hohda S, Inagaki N, Takahashi M, Hori H, Yasunami M, Nishi H, Koga Y, Nakamura H, Matsuzaki M, Choi BY, Bae SW, You CW, Han KH, Park JE, Knöll R, Hoshijima M, Chien KR, Kimura A (2004). Tcap gene mutations in hypertrophic cardiomyopathy and dilated cardiomyopathy. *J Am Coll Cardiol*. 44(11):2192-201.

Hegedüs T, Sessler T, Scott R, Thelin W, Bakos E, Váradi A, Szabó K, Homolya L, Milgram SL, Sarkadi B (2003). C-terminal phosphorylation of MRP2 modulates its interaction with PDZ proteins. *Biochem Biophys Res Commun*. 302(3):454-61.

Heineke J, Ruetten H, Willenbockel C, Gross SC, Naguib M, Schaefer A, Kempf T, Hilfiker-Kleiner D, Caroni P, Kraft T, Kaiser RA, Molkentin JD, Drexler H, Wollert KC (2005). Attenuation of cardiac remodeling after myocardial infarction by muscle LIM protein-calcineurin signaling at the sarcomeric Z-disc. *Proc Natl Acad Sci U S A*. 102(5):1655-60.

Herrera AM, McParland BE, Bienkowska A, Tait R, Pare PD, Seow CY (2005). 'Sarcomeres' of smooth muscle: functional characteristics and ultrastructural evidence. *J Cell Sci*. 118: 2381-92.

Honda K, Yamada T, Endo R, Ino Y, Gotoh M, Tsuda H, Yamada Y, Chiba H, Hirohashi S (1998). Actinin-4, a novel actin-bundling protein associated with cell motility and cancer invasion. *J Cell Biol*. 140(6):1383-93.

Huang C, Zhou Q, Liang P, Hollander MS, Sheikh F, Li X, Greaser M, Shelton GD, Evans S, Chen J (2003). Characterization and in vivo functional analysis of splice variants of cypher. *J Biol Chem*. 278(9):7360-5.

Hung AY, and Sheng M (2002). PDZ domains: structural modules for protein complex assembly. *J Biol Chem*. 277(8):5699-702.

Huxley HE (2008). Memories of early work on muscle contraction and regulation in the 1950's and 1960's. *Biochem Biophys Res Commun*. 369(1):34-42.

Ikeda K, Emoto N, Matsuo M, Yokoyama M (2003). Molecular identification and characterization of a novel nuclear protein whose expression is up-regulated in insulin-resistant animals. *J Biol Chem*. 278(6):3514-20.

Jeleń F, Oleksy A, Smietana K, Otlewski J (2003). PDZ domains - common players in the cell signaling. *Acta Biochim Pol*. 50(4):985-1017.

Jeyaseelan R, Poizat C, Baker RK, Abdishoo S, Isterabadi LB, Lyons GE, Kedes L (1997). A novel cardiac-restricted target for doxorubicin. CARP, a nuclear modulator of gene expression in cardiac progenitor cells and cardiomyocytes. *J Biol Chem*. 272(36):22800-8.

Jo K, Rutten B, Bunn RC, Bredt DS (2001). Actinin-associated LIM protein-deficient mice maintain normal development and structure of skeletal muscle. *Mol Cell Biol*. 21(5):1682-7.

Kang BS, Cooper DR, Jelen F, Devedjiev Y, Derewenda U, Dauter Z, Otlewski J, Derewenda ZS (2003). PDZ tandem of human syntenin: crystal structure and functional properties. *Structure*. 11(4):459-68.

Kemp TJ, Sadusky TJ, Saltisi F, Carey N, Moss J, Yang SY, Sassoon DA, Goldspink G, Coulton GR (2000). Identification of Ankrd2, a novel skeletal muscle gene coding for a stretch-responsive ankyrin-repeat protein. *Genomics*. 66(3):229-41.

Kiess M, Scharm B, Aguzzi A, Hajnal A, Klemenz R, Schwarte-Waldhoff I, Schäfer R (1995). Expression of ril, a novel LIM domain gene, is down-regulated in Hras-transformed cells and restored in phenotypic revertants. *Oncogene*. 10(1):61-8.

Kim E, and Sheng M (2004). PDZ domain proteins of synapses. *Nat Rev Neurosci*. 5(10):771-81.

Klaavuniemi T, Kelloniemi A, Ylänne J (2004). The ZASP-like motif in actinin-associated LIM protein is required for interaction with the alpha-actinin rod and for targeting to the muscle Z-line. *J Biol Chem*. 279(25):26402-10.

Klaavuniemi T, and Ylänne J (2006). Zasp/Cypher internal ZM-motif containing fragments are sufficient to co-localize with alpha-actinin--analysis of patient mutations. *Exp Cell Res*. 312(8):1299-311.

Klaavuniemi T (2006). PDZ-LIM domain proteins and α-actinin at the muscle Z-disk. http://herkules.oulu.fi/isbn9514282647/.

Knöll R, Hoshijima M, Hoffman HM, Person V, Lorenzen-Schmidt I, Bang ML, Hayashi T, Shiga N, Yasukawa H, Schaper W, McKenna W, Yokoyama M, Schork NJ, Omens JH, McCulloch AD, Kimura A, Gregorio CC, Poller W, Schaper J, Schultheiss HP, Chien KR (2002). The cardiac mechanical stretch sensor machinery involves a Z disc complex that is defective in a subset of human dilated cardiomyopathy. *Cell*. 111(7):943-55.

Kojic S, Medeot E, Guccione E, Krmac H, Zara I, Martinelli V, Valle G, Faulkner G (2004). The Ankrd2 protein, a link between the sarcomere and the nucleus in skeletal muscle. *J Mol Biol*. 339(2):313-25.

Kong Y, Flick MJ, Kudla AJ, Konieczny SF (1997). Muscle LIM protein promotes myogenesis by enhancing the activity of MyoD. *Mol Cell Biol*. 17(8):4750-60.

Kotaka M, Ngai SM, Garcia-Barcelo M, Tsui SK, Fung KP, Lee CY, Waye MM (1999). Characterization of the human 36-kDa carboxyl terminal LIM domain protein (hCLIM1). *J Cell Biochem*. 72(2):279-85.

Kotaka M, Kostin S, Ngai S, Chan K, Lau Y, Lee SM, Li H, Ng EK, Schaper J, Tsui SK, Fung K, Lee C, Waye MM (2000). Interaction of hCLIM1, an enigma family protein, with alpha-actinin 2. *J Cell Biochem*. 78(4):558-65.

Kotaka M, Lau YM, Cheung KK, Lee SM, Li HY, Chan WY, Fung KP, Lee CY, Waye MM, Tsui SK (2001). Elfin is expressed during early heart development. *J Cell Biochem*. 83(3):463-72.

Krishnamoorthy RV (1977). Increased histaminase activity in the atrophic muscle of denervated frog. *Enzyme*. 22(2):73-9.

Kruger M, Wright J, Wang K (1991). Nebulin as a length regulator of thin filaments of vertebrate skeletal muscles: correlation of thin filament length, nebulin size, and epitope profile. *J Cell Biol*. 115(1):97-107.

Kuo H, Chen J, Ruiz-Lozano P, Zou Y, Nemer M, Chien KR (1999). Control of segmental expression of the cardiac-restricted ankyrin repeat protein gene by distinct regulatory pathways in murine cardiogenesis. *Development*. 126(19):4223-34.

Kuroda S, Tokunaga C, Kiyohara Y, Higuchi O, Konishi H, Mizuno K, Gill GN, Kikkawa U (1996). Protein-protein interaction of zinc finger LIM domains with protein kinase C. *J Biol Chem*. 271(49):31029-32.

Labeit S, and Kolmerer B (1995). The complete primary structure of human nebulin and its correlation to muscle structure. *J Mol Biol*. 248(2):308-15.

Lanfranchi G, Muraro T, Caldara F, Pacchioni B, Pallavicini A, Pandolfo D, Toppo S, Trevisan S, Scarso S, Valle G (1996). Identification of 4370 expressed sequence tags from a 3'-end-specific cDNA library of human skeletal muscle by DNA sequencing and filter hybridization. *Genome Res*. 6(1):35-42.

Lange S, Himmel M, Auerbach D, Agarkova I, Hayess K, Fürst DO, Perriard JC, Ehler E (2005). Dimerisation of myomesin: implications for the structure of the sarcomeric M-band. *J Mol Biol*. 345(2):289-98.

Liu Y, Hair GA, Boden SD, Viggeswarapu M, Titus L (2002). Overexpressed LIM mineralization proteins do not require LIM domains to induce bone. *J Bone Miner Res*. 17(3):406-14.

Lodish H, Baltimore D, Berk A, Zipursky SL, Matsudaira P, Darnell J (1995). Molecular cell biology. Third edition. WH Freeman and Company, New York.

Loo DT, Kanner SB, Aruffo A (1998). Filamin binds to the cytoplasmic domain of the beta1-integrin. Identification of amino acids responsible for this interaction. *J Biol Chem*. 273(36):23304-12.

Loughran G, Healy NC, Kiely PA, Huigsloot M, Kedersha NL, O'Connor R (2005). Mystique is a new insulin-like growth factor-I-regulated PDZ-LIM domain protein that promotes cell attachment and migration and suppresses Anchorage-independent growth. *Mol Biol Cell*. 16(4):1811-22.

Louis HA, Pino JD, Schmeichel KL, Pomiès P, Beckerle MC (1997). Comparison of three members of the cysteine-rich protein family reveals functional conservation and divergent patterns of gene expression. *J Biol Chem*. 272(43):27484-91.

Luther PK, Barry JS, Squire JM (2002). The three-dimensional structure of a vertebrate wide (slow muscle) Z-band: lessons on Z-band assembly. *J Mol Biol*. 315(1):9-20.

Maeno-Hikichi Y, Chang S, Matsumura K, Lai M, Lin H, Nakagawa N, Kuroda S, Zhang JF (2003). A PKC epsilon-ENH-channel complex specifically modulates N-type Ca2+ channels. *Nat Neurosci*. 6(5):468-75.

Marino JH, Cook P, Miller KS (2003). Accurate and statistically verified quantification of relative mRNA abundances using SYBR Green I and real-time RT-PCR. *J Immunol Methods*. 283(1-2):291-306.

Mayans O, van der Ven PF, Wilm M, Mues A, Young P, Fürst DO, Wilmanns M, Gautel M (1998). Structural basis for activation of the titin kinase domain during myofibrillogenesis. *Nature*. 395(6705):863-9.

McKenna NM, Johnson CS, Wang YL (1986). Formation and alignment of Z lines in living chick myotubes microinjected with rhodamine-labeled alpha-actinin. *J Cell Biol*. 103:2163-71.

Mckoy G, Hou Y, Yang SY, Vega Avelaira D, Degens H, Goldspink G, Coulton GR (2005). Expression of Ankrd2 in fast and slow muscles and its response to stretch are consistent with a role in slow muscle function. *J Appl Physiol*. 98(6):2337-43; discussion 2320.

Miller MK, Bang ML, Witt CC, Labeit D, Trombitas C, Watanabe K, Granzier H, McElhinny AS, Gregorio CC, Labeit S (2003). The muscle ankyrin repeat proteins: CARP, ankrd2/Arpp and DARP as a family of titin filament-based stress response molecules. *J Mol Biol*. 333(5):951-64.

Miller MK, Granzier H, Ehler E, Gregorio CC (2004). The sensitive giant: the role of titin-based stretch sensing complexes in the heart. *Trends Cell Biol*. 14(3):119-26.

Millevoi S, Trombitas K, Kolmerer B, Kostin S, Schaper J, Pelin K, Granzier H, Labeit S (1998). Characterization of nebulette and nebulin and emerging concepts of their roles for vertebrate Z-discs. *J Mol Biol*. 282(1):111-23.

Mohapatra B, Jimenez S, Lin JH, Bowles KR, Coveler KJ, Marx JG, Chrisco MA, Murphy RT, Lurie PR, Schwartz RJ, Elliott PM, Vatta M, McKenna W, Towbin JA, Bowles NE (2003). Mutations in the muscle LIM protein and alpha-actinin-2 genes in dilated cardiomyopathy and endocardial fibroelastosis. *Mol Genet Metab*. 80(1-2):207-15.

Moncman CL, and Wang K (1995). Nebulette: a 107 kD nebulin-like protein in cardiac muscle. *Cell Motil Cytoskeleton*. 32(3):205-25.

Moreira ES, Wiltshire TJ, Faulkner G, Nilforoushan A, Vainzof M, Suzuki OT, Valle G, Reeves R, Zatz M, Passos-Bueno MR, Jenne DE (2000). Limb-girdle muscular dystrophy type 2G is caused by mutations in the gene encoding the sarcomeric protein telethonin. *Nat Genet*. 24(2):163-6.

Moriyama M, Tsukamoto Y, Fujiwara M, Kondo G, Nakada C, Baba T, Ishiguro N, Miyazaki A, Nakamura K, Hori N, Sato K, Shomori K, Takeuchi K, Satoh H, Mori S, Ito H (2001). Identification of a novel human ankyrin-repeated protein homologous to CARP. *Biochem Biophys Res Commun*. 285(3):715-23.

Mounier N, and Sparrow JC (1997). Structural comparisons of muscle and nonmuscle actins give insights into the evolution of their functional differences. *J Mol Evol*. 44(1):89-97.

Moza M, Mologni L, Trokovic R, Faulkner G, Partanen J, Carpén O (2007). Targeted deletion of the muscular dystrophy gene myotilin does not perturb muscle structure or function in mice. *Mol Cell Biol*. 27(1):244-52.

Mykkänen OM, Grönholm M, Rönty M, Lalowski M, Salmikangas P, Suila H, Carpén O (2001). Characterization of human palladin, a microfilament-associated protein. *Mol Biol Cell*. 12(10):3060-73.

Nakada C, Oka A, Nonaka I, Sato K, Mori S, Ito H, Moriyama M (2003). Cardiac ankyrin repeat protein is preferentially induced in atrophic myofibers of congenital myopathy and spinal muscular atrophy. *Pathol Int*. 53(10):653-8.

Nakagawa N, Hoshijima M, Oyasu M, Saito N, Tanizawa K, Kuroda S (2000). ENH, containing PDZ and LIM domains, heart/skeletal muscle-specific protein, associates with cytoskeletal proteins through the PDZ domain. *Biochem Biophys Res Commun*. 272(2):505-12.

Nave R, Fürst DO, Weber K (1990). Interaction of alpha-actinin and nebulin in vitro. Support for the existence of a fourth filament system in skeletal muscle. *FEBS Lett*. 269(1):163-6.

Naya FJ, Mercer B, Shelton J, Richardson JA, Williams RS, Olson EN (2000). Stimulation of slow skeletal muscle fiber gene expression by calcineurin *in vivo*. *J Biol Chem*. 275(7):4545-8.

Niederländer N, Fayein NA, Auffray C, Pomiès P (2004). Characterization of a new human isoform of the enigma homolog family specifically expressed in skeletal muscle. *Biochem Biophys Res Commun*. 325(4):1304-11.

Nigro V, de Sá Moreira E, Piluso G, Vainzof M, Belsito A, Politano L, Puca AA, Passos-Bueno MR, Zatz M (1996). Autosomal recessive limb-girdle muscular dystrophy, LGMD2F, is caused by a mutation in the delta-sarcoglycan gene. *Nat Genet*. 14(2):195-8.

North KN, Yang N, Wattanasirichaigoon D, Mills M, Easteal S, Beggs AH (1999). A common nonsense mutation results in alpha-actinin-3 deficiency in the general population. *Nat Genet*. 21(4):353-4.

Olivé M, Goldfarb LG, Shatunov A, Fischer D, Ferrer I (2005). Myotilinopathy: refining the clinical and myopathological phenotype. *Brain*. 128(Pt 10):2315-26.

Osio A, Tan L, Chen SN, Lombardi R, Nagueh SF, Shete S, Roberts R, Willerson JT, Marian AJ (2007). Myozenin 2 is a novel gene for human hypertrophic cardiomyopathy. *Circ Res*. 100(6):766-8.

Otey CA, Rachlin A, Moza M, Arneman D, Carpen O (2005). The palladin/myotilin/myopalladin family of actin-associated scaffolds. *Int Rev Cytol*. 246:31-58.

Ottenheijm CA, Heunks LM, Dekhuijzen RP (2008). Diaphragm adaptations in patients with COPD. *Respir Res*. 9(1):12.

Pallavicini A, Kojić S, Bean C, Vainzof M, Salamon M, Ievolella C, Bortoletto G, Pacchioni B, Zatz M, Lanfranchi G, Faulkner G, Valle G (2001). Characterization of human skeletal muscle Ankrd2. *Biochem Biophys Res Commun*. 285(2):378-86.

Parast MM, and Otey CA (2000). Characterization of palladin, a novel protein localized to stress fibers and cell adhesions. *J Cell Biol*.;150(3):643-56.

Pashmforoush M, Pomiès P, Peterson KL, Kubalak S, Ross J Jr, Hefti A, Aebi U, Beckerle MC, Chien KR (2001). Adult mice deficient in actinin-associated LIM-domain protein reveal a developmental pathway for right ventricular cardiomyopathy. *Nat Med*. 7(5):591-7.

Passier R, Richardson JA, Olson EN (2000). Oracle, a novel PDZ-LIM domain protein expressed in heart and skeletal muscle. *Mech Dev*. 92(2):277-84.

Pfaffl MW (2001). A new mathematical model for relative quantification in real-time RT-PCR. *Nucleic Acids Res*. 29(9):e45.

Pogue-Geile KL, Chen R, Bronner MP, Crnogorac-Jurcevic T, Moyes KW, Dowen S, Otey CA, Crispin DA, George RD, Whitcomb DC, Brentnall TA (2006). Palladin mutation causes familial pancreatic cancer and suggests a new cancer mechanism. *PLoS Med*. 3(12):e516.

Pomiès P, Macalma T, Beckerle MC (1999). Purification and characterization of an alpha-actinin-binding PDZ-LIM protein that is up-regulated during muscle differentiation. *J Biol Chem*. 274(41):29242-50.

Posch MG, Thiemann L, Tomasov P, Veselka J, Cardim N, Garcia-Castro M, Coto E, Perrot A, Geier C, Dietz R, Haverkamp W, Ozcelik C (2008). Sequence analysis of myozenin 2 in 438 European patients with familial hypertrophic cardiomyopathy. *Med Sci Monit*. 14(7):CR372-4.

Puntervoll P, Linding R, Gemünd C, Chabanis-Davidson S, Mattingsdal M, Cameron S, Martin DM, Ausiello G, Brannetti B, Costantini A, Ferrè F, Maselli V, Via A, Cesareni G, Diella F, Superti-Furga G, Wyrwicz L, Ramu C, McGuigan C, Gudavalli R, Letunic I, Bork P, Rychlewski L, Küster B, Helmer-Citterich M, Hunter WN, Aasland R, Gibson TJ (2003). ELM server: A new resource for investigating short functional sites in modular eukaryotic proteins. *Nucleic Acids Res*. 31(13):3625-30.

Pyle WG, and Solaro RJ (2004). At the crossroads of myocardial signaling: the role of Z-discs in intracellular signaling and cardiac function. *Circ Res*. 94(3):296-305.

Reggiani C, Bottinelli R, Stienen GJ (2000). Sarcomeric Myosin Isoforms: Fine Tuning of a Molecular Motor. *News Physiol Sci*. 15:26-33.

Rönty M, Taivainen A, Moza M, Otey CA, Carpén O (2004). Molecular analysis of the interaction between palladin and alpha-actinin. *FEBS Lett*. 566(1-3):30-4.

Roos H (2001). Biosensor systems and Biacore Technology. http://hermes.material.uu.se/~klas/S&A-Biochem+Biacore.pdf.

Salmikangas P, Mykkänen OM, Grönholm M, Heiska L, Kere J, Carpén O (1999). Myotilin, a novel sarcomeric protein with two Ig-like domains, is encoded by a candidate gene for limb-girdle muscular dystrophy. *Hum Mol Genet*. 8(7):1329-36.

Salmikangas P, van der Ven PF, Lalowski M, Taivainen A, Zhao F, Suila H, Schröder R, Lappalainen P, Fürst DO, Carpén O (2003). Myotilin, the limb-girdle muscular dystrophy 1A (LGMD1A) protein, cross-links actin filaments and controls sarcomere assembly. *Hum Mol Genet*. 12(2):189-203.

Sanger JW, Ayoob JC, Chowrashi P, Zurawski D, Sanger JM (2000). Assembly of myofibrils in cardiac muscle cells. *Adv Exp Med Biol*. 481:89-102; discussion 103-5.

Sanger JW, and Sanger JM (2001). Fishing out proteins that bind to titin. *J Cell Biol*. 154(1):21-4.

Schultheiss T, Choi J, Lin ZX, DiLullo C, Cohen-Gould L, Fischman D, Holtzer H (1992). A sarcomeric alpha-actinin truncated at the carboxyl end induces the breakdown of stress fibers in PtK2 cells and the formation of nemaline-like bodies and breakdown of myofibrils in myotubes. *Proc Natl Acad Sci U S A*. 89(19):9282-6.

Schultz J, Milpetz F, Bork P, Ponting CP (1998). SMART, a simple modular architecture research tool: identification of signaling domains. *Proc Natl Acad Sci U S A*. 95(11):5857-64.

Schulz TW, Nakagawa T, Licznerski P, Pawlak V, Kolleker A, Rozov A, Kim J, Dittgen T, Köhr G, Sheng M, Seeburg PH, Osten P (2004). Actin/alpha-actinin-dependent transport of AMPA receptors in dendritic spines: role of the PDZ-LIM protein RIL. *J Neurosci*. 24(39):8584-94.

Selcen D, and Engel AG (2004). Mutations in myotilin cause myofibrillar myopathy. *Neurology*. 62(8):1363-71.

Selcen D, and Engel AG (2005). Mutations in ZASP define a novel form of muscular dystrophy in humans. *Ann Neurol*. 57(2):269-76.

Sellers JR (2000). Myosins: a diverse superfamily. *Biochim Biophys Acta*. 1496(1):3-22.

Small JV, and Gimona M (1998). The cytoskeleton of the vertebrate smooth muscle cell. *Acta Physiol Scand*. 164(4):341-8.

Somlyo AP, and Somlyo AV (1994). Signal transduction and regulation in smooth muscle. *Nature*.372: 231-6.

Songyang Z, Fanning AS, Fu C, Xu J, Marfatia SM, Chishti AH, Crompton A, Chan AC, Anderson JM, Cantley LC (1997). Recognition of unique carboxyl-terminal motifs by distinct PDZ domains. *Science*. 275(5296):73-7.

Spangenburg EE, and Booth FW (2003). Molecular regulation of individual skeletal muscle fibre types. *Acta Physiol Scand*. 178(4):413-24.

Stephens NL (2001). Airway smooth muscle. *Lung*. 179: 333-73.

Takada F, Vander Woude DL, Tong HQ, Thompson TG, Watkins SC, Kunkel LM, Beggs AH (2001). Myozenin: an alpha-actinin- and gamma-filamin-binding protein of skeletal muscle Z lines. *Proc Natl Acad Sci U S A*. 98(4):1595-600.

Tang J, Taylor DW, Taylor KA (2001). The three-dimensional structure of alpha-actinin obtained by cryoelectron microscopy suggests a model for Ca(2+)-dependent actin binding. *J Mol Biol*. 310(4):845-58.

Te Velthuis AJ, Isogai T, Gerrits L, Bagowski CP (2007). Insights into the molecular evolution of the PDZ/LIM family and identification of a novel conserved protein motif. *PLoS ONE*. 2(2):e189.

Theis JL, Bos JM, Bartleson VB, Will ML, Binder J, Vatta M, Towbin JA, Gersh BJ, Ommen SR, Ackerman MJ (2006). Echocardiographic-determined septal morphology in Z-disc hypertrophic cardiomyopathy. *Biochem Biophys Res Commun*. 351(4):896-902.

Thompson TG, Chan YM, Hack AA, Brosius M, Rajala M, Lidov HG, McNally EM, Watkins S, Kunkel LM (2000). Filamin 2 (FLN2): A muscle-specific sarcoglycan interacting protein. *J Cell Biol*. 148(1):115-26.

Torrado M, Senatorov VV, Trivedi R, Fariss RN, Tomarev SI (2004). Pdlim2, a novel PDZ-LIM domain protein, interacts with alpha-actinins and filamin A. *Invest Ophthalmol Vis Sci*. 45(11):3955-63.

Torrado M, Nespereira B, López E, Centeno A, Castro-Beiras A, Mikhailov AT (2005). ANKRD1 specifically binds CASQ2 in heart extracts and both proteins are co-enriched in piglet cardiac Purkinje cells. *J Mol Cell Cardiol*. 38(2):353-65.

Tsukamoto Y, Senda T, Nakano T, Nakada C, Hida T, Ishiguro N, Kondo G, Baba T, Sato K, Osaki M, Mori S, Ito H, Moriyama M (2002). Arpp, a new homolog of carp, is preferentially expressed in type 1 skeletal muscle fibers and is markedly induced by denervation. *Lab Invest*. 82(5):645-55.

Tsukamoto Y, Hijiya N, Yano S, Yokoyama S, Nakada C, Uchida T, Matsuura K, Moriyama M (2008). Arpp/Ankrd2, a member of the muscle ankyrin repeat proteins (MARPs), translocates from the I-band to the nucleus after muscle injury. *Histochem Cell Biol*. 129(1):55-64.

Vaccaro P, and Dente L (2002). PDZ domains: troubles in classification. *FEBS Lett*. 512(1-3):345-9.

Valle G, Faulkner G, De Antoni A, Pacchioni B, Pallavicini A, Pandolfo D, Tiso N, Toppo S, Trevisan S, Lanfranchi G (1997). Telethonin, a novel sarcomeric protein of heart and skeletal muscle. *FEBS Lett*. 415(2):163-8.

Vallenius T, Luukko K, Mäkelä TP (2000). CLP-36 PDZ-LIM protein associates with nonmuscle alpha-actinin-1 and alpha-actinin-4. *J Biol Chem*. 275(15):11100-5.

Vallenius T, and Mäkelä TP (2002). Clik1: a novel kinase targeted to actin stress fibers by the CLP-36 PDZ-LIM protein. *J Cell Sci*. 115(Pt 10):2067-73.

Vallenius T, Scharm B, Vesikansa A, Luukko K, Schäfer R, Mäkelä TP (2004). The PDZ-LIM protein RIL modulates actin stress fiber turnover and enhances the association of alpha-actinin with F-actin. *Exp Cell Res*. 293(1):117-28.

van der Meer DL, Marques IJ, Leito JT, Besser J, Bakkers J, Schoonheere E, Bagowski CP (2006). Zebrafish cypher is important for somite formation and heart development. *Dev Biol*. 299(2):356-72.

van der Ven PF, Wiesner S, Salmikangas P, Auerbach D, Himmel M, Kempa S, Hayess K, Pacholsky D, Taivainen A, Schröder R, Carpén O, Fürst DO (2000). Indications for a novel muscular dystrophy pathway. gamma-filamin, the muscle-specific filamin isoform, interacts with myotilin. *J Cell Biol*. 151(2):235-48.

van Ham M, and Hendriks W (2003). PDZ domains-glue and guide. *Mol Biol Rep*. 30(2):69-82.

Vatta M, Mohapatra B, Jimenez S, Sanchez X, Faulkner G, Perles Z, Sinagra G, Lin JH, Vu TM, Zhou Q, Bowles KR, Di Lenarda A, Schimmenti L, Fox M, Chrisco MA, Murphy RT, McKenna W, Elliott P, Bowles NE, Chen J, Valle G, Towbin JA (2003). Mutations in Cypher/ZASP in patients with dilated cardiomyopathy and left ventricular non-compaction. *J Am Coll Cardiol*. 42(11):2014-27.

von Nandelstadh P, Grönholm M, Moza M, Lamberg A, Savilahti H, Carpén O (2005). Actin-organising properties of the muscular dystrophy protein myotilin. *Exp Cell Res*. 310(1):131-9.

von Nandelstadh P, Ismail M, Gardin C, Suila H, Zara I, Belgrano A, Valle G, Carpen O, Faulkner G (2009). A class III PDZ binding motif in myotilin and FATZ families binds Enigma family proteins - a common link for Z-disc myopathies. *Mol Cell Biol*. 29(3):822-834.

Vorgerd M, van der Ven PF, Bruchertseifer V, Löwe T, Kley RA, Schröder R, Lochmüller H, Himmel M, Koehler K, Fürst DO, Huebner A (2005). A mutation in the dimerization domain of filamin c causes a novel type of autosomal dominant myofibrillar myopathy. *Am J Hum Genet*. 77(2):297-304.

Waites GT, Graham IR, Jackson P, Millake DB, Patel B, Blanchard AD, Weller PA, Eperon IC, Critchley DR (1992). Mutually exclusive splicing of calcium-binding domain exons in chick alpha-actinin. *J Biol Chem*. 267(9):6263-71.

Wang K, and Wright J (1988). Architecture of the sarcomere matrix of skeletal muscle: immunoelectron microscopic evidence that suggests a set of parallel inextensible nebulin filaments anchored at the Z line. *J Cell Biol*. 107:2199-212.

Wang H, Harrison-Shostak DC, Lemasters JJ, Herman B (1995). Cloning of a rat cDNA encoding a novel LIM domain protein with high homology to rat RIL. *Gene*. 165(2):267-71.

Witt SH, Granzier H, Witt CC, Labeit S (2005). MURF-1 and MURF-2 target a specific subset of myofibrillar proteins redundantly: towards understanding MURF-dependent muscle ubiquitination. *J Mol Biol*. 350(4):713-22.

Wong ML, and Medrano JF (2005). Real-time PCR for mRNA quantitation. *Biotechniques*. 39(1):75-85.

Wu R, Durick K, Songyang Z, Cantley LC, Taylor SS, Gill GN (1996). Specificity of LIM domain interactions with receptor tyrosine kinases. *J Biol Chem*. 271(27):15934-41.
Wu RY, and Gill GN (1994). LIM domain recognition of a tyrosine-containing tight turn. *J Biol Chem*. 269(40):25085-90.

Xia H, Winokur ST, Kuo WL, Altherr MR, Bredt DS (1997). Actinin-associated LIM protein: identification of a domain interaction between PDZ and spectrin-like repeat motifs. *J Cell Biol*. 139(2):507-15.

Yao X, Chaponnier C, Gabbiani G, Forte JG (1995). Polarized distribution of actin isoforms in gastric parietal cells. *Mol Biol Cell*. 6(5):541-57.

Young P, Ferguson C, Bañuelos S, Gautel M (1998). Molecular structure of the sarcomeric Z-disk: two types of titin interactions lead to an asymmetrical sorting of alpha-actinin. *EMBO J*. 17(6):1614-24.

Young P, and Gautel M (2000). The interaction of titin and alpha-actinin is controlled by a phospholipid-regulated intramolecular pseudoligand mechanism. *EMBO J*. 19(23):6331-40.

Zhang Q, Fan JS, Zhang M (2001). Interdomain chaperoning between PSD-95, Dlg, and Zo-1 (PDZ) domains of glutamate receptor-interacting proteins. *J Biol Chem*. 276(46):43216-20.

Zhang Y, Kornfeld H, Cruikshank WW, Kim S, Reardon CC, Center DM (2001). Nuclear translocation of the N-terminal prodomain of interleukin-16. *J Biol Chem*. 276(2):1299-303.

Zhou Q, Ruiz-Lozano P, Martone ME, Chen J (1999). Cypher, a striated muscle-restricted PDZ and LIM domain-containing protein, binds to alpha-actinin-2 and protein kinase C. *J Biol Chem*. 274(28):19807-13.

Zhou Q, Chu PH, Huang C, Cheng CF, Martone ME, Knoll G, Shelton GD, Evans S, Chen J (2001). Ablation of Cypher, a PDZ-LIM domain Z-line protein, causes a severe form of congenital myopathy. *J Cell Biol*. 155(4):605-12.

Zou Y, Evans S, Chen J, Kuo HC, Harvey RP, Chien KR (1997). CARP, a cardiac ankyrin repeat protein, is downstream in the Nkx2-5 homeobox gene pathway. *Development*. 124(4):793-804.